



University of Pretoria

**Expression and Purification of an efficacious recombinant Pulpy  
Kidney subunit vaccine made in *N. Benthamiana***

by

**Tinyiko Mokoena**

Dissertation submitted in partial fulfilment of the requirement for the degree

**PHILOSOPHIAE DOCTORATE**

**Department of Plant Science  
Forestry and Agricultural Biotechnology Institute (FABI)**

in the

**Faculty of Natural and Agricultural Science  
University of Pretoria**

**Supervisors: Dr E Chakauya  
Dr T Tsekoa  
Dr M Crampton  
Dr R Chikwamba**

**29 SEPTEMBER 2016**

**DECLARATION**

I, Tinyiko E Mokoena, declare that the thesis, which I hereby submit for the degree Philosophiae Doctorate at the University of Pretoria is my own work has not previously been submitted by me for a degree at this or any other tertiary institution.

SIGNATURE: .....

DATE: .....

## Table of Contents

ABSTRACT.....	v
ACKNOWLEDGEMENTS .....	ix
ABBREVIATIONS AND SYMBOLS.....	x
Chapter 1 .....	1
INTRODUCTION.....	1
1.2 Impact of the sheep industry in South Africa.....	3
1.2.1 South Africa's competitiveness of the sheep industry.....	4
1.3 Molecular biology of the <i>Epsilon</i> toxin.....	5
1.4 Effect of the <i>Epsilon</i> toxin on MDCK cells .....	8
1.5 Effects of the <i>Epsilon</i> toxin on animals and tissues.....	9
1.6 Evidence for neurotoxicity .....	11
1.7 Crystal structure of the $\epsilon$ -toxin .....	12
1.8 Pore formation by <i>Epsilon</i> toxin.....	15
1.9 Pulpy Kidney Disease vaccine production and challenges .....	18
1.10 Plant-derived biopharmaceutical products .....	21
1.11 Tobacco as an expression host .....	23
1.12 <i>Agrobacterium</i> -mediated delivery.....	24
1.13 Downstream processing.....	25
1.14 The development of expression vectors.....	26
2 INTRODUCTION.....	31
2.1 Pulpy Kidney Disease.....	31
2.2 Materials and method.....	37
2.3 Results .....	48
2.4 Discussion.....	63
2.5 Conclusion .....	67
Chapter 3 .....	69
3.1 Introduction.....	71
3.2 Materials and methods .....	73
3.3 Results .....	75
3.4 Discussion.....	82

<b>CYTOTOXICITY AND EFFICACY OF THE PLANT-DERIVED EtxD ANTIGEN .....</b>	<b>84</b>
<b>ABSTRACT.....</b>	<b>85</b>
<b>4. INTRODUCTION.....</b>	<b>86</b>
<b>4.1 Current production and formulation methods of the Pulpy Kidney Disease vaccine ....</b>	<b>86</b>
<b>4.2 Materials and methods .....</b>	<b>88</b>
<b>4.4 Results .....</b>	<b>94</b>
<b>4.5 Discussion.....</b>	<b>99</b>
<b>4.6 CONCLUSION .....</b>	<b>101</b>
<b>SUMMARY AND PERSPECTIVE.....</b>	<b>102</b>
<b>5.1 SUMMARY .....</b>	<b>103</b>
<b>5.2 Limitation and drawbacks of the product .....</b>	<b>104</b>
<b>5.3 FUTURE RESEARCH.....</b>	<b>105</b>
<b>References.....</b>	<b>106</b>
<b>Appendix A .....</b>	<b>119</b>

## ABSTRACT

*Epsilon* toxin (Etx) produced by *Clostridium perfringens* type D is responsible for a fatal Enterotoxemia (Pulpy Kidney Disease) in economically significant livestock such as sheep and goats. The only practical means of controlling this disease is by immunisation and avoiding the circumstances that are conducive to its occurrence. All currently available Pulpy Kidney Disease vaccines are based on a formalinised toxoid of *Clostridium perfringens* (*Welchii*) type D. This is either as an alum-precipitate, oil-emulsion formulation of the whole cell culture or a bacterial culture filtrate (Deepika, 2010). The current vaccine has several drawbacks. First, it is generally accepted that its chemical inactivation with formalin is difficult to standardise. Second, the classical methods of detoxification usually alter the overall protein structure in a random manner. Consequently, the immunogenicity of this type of a vaccine is decreased substantially. Third, there is a narrow range in balancing the detoxification (the strength of formalin commonly used is 1%) and the immunogenicity of the vaccine (Robertson et al. 2011). Alternatives to formalin inactivation have been proposed because of these challenges. These include ectopically expressing the mutated toxoids in other gram-positive microorganisms.

Apparently, plants provide a genuine alternative for the expression of an immunogenic and non-toxic vaccine for the Pulpy Kidney Disease. Thus, in this study, the hypothesis was that the EtxD protein could be transiently expressed efficiently in *Nicotiana benthamiana* plants via deconstructed viral vectors, targeting the EtxD protein expression into the apoplast or the cytosol. This resulted in the investigation of the following six research topics:

1. The feasibility of producing the *Epsilon* toxin recombinantly in *N. benthamiana*.
2. The role of subcellular targeting in the observed level of expression and accumulation of the target protein.
3. The methods of purification that could be explored to recover and purify the EtxD protein that was transiently expressed recombinantly in the *N. benthamiana* leaves.
4. The suitability of the plant-derived purified EtxD protein as an antigen for Pulpy Kidney Disease vaccine production.
5. An evaluation of the toxicity of the plant-derived EtxD protein.
6. Testing the efficacy of the recombinant plant-derived EtxD antigen.

In this context, the *EtxD* gene, accession number AY858558, and the genetic region from the NCBI and EMBL databases was targeted for this study since the *EtxD* gene is well-reported in published data and is similar to the *EtxD*-gene strain produced in South Africa. The targeted gene was then codon-optimised to be expressed in *N. benthamiana* plants and chemically synthesised by GeneArt. The codon-optimised *EtxD* gene was directly cloned into an Icon-deconstructed vector and vacuum infiltrated via an *Agrobacterium*- mediated transfer. Leaves of *N. benthamiana* were transfected by vacuum infiltration to deliver the *EtxD* gene transiently into the apoplast and the cytosol respectively. The plant-derived EtxD protein was then isolated from the plant matrix and biochemically analysed by SDS-PAGE, N-terminal peptide sequencing and Western Blot analysis. The EtxD protein was visible as a 34 kDa protein band on an SDS-PAGE gel. The protein band was isolated, and the sequence was confirmed by N-terminal sequencing, as well as by Western Blot analysis using a secondary polyclonal guinea pig anti-EtxD antibody. The plant-derived EtxD protein was then quantified by ELISA and thereafter the expression levels were established at 380 mg/kg fresh weight when targeted to the apoplast, and 300 mg/kg fresh weight when targeted to the cytosol. The apoplast plant-made EtxD protein was purified using a two-step chromatography method, namely ion exchange and size exclusion, with a 50% recovery of the EtxD protein on the final step of purification.

To investigate the suitability of the plant-derived purified EtxD protein as an antigen for the Pulpy Kidney Disease vaccine, the toxicity of the EtxD protein was evaluated and the efficacy of the derived EtxD protein was tested. For these, both in vitro and in vivo studies were conducted. The LD<sub>50</sub> studies on mice revealed that the plant-derived EtxD protein was slightly toxic, which correlated with the IC<sub>50</sub> results on MDCK cells. For the animal-challenge results, two formulations of vaccines were prepared from the recombinant antigen EtxD protein and administered intravenously to mice. The formulations that contained the plant-derived EtxD protein that were not activated by trypsin were unable to protect mice against the *Epsilon* toxin challenge. This indicates that the *Epsilon* toxin in the purified plant extract was not immunogenic. When the plant-derived EtxD protein was treated with trypsin, inactivated with formalin and formulated with the adjuvant, alum, it was also non-protective. However, the formulation containing the plant-derived EtxD protein and Disease Control Africa (DCA) immune stimulant was protective. These findings indicated that the plant-derived *Epsilon* toxin is a viable recombinant antigenic vaccine when formulated with the immune stimulant DCA.

In conclusion, this study has demonstrated that tobacco is a suitable host for the production of the EtxD protein. The ELISA results of the infiltrated tobacco leaf samples have demonstrated the successful expression of the 34 kDa EtxD protein together with *glucan-endo-1, 3-beta-glucanase* of about 25 kDa. The cytosol targeted strategy generated the lowest EtxD protein production at 300, 200 and 10 µg/kg fw of the protein. For large scale-production of the EtxD protein, transient expression targeting to the apoplast is preferable because of the high yield of protein per fresh leaf weight achieved in this study.

It has been shown in the study that a transiently expressed EtxD protein can be efficiently purified from tobacco to a high purity and yield by using just two main steps after the initial extraction. Up to 49,85% product yield (based on the initial recombinant EtxD protein concentration) could be recovered after the final step, as visualised on the SDS-PAGE. The recombinant EtxD protein was recovered to purity, as judged by the fact that a Coomassie stained SDS-PAGE has a single band. The results suggest that the transiently expressed EtxD protein may be efficiently purified from *N. benthamiana* extracts. The purification steps incorporated in the study also suggest that this purification scheme has the potential to be scaled-up. It has also been determined that it is possible to produce a relevant and less toxic Pulpy Kidney Disease vaccine in plants by means of *Nicotiana sp.* transient expression via the recombinant *A. tumefaciens*. Based on the results, the plant-derived purified EtxD protein needs to be trypsin-activated and formulated with a strong adjuvant, such as the DCA immune stimulant, to obtain full protection in mice. Further work needs to be undertaken to establish the dose response and techno-economic model for production of this candidate vaccine.

The current study thus demonstrates the feasibility of producing a safe and potent subunit vaccine for Pulpy Kidney Disease vaccine. This is the first reported case of such an achievement with this particular disease.

## THESIS COMPOSITION

In five chapters, this thesis describes a doctoral study aimed at efficiently producing a Pulpy Kidney Disease vaccine in *N. benthamiana* plants.

**Chapter 1** discusses the clinical importance of the *Epsilon* toxin responsible for the Pulpy Kidney Disease in economically important livestock. The chapter also provides information on the molecular biology of the  $\epsilon$ -toxin; the effects of the *Epsilon* toxin on MDCK cells; the effects of the toxin on animals; tissue, evidence of neurotoxicity; the crystal structure of the toxin; pore formation by *Epsilon* toxin; Pulpy Kidney Disease vaccine production and its challenges; and the plant-derived biopharmaceutical product. The chapter concludes with the introduction of tobacco as an expression host and *Agrobacterium* mediated transformation.

**Chapter 2** presents the methods and data of experiments relating to the expression feasibility and biochemical characterisation of a recombinant *Epsilon* toxin (EtxD) produced transiently as a soluble protein in *N. benthamiana* leaves.

**Chapter 3** informs on the methods used and the data obtained from experiments relating to the purification of the recombinant plant-derived EtxD protein in *N. benthamiana* plants, as well as the biochemical characterisation that confirms the presence and levels of protein.

**Chapter 4** presents the methods used and data obtained from experiments relating to the *in vivo* and *in vitro* studies undertaken to investigate the suitability of the plant-derived purified EtxD protein as an antigen for Pulpy Kidney Disease vaccine production, the evaluation of the toxicity of the plant-derived EtxD protein and the testing of the efficacy of the plant-derived Pulpy Kidney Disease vaccine.

**Chapter 5** summarises and provides perspective on the study followed by all the references that are cited within this thesis.

## ACKNOWLEDGEMENTS

To Jehovah, thank You very much for the divine interventions and all the blessing you have provided through this journey.

A heartfelt gratitude to my supervisors, Dr Rachel Chikwamba, Dr Ereck Chakauya, Dr Tsepko Tsekoa and Dr Michael Crampton, for their leadership and support that has made this achievement possible.

DCA Lab for the *in vivo* studies undertaken to investigate the suitability of the plant-derived purified EtxD protein as an antigen for Pulpy Kidney Disease vaccine production

I would like to also express my gratitude to my husband and family for their unfailing support and encouragement. Gogo nasiMelane, this is for you.

## ABBREVIATIONS AND SYMBOLS

BeYDV	Yellow dwarf virus
bp	Base pair
BSA	Bovine serum albumin
BME	2-mercaptoethanol
CAI	Codon adaptation index
CAM	Calmodulin
CMV	Cucumber mosaic virus
CPMV	Cowpea mosaic virus
CPPX	Cationic peanut peroxidase
CSIR	Council for Industrial and Scientific Research
cv	Column volumes
DCA	Disease Control Africa
DEAE	Diethylaminoethanol
dpi	Days post infection
DRM	Detergent resistant membranes
DTT	Dithiothreitol
EDTA	Ethylenediaminetetraacetic acid
EtxD	<i>Epsilon</i> toxin type D
EMBL	European Molecular Biology Laboratory
FLPC	Fast-performance liquid chromatography
GFP	Green fluorescence protein
GMCSF	Granulocyte-macrophage colony stimulating factor
GUS	<i>Beta glucuronidase</i>

His	Histidine
HPLC	High-pressure liquid chromatography
IMAC	Immobilised metal affinity chromatography
IMPACT	Implant activation technology
IU	International units
Kb	Kilo-base pair
kDa	Kilo Daltons
LIR	Long intergenic region
MDCK	Madin-Darby Canine Kidney
MMPMSF	Phenylmethyl sulphonyl fluoride
MTS	Methanethiosulfate
MWCO	Molecular weight cut-off
NCBI	National Centre for Biotechnology information
Nos	Neopaline synthase
OBP	Onderstepoort Biological Products
PAGE	Polyacrylamide gel
pI	Isoelectric point
PMSF	Phenylmethanesulphonyl fluoride
PR	Pathogenesis-related
PVDF	Polyvinylidene difluoride
PVPP	Phenolic-binding agents (polyvinylpyrrolidone)
ROS	Reactive oxygen species
rpm	Revolutions per minute
SA	South African
SDS	Sodium dodecyl sulphate
SEAP	Secreted alkaline phosphatase
SIR	Short intergenic region

T <sub>i</sub>	Tumour-inducing
T-DNA	Transferred DNA
TMV	Tobacco mosaic virus
v/v	Volume/volume

## INDEX OF FIGURES

	<b>Page</b>
<b>Figure 1.1</b>	<b>7</b>
The primary structure of the <i>Etx</i> gene product	
<b>Figure 1.2</b>	<b>9</b>
Effect of <i>Epsilon</i> toxin on the brain cells	
<b>Figure 1.3</b>	<b>10</b>
Intestinal oedema of a mouse inoculated with <i>Epsilon</i> toxin	
<b>Figure 1.4</b>	<b>13</b>
The structures of members of the aerolysin-like, $\beta$ -pore-forming toxin family as determined by X-ray crystallography	
<b>Figure 2.1</b>	<b>41</b>
Cloning of <i>EtxD</i> sequence into expression vectors	
<b>Figure 2.2</b>	<b>46</b>
Optimisation of sample standards for ELISA analysis	
<b>Figure 2.3</b>	<b>50</b>
Multiple amino acid sequence alignment of the different <i>C. perfringens</i> EtxD protein found in other countries with the EtxD protein found in the South African isolate	
<b>Figure 2.4</b>	<b>51</b>
Dendrogram based on a neighbour-joining algorithm showing the phylogenetic relationships among the protein sequence of the five <i>C. perfringens</i> type-D <i>Epsilon</i> toxins	
<b>Figure 2.5</b>	<b>52</b>
Multiple nucleic acid sequence alignment comparing the sequence of the targeted <i>C.</i>	

*perfringens* EtxD protein with the codon optimised *EtxD* gene

<b>Figure 2.6</b>	<b>54</b>
Transient expression of the <i>GFP</i> gene in the leaves of <i>N. benthamiana</i>	
<b>Figure 2.7</b>	<b>55</b>
Images of <i>N. benthamiana</i> leaves after agroinfiltration with the recombinant <i>EtxD</i> gene directed into cytosol	
<b>Figure 2.8</b>	<b>56</b>
An SDS-PAGE (12%) gel analysis of the agroinfiltrated recombinant EtxD protein	
<b>Figure 2.9</b>	<b>57</b>
Characterisation of guinea-pig blood serum and the secondary antibody for cross-reaction	
<b>Figure 2.10</b>	<b>58</b>
Western Blot analysis of the EtxD protein expressed in tobacco leaves	
<b>Figure 2.11</b>	<b>61</b>
Peptide sequencing of plant-produced proteins by mass spectrometer	
<b>Figure 2.12</b>	<b>62</b>
Expression levels of EtxD protein targeted to different subcellular compartments as measured by ELISA	
<b>Figure 2.13</b>	<b>63</b>
EtxD protein in different subcellular compartments as a percentage of total soluble protein from <i>N. benthamiana</i> leaves	
<b>Figure 3.1</b>	<b>76</b>
Capto Q anion-exchange chromatography of agroinfiltrated tobacco leaves extract and corresponding fraction analysis of plant-derived EtxD protein activity	

<b>Figure 3.2</b>	<b>77</b>
An SDS-PAGE analysis of partially purified EtxD transiently expressed in <i>N. benthamiana</i> leaves	
<b>Figure 3.3</b>	<b>78</b>
Chromatogram of Superdex 75 gel filtration chromatography of the unpurified EtxD sample	
<b>Figure 3.4</b>	<b>79</b>
SDS-PAGE analysis of purified EtxD protein transiently expressed in <i>N. benthamiana</i> leaves purified with a gel infiltration	
<b>Figure 3.5</b>	<b>80</b>
SDS-PAGE (12%) analysis of the plant-derived purified EtxD protein fractions pooled together	
<b>Figure 3.6</b>	<b>81</b>
A Western Blot analysis of EtxD protein	
<b>Figure 4.1</b>	<b>95</b>
Graphs showing the determination of the IC <sub>50</sub> level of the EtxD protein	
<b>Figure 4.2</b>	<b>96</b>
Microscopy images showing the biological activity of the plant-derived-purified EtxD protein	

## INDEX OF TABLES

	<b>Page</b>
<b>Table 1.1</b>	<b>2</b>
Toxins produced by strains of <i>C. perfringens</i>	
<b>Table 2.1</b>	<b>35</b>
Plant-based vaccines for veterinary use	
<b>Table 2.2</b>	<b>38</b>
<i>E. coli</i> and <i>A. tumefaciens</i> strains	
<b>Table 2.3</b>	<b>49</b>
Gene bank sequences of EtxD proteins from different countries	
<b>Table 2.4</b>	<b>60</b>
Sequencing data for the putative <i>Epsilon</i> protein bands from SDS-PAGE proteins	
<b>Table 3.1</b>	<b>82</b>
The protein efficiency recovered from the EtxD	
<b>Table 4.1</b>	<b>97</b>
Toxicity of the <i>Epsilon</i> -toxin samples on mice	
<b>Table 4.2</b>	<b>99</b>
The challenge results of plant-produced EtxD vaccine	

# **Chapter 1**

## **INTRODUCTION**

# 1. EPSILON TOXIN CLOSTRIDIUM PERFRINGENS

## 1.1 Clinical importance of the *Epsilon* toxin from *C. perfringens*

According to Robinson et al. (2017), the *Clostridium* genus encompasses more than 80 species that form a diverse group of rod-shaped, Gram positive bacteria that have the ability to form spores. These organisms are principally obligate anaerobes, although some species are able to survive in the presence of trace amounts of oxygen (Bokori-Brown et al., 2011; Stiles et al., 2013). *Clostridia* are omnipresent bacteria that is found in soil and water, as well as in decomposing animal and plant matter. In addition, some *Clostridia* species can be found in the gastrointestinal tract of humans and animals where they form part of the normal gut flora. However, under certain circumstances some of these species are able to cause severe diseases in humans and domestic animals as a result of a variety of toxins being produced (Stiles et al., 2013). *Clostridium perfringens* is one of the most pathogenic species in the *Clostridium* genus as it is able to produce at least 17 toxins (Alouf, 2006; Bokori-Brown et al., 2011). Depending on their ability to produce the four typing toxins ( $\alpha$ ,  $\beta$ ,  $\epsilon$  and  $\iota$ -toxins), *C. perfringens* strains are classified into five toxinotypes (Table 1.1) (Petit et al., 1999; Bokori-Brown et al., 2011; Stiles et al., 2013; Jemal., 2016).

**Table 1.1: Toxins produced by strains of *C. perfringens***

Toxins names				
Strain(s)	Alpha	Beta	<i>Epsilon</i>	Iota
A	x			
B	x	x		
C	x	x		
D	x		x	
E	x			x

In addition to the typing toxins, the bacterium is able to produce a number of toxins not used for typing, such as  $\beta_2$ ,  $\delta$ ,  $\kappa$ ,  $\mu$ ,  $\gamma$ ,  $\nu$ ,  $\theta$  and enterotoxin (Stiles et al., 2013). As bacterial toxins often act in concert, causing virulent effects, their individual significance and roles in disease can be difficult to assess. The *Epsilon* toxin is produced by the *C. perfringens* toxinotypes B and D, which also produces the  $\beta$ -toxin, is the aetiological agent of dysentery in new-born

lambs. It is also associated with enteritis and enterotoxaemia in goats, calves and foals (Berger, 2016).

*C. perfringens* type D affects mainly sheep (including lambs) that are on rich diets, but it can also cause infection in goats and calves (Bokori-Brown et al., 2011). The most important factor that initiates the disease is the disruption of the microbial balance in the gut as a result of overeating. This leads to the passage of large amounts of undigested carbohydrates from the rumen into the intestine. Here, *C. perfringens* is then able to proliferate in large numbers and produce the  $\epsilon$ -toxin. The overproduction of this toxin causes increased intestinal permeability, facilitating the entry of the toxin into the bloodstream and then spreading to various organs, including the brain, lungs and Kidneys, which causes severe oedema (Bokori-Brown et al., 2011). While infection of the central nervous system results in neurological disorders, a further effect is sudden death (Finnie, 2003; Bokori-Brown et al., 2011).

The US Government Centre for Disease Control and Prevention considers the toxin to be a potential bio-warfare or bio-terrorism agent (Berger, 2016). The use of biological weapons in conventional warfare has been banned by the Biological and Toxic Weapons Convention, initiated by the USA in 1972. Western states are particularly concerned about the availability of toxins to terrorist groups. The fact that a 50% dose (LD<sub>50</sub>) of *Epsilon* toxin in mice (50 ng/kg) is lethal (Berger, 2016), indicates the potential for using this toxin as a bio-terrorist weapon and highlights the need to understand the molecular basis of the toxicity so that an effective vaccine can be developed.

## **1.2 Impact of the sheep industry in South Africa**

Sheep production in South Africa is a significant contributor to food security and clothing. In addition, the industry adds considerable value to the country's economy. For these reasons and to ensure the industry's healthy growth, efficient and affordable vaccines are required to prevent diseases such as Pulpy Kidney Disease (Bath et al., 2016). As Pulpy Kidney Disease is the most important disease that constrain small-ruminant livestock farming growth (Jemal et al., 2016). Furthermore, this supports the contention that animal disease control requires significant continued support and lack of access to veterinary support including vaccines is a major challenge to farming SMEs. Hence, the development of affordable, easily accessible, safe and quality vaccine such as plant-based Pulpy Kidney Disease vaccine is required. The

current OBP price for a Pulpy Kidney Disease vaccine is R155, 48c/100 ml excluding tax. The constant monitoring of sheep after grazing for the disease and revaccination makes the vaccination process expensive to small-ruminant livestock farmers and hinders their growth (Bath et al., 2016).

Sheep farming is practiced throughout South Africa, although it is concentrated in the more arid parts of the country such as the Northern, Eastern and Western Cape, the Free State and Mpumalanga. The industry encompasses approximately 8 000 commercial sheep farms and about 5 800 communal farmers. The number of sheep in South Africa is estimated to number 28,8 million. Sheep farmers are represented by organisations such as the Dorper Sheep Breeders' Society of South Africa and Merino SA (Snyman, 2014). The Dorper is a highly successful South African mutton breed developed specially for the more arid areas of the country. Its excellent carcass qualities in terms of conformation and fat distribution generally qualify it for top classification. Other mutton breeds that also produce wool are Damara, Meatmaster, Ille de France, Dormer, Suffolk, Van Rooy and Vador (Snyman, 2014). The gross value of mutton production is dependent on the price and quantity of meat produced. Over the past ten years the average gross production value amounted to R3,4 billion per year. This value has increased continuously over the years (Snyman, 2014).

### ***1.2.1 South Africa's competitiveness of the sheep industry***

South Africa is a net importer of mutton as it only produces approximately 83% of its domestic consumption. Given the current maize surplus and a low world maize price, with grain prices expected to remain under pressure, there should be a further improvement in profitability by supplementary feeding. Domestic mutton prices are expected to move with the normal seasonal price trend, which declines during October and increase during the braai months. It is therefore expected that prices will strengthen due to strong consumer demand during this period (Pieter, 2017).

### ***1.2.2 The competitiveness of the sheep industry in exports***

The South African wool industry is in a privileged position and has ample opportunity for growth. Sheep commodity prices are doing remarkably well, and economists believe this trend will continue because of international market demand exceeds supply (Trade probe report, 2017). Concerning mutton, the greatest share of South African exports is destined for Mozambique, which in 2013 commanded a 41,4% share, followed by the DRC with 27,6% and the Congo with 20,7%.

### **1.3 Molecular biology of the *Epsilon* toxin**

The  $\mathcal{E}$ -toxin gene, *Etx*, is located on plasmids in both toxinotypes B and D (Bokori-Brown et al., 2011). In toxinotype B isolates, the *Etx* gene is carried on a 65 kb plasmid that may also carry the *cpb2* gene for the  $\beta$ 2-toxin (Sayeed and McClane, 2010; Bokori-Brown et al., 2011), while the *cpb* gene that encodes the  $\beta$ -toxin resides on a separate plasmid. In the toxinotype D isolates, the *Etx* gene is present on plasmids ranging from 48 to 110 kb (Sayeed and McClane, 2010; Bokori-Brown et al., 2011). Interestingly, the larger plasmids have been found to carry up to three different toxin-encoding genes (*Etx*, *cpe* and *cpb2*) (Sayeed and McClane, 2010; Bokori-Brown et al., 2011).

A common theme in both toxinotypes is the association of the *Etx* gene with insertion sequences. The transposable element IS1151 has been found upstream of the *Etx* gene in plasmids from both toxinotypes, although in opposite orientations (Miyamoto et al., 2008; Bokori-Brown et al., 2011). This association has led to speculation about possible virulence gene mobilisation and exchange between plasmids. Support for this hypothesis was provided by the identification of circular transposition intermediates containing IS406-*Etx*-IS1151 (Bokori-Brown et al., 2011). These findings have implications for the evolution of *C. perfringens* and help to explain how some plasmids carry multiple toxin genes. Additional evidence for genetic exchange among toxinotypes is provided by the finding that the *tcp* locus, required for conjugation (Bokori-Brown et al., 2011), is present in some *Etx* plasmids from both toxinotype B and D isolates (Sayeed and McClane, 2010). Hughes et al. (2007) demonstrated the conjugative transfer of an *Etx* plasmid from a toxinotype D to a type A isolate,

thus essentially converting type A to type D, both genotypically and phenotypically (Hughes et al., 2007; Bokori-Brown et al., 2011).

In all strains,  $\epsilon$ -toxin is expressed with a signal sequence of 32 amino acids that direct an export of the prototoxin from *C. perfringens* (Bokori-Brown et al., 2011). Sequencing of *EtxB* and *EtxD* revealed only two nucleotide differences in the open reading frames. The first change, at position 762, does not result in an amino acid substitution. The second change, at position 962, results in a substitution from serine, in *EtxB*, to tyrosine in *EtxD* (Bokori-Brown et al., 2011). The upstream regions of the *EtxB* and *EtxD* genes are not identical and have different putative -10 and -35 promoter regions (Bokori-Brown et al., 2011). This suggests that the expression of these genes may be regulated in different ways in type B and D strains of *C. perfringens*. This possibility is supported by the observation that the strain from which the *EtxD* gene was isolated (NCTC 8346) produced ten times more  $\epsilon$ -toxin than the strain from which the *EtxB* gene was isolated (NCTC 8533) (Havard et al., 1992). The relatively inactive secreted prototoxin of 296 amino acids (32,9 kDa) is converted to the fully active mature toxin by a proteolytic cleavage in the gut lumen. This is either by digestive proteases of the host, such as trypsin and chymotrypsin (Bhown and Haberb, 1993), or by *C. perfringens* k-protease (Minami et al., 1997; Bokori-Brown et al., 2011).

Proteolytic activation of the toxin can also be achieved in the laboratory by controlled enzyme digestion (Bokori-Brown et al., 2011). Depending on the protease, proteolytic cleavage results in the removal of 10 to 13 amino-terminal amino acids and 22 to 29 carboxy-terminal amino acids (Bhown and Haberb, 1993; Bokori-Brown et al., 2011). Maximal activation of the toxin occurs with a combination of trypsin and chymotrypsin, resulting in the loss of 13 N-terminal residues and 29 C-terminal residues (see Figure 1.1).

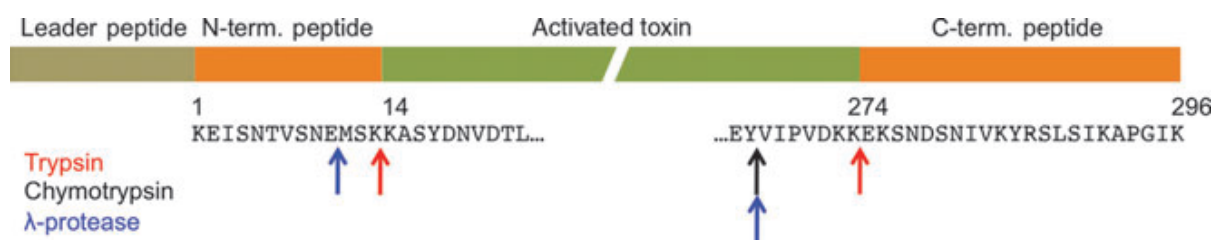


**Figure 1.1: The primary structure of the *Etx* gene product.** After secretion, the prototoxin is activated by a removal of N and C-terminal peptides at the indicated positions. Residue numbers are given according to the numbering system for prototoxin (Bokori-Brown et al., 2011).

This produces a mature toxin that is over 1 000-fold more toxic than the prototoxin (Bokori-Brown et al., 2011), with an LD<sub>50</sub> of 50 to 65 ng/kg in mice. This makes *Epsilon* toxin the most potent clostridial toxin after the botulinum and tetanus neurotoxins. If trypsin alone is used for activation, only 22 residues are removed from the C-terminus, resulting in a lower toxicity in mice, with an LD<sub>50</sub> of 320 ng/kg (Bokori-Brown et al., 2011; Minami et al., 1997). If *C. perfringens* k-protease is used for activation, the C-terminus is cleaved at the same position as with chymotrypsin, but leaves three extra residues at the N-terminus, resulting in activity close to the maximal level, with an LD<sub>50</sub> of 110 ng/kg (Bokori-Brown et al., 2011).

Proteolytic cleavage also causes a marked shift in pI from 8,02 in the prototoxin to 5.36 in the mature toxin. However, an additional moiety with a pI of 5,74, which is thought to correspond to the partially activated toxin, can also be detected. The primary structure of  $\epsilon$ -toxin bears no sequence similarity to any protein with a known structure in the current protein data bank (<http://www.rcsb.org/pdb>) as detectable by sequence comparison methods. However, the amino acid sequence of  $\epsilon$ -toxin shows some homology to the *Bacillus sphaericus* mosquitocidal toxins *Mtx2* and *Mtx3*, with a 26% and a 23% sequence identity, respectively. The *B. sphaericus* toxins are also activated by proteolytic cleavage (Liu et al., 1996), giving further support to the idea that they have a similar function to the  $\epsilon$ -toxin. In addition, there is a similar level of sequence identity to a number of putative bacterial proteins of unknown function, identified by genome sequencing projects, including a number of proteins from *B. thuringiensis* (UniProt ID: C3GC23 or C3FC62).

## 1.4 Effect of the *Epsilon* toxin on MDCK cells

The effects of  $\epsilon$ -toxin on several cell lines have been tested on cultured cells over the past few decades to identify a suitable in vitro model for the study of the *Epsilon* toxin. The Madin-Darby Canine Kidney (MDCK) cell line of epithelial origin, derived from the distal collecting tubule, was initially identified to be toxin sensitive by a microscopic examination of intoxicated cells (Bokori-Brown et al., 2011). Cytotoxicity assays on a further 11 Kidney cell lines of animal origin failed to identify additional cell lines sensitive to the toxin (Bokori-Brown et al., 2011). Cytotoxicity assays on 17 human cell lines (originating from the Kidney, brain, skin, bone, respiratory and intestinal tracts) identified the Caucasian renal leiomyoblastoma (G-402) cell line to be toxin-sensitive, although to a lesser extent than the MDCK cell line (Shortt et al., 2000). In MDCK cells, the dose of  $\epsilon$ -toxin needed to kill 50% of cells is reported to be 15 ng/ml, while the MDCK cells that have *Epsilon* toxin in their system undergo morphological changes that include swelling and formation of membrane blebs (Bokori-Brown et al., 2011; Takeyana et al., 2015).

The rapid death of cells exposed to the toxin results in the formation of a large membrane complex on the target cell surface (Donelli et al., 2003; Bokori-Brown et al., 2011) leading to pore formation, an efflux of  $K^+$  and an influx of  $Na^+$  and  $Cl^-$  ions (Petit et al., 2001). In addition, cytotoxicity is temperature and pH-dependent (Lindsay, 1996) and is potentiated by EDTA (Bokori-Brown et al., 2011). Recently, the cytotoxic effect of  $\epsilon$ -toxin was demonstrated in a highly differentiated murine renal cortical collecting duct principal cell line, mpkCCDcl4 (Chassin et al., 2007). These cells retain the specific ion transport properties of the distal collecting duct cells from which they are derived (Chassin et al., 2007; Bokori-Brown et al., 2011). According to Buxton (1990), in mpkCCDcl4 cells, a toxin-induced intracellular  $Ca^{2+}$  rise and an ATP depletion-mediated cell death occurred even under conditions that prevented toxin oligomerisation and thus pore formation. Some primary cells are also susceptible to the toxin. For example, guinea pig peritoneal macrophages exposed to the toxin show a blistering of the nuclear membrane, an ill-defined chromatin and a swollen cytoplasm without structure.

Mixed glial primary cell cultures, isolated from mice brains, are also toxin-sensitive (Soler-Jover et al., 2007). Primary cultures of mice cerebellar cortex identified granule cells are also targeted and affected by the *Epsilon* toxin, leading to membrane severing,  $Ca^{2+}$  influx and

glutamate efflux (Lonchamp et al., 2010). Primary cultures of the human renal tubular epithelial cells also showed a toxin-induced swelling of cells and the formation of membrane blebs (Fernandez-Miyakawa et al., 2010).

### 1.5 Effects of the *Epsilon* toxin on animals and tissues

Enterotoxaemia in naturally infected animals is usually characterised by enterocolitis in goats and systemic lesions in sheep (Bokori-Brown et al., 2011; Takeyama et al., 2015). It is postulated that a proteolytic activation of the toxin in the gastrointestinal tract compromises an intestinal barrier in the intoxicated animals, allowing the dissemination of the toxin via the bloodstream to the main target organs of the Kidneys and brain (Figure 1.2).

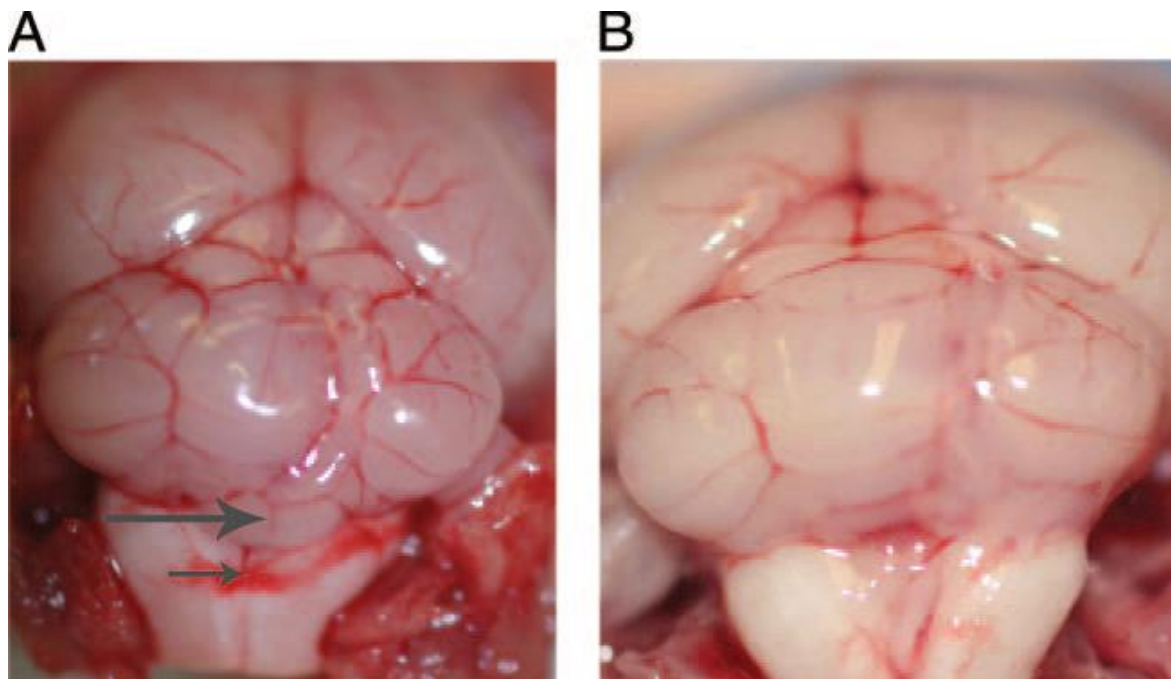


**Figure 1.2: Effect of *Epsilon* toxin on brain cells.** (A) The brain of a sealed mouse inoculated intragastrically with a *C. perfringens* type D isolate. Note the cerebellar coning (the vermis of the cerebellum protrudes slightly backwards) (large arrow) and haemorrhage on the dorsal part of the medulla (small arrow). (B) The brain of a healthy control mouse shown for comparison (Fernandez-Miyakawa et al., 2007; Allaart et al., 2014).

The mechanism of  $\mathcal{E}$ -toxin absorption from the gastrointestinal tract is not well understood. A histological analysis of the ligated intestinal loops of sheep and goats exposed to *Epsilon* toxin revealed a necrosis of the colonic epithelium in both species. This suggests that an alteration of permeability of the large intestine might play a role in toxin absorption (Fernandez-Miyakawa, 2003). Figure 1.3 shows the results of the study conducted by Fernandez-Miyakawa

et al. in 2007 revealing the intestinal oedema of a mouse inoculated with a *C. perfringens* type D isolate.

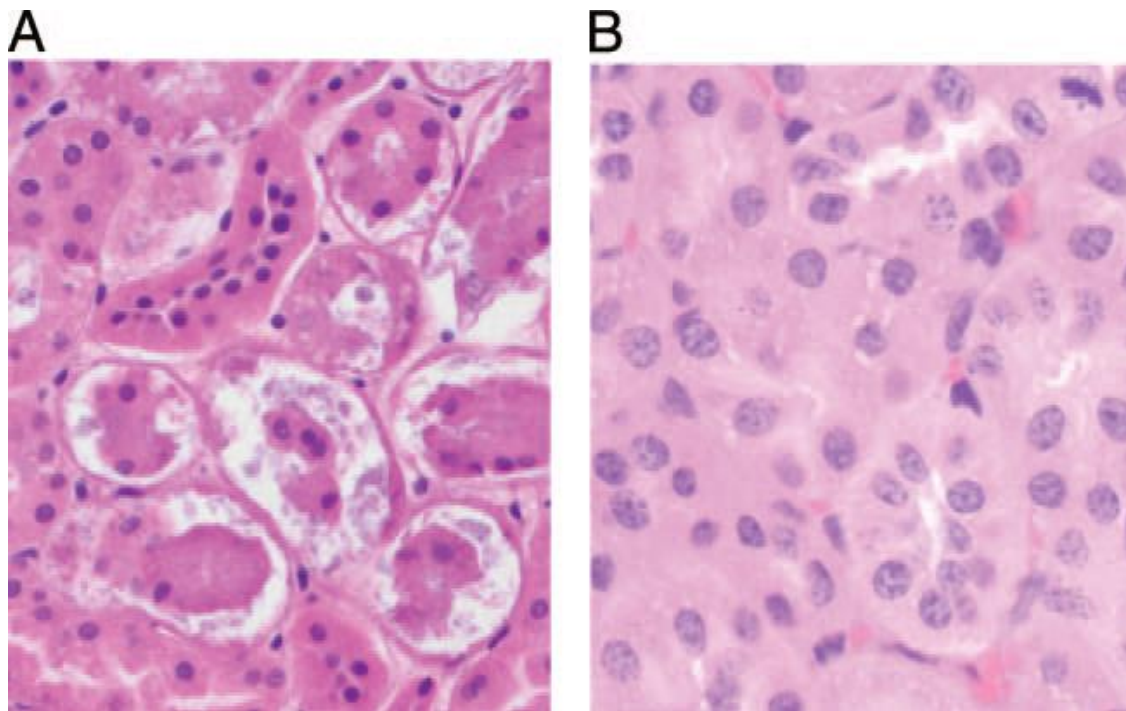


**Figure 1.3: Intestinal oedema of a mouse inoculated with *Epsilon* toxin.** (A) Interstitial oedema in the brain of a sealed mouse inoculated intragastrically with a *C. perfringens* type D isolate. Observe the presence of diffuse acidophilic fluid and vacuolation of the interstitium. (B) The brain of a healthy control mouse shown for comparison. The tissues were stained with hematoxylin and eosin. Magnification x 200 (Fernandez-Miyakawa et al., 2007; Allaart et al., 2014).

In mice and rats, *in vivo* transmission electron microscopy studies have revealed that the toxin alters the small intestinal permeability. This is predominantly the result of the mucosa tight junction opening up, indicating that the small intestine might also have a role in the absorption of the toxin (Goldstein et al., 2009). Previous studies suggested that a toxin-induced oedema of the brain is because of the damaging action of the toxin on vascular endothelial cells (Uzal and Kelly, 1997). A toxin-induced increase in vascular permeability in the brain was initially visualised by the use of vascular tracers, such as the horseradish peroxidase (Morgan et al., 1995; Bokori-Brown et al., 2011) or radiolabelled serum albumin (Griner and Carlson, 1961; Bokori-Brown et al., 2013).

## 1.6 Evidence for neurotoxicity

The terminal phase of enterotoxaemia is characterised by severe neurological disorders that include opisthotonus, seizures and agonal struggling, both in natural hosts and in experimental animal models (Finnie, 2003; Bokori-Brown et al., 2011). Several studies provide evidence that neurological damage in intoxicated animals is induced by the increased vascular permeability of brain blood vessels, leading to vasogenic oedema. This is a common feature of animals suffering from *C. perfringens* enterotoxaemia. There is also evidence that the toxin acts directly on neuronal tissues of intoxicated animals. For example, in mice and rat brains, intoxication causes both selective and extensive neurotoxicity, depending on the dose of the toxin administered (Bokori-Brown et al., 2011). Extensive neuronal damage was also observed in a rat brain after an intravenous toxin was administered at a minimal lethal dose. While a sublethal dose caused neuronal damage predominantly in the hippocampus, including the mossy fibre layers this was not because of a change in the cerebral blood flow (Bokori-Brown et al., 2011). A subacute or chronic intoxication of rats also produced the degeneration and necrosis of neuronal cells (Bokori-Brown et al., 2011). In intravenously injected mice, a pre-injection of the prototoxin inhibited the preferential accumulation and lethal activity in the brain of a radiolabelled toxin, which indicates that the toxin specifically binds to and acts on the brain (Bokori-Brown et al., 2011).

High affinity binding of a radiolabelled toxin to rat brain homogenates and synaptosomal membrane fractions has also suggested the presence of specific binding sites in the brain tissue (Bokori-Brown et al., 2011). Pre-treatment of the synaptosomal membrane fractions with pronase, heat and neuraminidase decreased toxin binding. This indicates that the interaction of toxin with cell membranes in the brain is facilitated by a sialoglycoprotein (Bokori-Brown et al., 2011). A pre-treatment of the synaptosomal membrane fractions with the presynaptic neurotoxin  *$\beta$ -bungarotoxin* also inhibited the toxin binding in a dose-dependent manner (Nagahama and Sakurai, 1992). A number of studies suggest that  $\epsilon$ -toxin exhibits neurotoxicity towards the brain by stimulating a neurotransmitter release. In mice, the lethal activity of the toxin was reduced by dopamine receptor antagonists and by drugs that directly or indirectly inhibit dopamine release. This suggests that the toxin specifically stimulates the release of dopamine from dopaminergic nerve endings (Nagahama and Sakurai, 1992). In another study, prior injection of either a presynaptic glutamate release inhibitor or a glutamate receptor

antagonist protected the rat hippocampus from toxin-induced neuronal damage, indicating that the toxin specifically stimulates glutamate release (Miyamoto et al., 1998). The stimulated release of glutamate was also demonstrated in the mouse hippocampus after an intravenous administration of the toxin, which led to seizure and neuronal damage (Miyamoto et al., 2000).

Recent electrophysiological and pharmacological analysis of cultured mouse cerebellar slices has demonstrated that the stimulation of glutamate release is the result of the toxin's direct action on granule cell somata (Lonchamp et al. 2010). The identity of the cells targeted by the toxin remains a debatable point. A study undertaken by Lonchamp et al. (2010) found no evidence that the toxin has a direct effect on glutamatergic nerve terminals, which is in contrast to the findings of previous biochemical studies performed on rat brain synaptosomal membrane fractions. In the latter experiment, binding of a radiolabelled toxin to rat synaptosomes was associated with the formation of a stable, high-molecular weight complex, leading to pore formation (Bokori-Brown et al., 2011). A study by Dorca- Arevalo et al., (2008) also disputes the direct action of GFP-tagged *Epsilon* toxin on nerve terminals, based on the failure of the toxin to trigger glutamate release from the toxin-treated mouse brain synaptosomal fractions. In this study, synaptosomal preparations were found to be contaminated by myelin structures, identified as the main toxin binding sites in preparations (Dorca-Arevalo et al., 2008).

## **1.7 Crystal structure of the $\epsilon$ -toxin**

The three-dimensional structure of the  $\epsilon$ -toxin has been determined by multi-wavelength anomalous dispersion (<http://www.rcsb.org/pdb>) (PDB ID: 1UYJ). The crystal structure revealed that  $\epsilon$ -toxin is a very elongated molecule ( $100 \text{ \AA} \cdot 20 \text{ \AA} \cdot 20 \text{ \AA}$ ) and is composed mainly of  $\beta$ -sheets (Figure 1.4). The toxin structure can be divided into three domains. The first domain contains an  $\alpha$ -helix and a three-stranded anti-parallel sheet upon which the large  $\alpha$ -helix lies. The second domain is a  $\beta$ -sandwich, containing a five-stranded sheet and a  $\beta$ -hairpin (both of which are anti-parallel). The third domain is a  $\beta$ -sandwich composed of one four-stranded sheet and one three-stranded sheet, the latter containing the only parallel strand in the structure. The overall fold of the  $\epsilon$ -toxin structure shows similarity to aerolysin from the Gram-negative bacterium *Aeromonas hydrophila* (Parker et al., 1994; Bokori-Brown et al., 2011) to

parasporin-2 (PS) from *B. thuringiensis* and to a pore-forming lectin, LSL, from *Laetiporus sulphureus* (Mancheno et al., 2005).

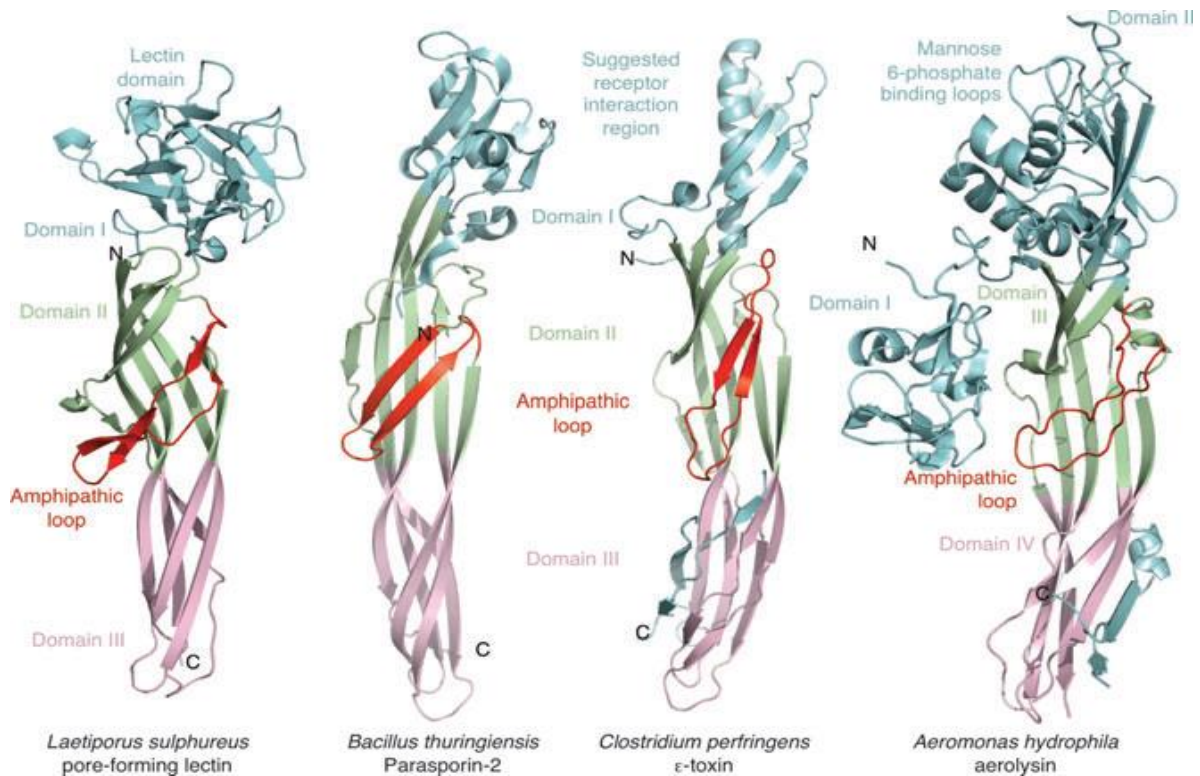


**Figure 1.4: The structures of members of the aerolysin-like,  $\beta$ -pore-forming toxin family as determined by X-ray crystallography.** The colour cyan indicates the N-terminal membrane interacting and other non-related regions, pale green and pink show domains important for oligomerisation and membrane interaction, and red is for the  $\beta$ -hairpin predicted to insert into the membrane (Bokori-Brown et al., 2011).

Despite the low identity (<20%) between the primary sequences of all the above proteins, the structures show remarkably similar  $\beta$ -sheet arrangements (Figure 1.4) in their two C-terminal domains (domains III and IV in aerolysin, and domains II and III in the others). All these proteins form pores, though aerolysin and  $\epsilon$ -toxin, are predicted to be heptameric (Moniatte et al., 1996; Bokori-Brown et al., 2011), while LSL is thought to be hexameric. Parasporin-2 is known to oligomerise at cell surfaces, even though the size of the oligomers has not been accurately determined (Abe et al., 2008; Bokori-Brown et al., 2011). Aerolysin,  $\epsilon$ -toxin and PS are all secreted as prototoxins and are activated by proteolytic removal of the N and C-terminal sequences. There is greater structural variation between the N-terminal domains of the above proteins than between the C-terminal domains.

The N-terminal domains are expected to be important for substrate or receptor binding. In aerolysin, the N-terminal domain has been postulated to be responsible for the initial interaction with cells (MacKenzie et al., 1999; Bokori-Brown et al., 2011). Aerolysin binds to the glycosylphosphatidylinositol (GPI)-anchored proteins that are found in detergent-resistant membranes (DRMs) via domain II. The crystal structure of an oligomerising but not pore-forming mannose-6 phosphate bound aerolysin is now available (PDB ID: 3C0O). Domain I of the  $\epsilon$ -toxin and PS (Figure 1.4) are similar and have some limited similarity to aerolysin. It has been suggested that this domain performs a similar function in  $\epsilon$ -toxin (Cole et al., 2004; Akiba et al., 2009; Bokori-Brown et al., 2011). However, none of the residues involved in sugar-binding in aerolysin are present in the  $\epsilon$ -toxin or PS. Therefore, it seems likely that these proteins have a different cell-surface receptor. In complete contrast, the domain I of LSL has a  $\beta$ -trefoil lectin fold (Figure 1.4) in which lactose and N-acetyl-D lactosamine have been observed crystallographically. It is probable that the major reported differences in the target cell specificities of aerolysin and  $\epsilon$ -toxin, and the different function of LSL, are the result of the different structures and properties of these domains. The second and third domains of  $\epsilon$ -toxin exhibit obvious structural similarities to the third and fourth domains of aerolysin, and to the second and third domains of LSL and PS. As described previously, domain II is composed of a five-stranded sheet with an amphipathic  $\beta$ -hairpin (residues 124 to 146) lying against it, while domain III is a  $\beta$ -sandwich composed of four and three-stranded  $\beta$ -sheets.

This amphipathic  $\beta$ -hairpin in  $\epsilon$ -toxin has been predicted to form the membrane insertion domain owing to its alternating hydrophilic-hydrophobic character (Cole et al., 2004; Bokori-Brown et al., 2011). This hairpin was studied by Knapp et al. (2009). This group showed that certain residues in the hairpin were accessible to methanethiosulfate (MTS) reagents, which resulted in reduced pore conductance of the planar bilayer-embedded *Epsilon* toxin, suggesting that these residues must be facing the lumen of the pore. In addition, Pelish and McClain (2009) have shown that by creating disulphide bonds between pairs of the introduced cysteines (one in the amphipathic loop and one in an adjacent strand) prevented conformational changes in the amphipathic loop, thereby preventing pore formation but not receptor binding or oligomerisation and confirming that these residues are important for pore formation. The amphipathic pattern is present in the other  $\beta$ -pore-forming toxins, including aerolysin, LSL and PS. The corresponding hairpin in domain III of aerolysin was shown to form the membrane

pore. Alternating residues on either side of the hairpin were accessible to MTS probes added to the trans-side of the planar bilayers, which is consistent with these residues lining the lumen of the pore. Interestingly, a hydrophobic loop connecting the two amphipathic sides of the hairpin was inaccessible, indicating that it is buried in the bilayer. It is proposed that this hydrophobic sequence drives membrane insertion and possibly acts as a rivet, stabilising the pore. However, the effect was not seen in  $\epsilon$ -toxin, where turn residues could be accessed from the trans-side by antibodies (Bokori-Brown et al., 2011).

In the *C. septicum*  $\alpha$ -toxin, a protein with significant sequence homology to aerolysin, the region equivalent to this hairpin was tested for membrane insertion. This was undertaken using sequential cysteine mutation modified with a fluorescent probe sensitive to changes from an aqueous to a lipid environment (Bokori-Brown et al., 2011). This technique showed that, alternately, these residues point into a lipid and then an aqueous environment when bound to a membrane, indicating an insertion of the two stranded sheets in a similar manner to the *Staphylococcus aureus*  $\alpha$ -toxin. The final domain of the  $\epsilon$ -toxin has been associated with heptamerisation (Miyata et al., 2001; Bokori-Brown et al., 2011). In the precursor forms of both  $\epsilon$ -toxin and aerolysin, the C-terminal peptides appear to block oligomerisation. Electron microscopy of the water-soluble, non-pore forming heptamer created by an aerolysin mutant, Y221G, was performed. This showed that the interface between a pair of monomers in the heptamer is made up of one face from one monomer and the opposite face from the other monomer (Tsitrin et al., 2002; Bokori-Brown et al., 2011), as is the case for any ring formed of monomers. If the C-terminal peptide is not removed by activation, it will be located in a similar position between monomers in the oligomer, thus blocking interaction.

## **1.8 Pore formation by *Epsilon* toxin**

The binding of  $\epsilon$ -toxin to MDCK cells (and rat synaptosomal membranes) is associated with the formation of a stable, high-molecular weight complex (Petit et al., 1997; Bokori-Brown et al., 2011). The formation of large complexes with the related pore forming bacterial toxins, *C. septicum*  $\alpha$ -toxin (Bokori-Brown et al., 2011), aerolysin (Wilmsen et al., 1992) and PS (Abe et al., 2008) has also been observed. A fully activated  $\epsilon$ -toxin is cleaved at both the N and C-termini. The recombinant constructs of the toxin possessing the C-terminal sequence have never been observed to form large complexes, unlike those missing this sequence (Miyata et

al., 2001; Bokori-Brown et al., 2011). The ability of the D-C and D-ND-C toxin derivatives to form a large complex has made it possible to ascertain the number of monomers present in the membrane complex. Heterogeneous mixtures of the two toxin molecules mixed at various molar ratios produce autoradiographs with six intermediary bands, indicating that the complex formed is a hexamer. This is consistent with that observed for the related toxin, aerolysin. The possible pore-forming ability of  $\epsilon$ -toxin has also been investigated via experiments using lipid bilayers.

Activated  $\epsilon$ -toxin added to bilayer membranes causes an increase in conductance across the membrane in a stepwise fashion after about two minutes. After about 30 minutes, the increase is of about three orders of magnitude (Petit et al., 2001; Bokori-Brown et al., 2011). This stepwise increase indicates not only the presence of pores within a membrane after the addition of  $\epsilon$ -toxin, but also that these pores are long-lived and do not have an association–dissociation equilibrium. These results have shown that pores can be formed in the absence of a membrane receptor. Although various lipids were used in these experiments, the toxin was not shown to have a lipid preference (Petit et al., 2001; Bokori-Brown et al., 2011). However, lipids with low melting points seem to favour membrane insertion under the same experimental conditions (Nagahama et al., 2006; Bokori-Brown et al., 2011). The toxin of this group had a 100-fold lower sensitivity to carboxyfluorescein-loaded liposomes compared to MDCK cells. This is not surprising, considering the absence of a receptor in the liposomes. The study also demonstrated the existence of heptameric assemblies formed in liposomes. However, the heptamers were not stable, as evidenced by the presence of intermediate species on an SDS-PAGE gel. *Epsilon* toxin appears to target the DRMs in membranes.

This is also the case for aerolysin (Bokori-Brown et al., 2011) and PS (Abe et al., 2008; Bokori-Brown et al., 2011). Both monomeric and heptameric  $\epsilon$ -toxin accumulate in the DRMs, while the depletion of cholesterol, a major constituent of DRMs, has an inhibitory effect on both the *Epsilon* toxin and PS (Miyata et al., 2001, Bokori-Brown et al., 2011). The  $\epsilon$ -prototoxin, unable to form heptamers, also binds mainly to the DRMs, indicating that heptamerisation is not a prerequisite for interactions with susceptible cells. Therefore, the putative receptor for both the  $\epsilon$ -prototoxin and  $\epsilon$ -toxin is thought to be present mainly in the DRMs. All steps, from binding to membrane insertion, are thought to occur in the DRMs. It has been shown that changes to the ganglioside content in the DRMs affects the binding of the *Epsilon* toxin (Bokori-Brown et

al., 2011). However, there is no direct evidence of toxin binding to the ganglioside, and the  $\epsilon$ -toxin shows high cell specificity. In contrast, the related toxin, aerolysin, can interact with many cell types via the GPI-anchored proteins. Additionally, the residues involved in the mannose six-phosphate binding in aerolysin are not conserved in  $\epsilon$ -toxin or PS. It has been shown that the PS requires a specific GPI-anchored protein receptor for efficient cytotoxic action and that this receptor is different from that of aerolysin, despite both being in the DRMs. Since the N-terminal domains of the  $\epsilon$ -toxin and PS are more similar to each other than they are to aerolysin, it may be that  $\epsilon$ -toxin acts in a similar manner. As  $\epsilon$ -toxin is capable of forming channels in lipid bilayers in the absence of a receptor, although with less efficiency (Bokori-Brown et al., 2011), it has been suggested that the receptors present in the DRMs act to concentrate the toxins, allowing heptamerisation.

The size of the pores formed by  $\epsilon$ -toxin has also been investigated. Petit et al. (2001) have suggested pore sizes in the 2-nm diameter range. However, toxicity associated with the polyethylene-glycol used to determine the pore size made the results slightly unreliable. A recent study using polyethylene-glycols of different molecular weights suggested that the pores formed by  $\epsilon$ -toxin are asymmetrical (Nestorovich et al., 2010). Here the pore size was estimated to be 0,4 nm on the side of toxin insertion and 1,0 nm on the opposite side. High-throughput screen methods identified some  $\epsilon$ -toxin inhibitors that appear to work by blocking the pores (Lewis et al., 2010) as they do not work by inhibiting cell-binding or oligomerisation and are effective in cells pre-treated with the toxin.

The likely mechanism of pore formation by  $\epsilon$ -toxin is predicted to be as follows. The prototoxin is secreted by the bacterium and activated, possibly locally, by *C. perfringens* k-protease or by host proteases, such as trypsin and/or chymotrypsin. Receptor binding may occur prior to or after activation. Once activated, heptamerisation occurs on the membrane, which may lead to the formation of a pre-pore complex. This has been observed in cholesterol-dependent cytolysins (Tilley et al., 2005; Bokori-Brown et al., 2011) and in *S. aureus*  $\alpha$ -toxin (Bokori-Brown et al., 2011). In fact, under certain conditions, heptamerisation of both the aerolysin (Tsitritin et al., 2002; Bokori-Brown et al., 2011) and *Epsilon* toxin (Pelish and McClain, 2009; Bokori-Brown et al., 2011) is possible without pore formation. The final step of pore formation might involve unfolding the amphipathic hairpin and inserting it into the membrane to form the walls of the pore composed of 14  $\beta$ -strands.

## 1.9 Pulpy Kidney Disease vaccine production and challenges

A number of commercially available vaccines exist for the prevention of *C. perfringens* enterotoxaemia and these have been used extensively over the past decades to prevent disease in domesticated livestock (Jemal et al., 2017). The vaccines are typically prepared by treating the *C. perfringens* type D culture filtrate with formaldehyde to toxoid components. Since relatively crude culture filtrates are used, the vaccines are likely to contain additional proteins other than the *Epsilon* toxoid. The typical immunisation regimens involve an initial course of two doses of vaccine, administered two to six weeks apart. Lambs can be immunised from the age of three months. Sheep require a boost annually, whereas goats are boosted every three to four months (Bokori-Brown et al., 2011; Bath et al., 2016). Adjuvants such as aluminium hydroxide are often used, which confer protection in animals if they induce antibody titres equivalent to five International Units (IU) of antitoxin. However, the immunogenicity of the *Epsilon* toxoid in some vaccine preparations has been reported to be poor or variable (Lobato et al., 2010; Bokori-Brown et al., 2011). Inflammatory responses following vaccination leading to reduced food consumption have also been reported (Stokka et al., 1994; Bokori-Brown et al., 2011).

Attempts to improve vaccine efficacy using a liposome formulation have reportedly not been successful (Uzal et al., 1997; Bokori-Brown et al., 2011). A method for the reliable production of  $\epsilon$ -toxoid vaccines remains one of the challenges facing the veterinary vaccine industry. One approach would involve using genetic engineering to produce the toxin and then use this recombinant protein for toxoiding. The expression of prototoxin or toxin in *Escherichia coli* has been reported (Lobato, 2010) with yields of 10 to 12 mg/l<sup>-1</sup> of culture (Chandran et al., 2010). Prototoxin requires trypsin activation (Lobato et al., 2010), but the recombinant expression of the toxin avoids this requirement (Chandran et al., 2010). After toxoiding with formaldehyde and formulation with an aluminium hydroxide adjuvant, a preparation is obtained that is reported to be immunogenic in rabbits, sheep, goats and cattle, and gives rise to > 5 IU of antitoxin after two doses (Lobato et al., 2010). This recombinant toxoid was reported to be a superior immunogen to the commercial vaccines available in Brazil (Lobato et

al., 2010). An alternative approach to the development of a toxoid vaccine would involve generating a gene encoding a non-toxic variant. This can then be expressed in *E. coli* or another easily cultured host.

An *Epsilon* toxin consists of three domains (Figure 1.4), which are dependent on two strands traversing the entire molecule (Cole et al., 2004). For this reason, the expression of the individual domains of  $\epsilon$ -toxin, which are likely to be non-toxic, is not straightforward. Site-directed mutants of the toxin have been produced, which show markedly reduced toxicity towards MDCK cells and these could be exploited as vaccines (Pelish and McClain, 2009). Although the evaluation of these mutants in mice has not been reported, the H106P variant protein H119P, following the numbering system for prototoxin without signal peptide, has been shown to be non-toxic to mice. The reason why the H106P protein is not toxic is not known. However, it may be relevant that chemical modification studies have previously shown that at least one histidine is essential for toxicity (Sakurai and Nagahama, 1987). It is also not clear which of the two histidine residues in  $\epsilon$ -toxin was chemically modified. It is possible that the mutation of histidine to proline at position 106 caused changes in the structure of the  $\epsilon$ -toxin. It is relevant that an antibody against a single epitope on the toxin has been shown to protect against *Epsilon* toxin (Percival et al., 1990).

There has been significant interest in the potential value of antibodies against  $\epsilon$ -toxin for the prevention of enterotoxaemia caused by  $\epsilon$ -toxin. The passive transfer of polyclonal antisera against the toxin into new-born lambs has reportedly been achieved either by injection (Odendaal et al., 1989) or by feeding the animals colostrum that contained antibodies reactive with *Epsilon* toxin (Clarkson et al., 1985). More recently, a number of workers have described the generation of monoclonal antibodies that are able to protect cultured cells (Bokori-Brown et al., 2011) and, in some cases, mice from intoxication. The finding that a single monoclonal antibody is able to provide good protection indicates that a single epitope is required for the induction of protection. In one study, the location of the epitope recognised by the protective monoclonal antibody has been mapped to amino acids 134 to 145 (peptide sequence SFANTNTNTNSK) and overlaps the putative membrane inserting loop (Bokori-Brown et al., 2011). It is not known whether other neutralising monoclonal antibodies recognise this loop. Any of these antibodies could have utility for the prevention or treatment of the disease.

An intriguing alternative to the use of antibodies is the use of dominant-negative inhibitors of toxicity. This approach involves generating variant forms of  $\epsilon$ -toxin that are inactive but are still able to oligomerise. In the work reported by Pelish and McClain (2009), variants were generated in which the putative membrane-insertion loop was locked into the folded conformation by the introduction of cysteines, which were then able to form disulphide bridges. Mixtures of the variant and wild-type toxin, in a ratio of at least 1:8, were non-toxic towards MDCK cells. Although these mixtures were able to form oligomers and bind to cells, they were unable to form heat-resistant and sodium dodecyl sulphate-resistant oligomers. It is conceivable that these variant forms of the toxin could be used to limit toxicity, but they may need to be given at the same time as exposure to the wild-type toxin, which would limit their therapeutic value.

The *Epsilon* toxin differs markedly from the other pore-forming toxins because of its remarkable potency and its specificity for certain cell types (Bokori-Brown et al., 2011). These properties may be linked and the ability of the toxin to be lethal in animals at low doses may be related to its ability to target neuronal cells. However, the precise molecular mechanism(s) by which the toxin causes death, and the mechanisms by which the toxin crosses the gut wall and is trafficked to target cells, are not known (Bokori-Brown et al., 2011). The specificity of the toxin is likely to reflect on its ability to bind to specific cell surface receptors, though the identity of these receptors is still not known (Bokori-Brown et al., 2011).

Some progress has been made in developing vaccines against  $\epsilon$ -toxin. The availability of the crystal structure of the toxin should now allow the protein to be rationally modified so that immunological identity is conserved but toxicity is abolished. Clearly, an understanding of the structure of the membrane-bound and multimeric forms of the toxin will further support work to devise vaccines. The development of other interventions to prevent or even reverse toxicity is likely to be dependent on a more detailed understanding of the molecular mechanisms of intoxication (Bokori-Brown et al., 2011). This study proposes to produce a less toxic *C. perfringens* Type D *Epsilon* toxoid subunit vaccine recombinantly in *N. benthamiana* as some proteins have already been efficiently expressed in variety of plants.

## **1.10 Plant-derived biopharmaceutical products**

Recombinant proteins have been expressed in plants for more than 20 years. Initially, most studies focused on the development of favourable agronomic traits such as insect resistance (Twyman et al., 2003) and disease control (Broglie et al., 1995; Holler, 2007). But within the past decade plants have emerged as a serious candidate for expressing valuable therapeutic-based recombinant proteins on a commercial scale, vying for a share of the multi-billion dollar biotechnology industry. Several plant-derived diagnostic and research proteins have already reached the market (Hood et al., 1997; Takeyama et al., 2015) and numerous other plant-derived biopharmaceuticals are in various stages of clinical trials (Witcher, 1998; Menkhaus et al., 2004). Antibodies, vaccines, growth regulators, human serum proteins and hormones have all been efficiently expressed in a variety of plants (Yao et al., 2015; Takeyama et al., 2015). Crops such as cereals (maize, rice), legumes (soybean, pea), fruits and vegetables (potato, tomato, banana) and leafy plants (tobacco, alfalfa, lettuce) have all been among the target hosts for recombinant protein production.

Each type of a plant has its own unique set of advantages and disadvantages when it comes to the production of recombinant proteins (Menkhaus et al., 2004). In general, plants may be comparable with or even advantageous to traditional systems, such as bacterial or mammalian cell cultures or transgenic animals for producing recombinant therapeutic proteins. Plant systems may prove to be safer, more economical and more convenient than the traditional systems (Holler, 2007; Claire et al., 2011). Plants do not harbour human pathogens and the threat of transmissible disease is therefore effectively eliminated. Furthermore, production of heterologous proteins in transgenic animals or mammalian cells raises safety and ethical concerns (Fischer et al., 1999; Claire et al., 2011). Whereas microbial systems cannot produce accurate post-translational modifications of eukaryotic proteins, plants do have the ability to produce functional proteins of eukaryotic origin, including human proteins (Holler, 2007; Claire et al., 2011).

Production of recombinant proteins in traditional systems is still expensive and difficult to scale up. However, the framework for cultivating, harvesting and processing large amounts of plant material is already established and well understood, which will help lower production costs (Holler, 2007). Several studies have been undertaken to assess the cost to produce recombinant

proteins from plants compared to traditional expression systems. It is estimated that the production of recombinant proteins in plants may be two to 10% of the cost for the same protein production in microbial systems such as *E. coli* fermentation, and 0,1% of the cost of mammalian cell cultures, depending on the type of plant and expression level (Holler, 2007). While plants have many advantages for recombinant protein production, there are also limitations and concerns. Many of these concerns are associated with safety when producing biopharmaceuticals in plants. Contamination of a food supply, or the release of recombinant protein products into the environment is a serious threat that must be closely regulated (Twyman et al., 2003). Furthermore, even though the protein synthesis pathways are largely conserved between plants and animals, some proteins may not be correctly processed (Holler, 2007). Some leafy plant species, like alfalfa, can produce homogeneous glycan chains for glycoproteins, whereas tobacco produces heterogeneous glycan structures (Fischer et al., 1999; Holler, 2007).

Improper post-translational modifications of biopharmaceuticals can lead to immunogenic or toxic effects in humans (Menkhaus et al., 2004). Therefore, the expression and production of recombinant biopharmaceutical proteins in plants must be closely monitored by safety and other regulatory standards, the number of which is growing rapidly (Menkhaus et al., 2004;). Another challenge for the recombinant protein production in plants is low protein expression and accumulation, largely because of poor protein stability. Expression levels and stability will ultimately dictate whether it is economically feasible to use a particular plant species for the production of a recombinant protein. A final hurdle, and one of the most difficult to overcome, is the downstream processing (protein extraction and purification) needed to obtain large quantities of a very pure protein. It is estimated that downstream processing may account for over 80% of the total cost associated with recombinant protein production in plants when a highly pure protein is needed (Twyman, et al., 2003). To circumvent this difficulty, great efforts have been devoted to the production of edible vaccines in corn, tomato, potato, banana and other food crops (Holler, 2007). Delivering the target protein orally avoids expensive downstream processing. However, this is not possible in the case of many recombinant proteins or for some plant species, such as tobacco.

Finally, there is a significant lack of published information with regard to the general purification processes that may have potential for commercial-scale application and do not rely

on affinity steps. For these reasons, new and improved downstream processes must be investigated for the purification of recombinant proteins expressed in plant systems such as tobacco and other non-edible plants (Holler, 2007).

### **1.11 Tobacco as an expression host**

The production and use of tobacco (*Nicotiana tabacum*), a major crop of the south-eastern United States, is on the decline because of the negative health issues associated with tobacco use, as well as increasing federal regulations (Holler, 2007). For these reasons, alternative uses for this crop are being explored. Tobacco has long been used as a model system for the production of recombinant proteins and shows promise as a host for large-scale protein production (Holler, 2007). Transformation procedures for the expression of foreign proteins in tobacco are well developed and accomplished by methods such as *A. tumefaciens* mediated DNA-transfer and plant viral vectors such as tobacco mosaic virus (TMV). Tobacco is considered a relatively safe crop for recombinant protein production. Like all other plants, tobacco does not harbour human pathogens, effectively eliminating the threat of transmissible diseases. It is also a non-food and non-feed crop, minimising the threat of contamination of a food or feed supply (Twyman et al., 2003). Recombinant protein expression in tobacco is usually directed to the leaf tissue, which translates to an abundance of transgenic biomass when plant production is increased. Farming practices for tobacco production are already well established and tobacco can be harvested several times a year (Holler, 2007). Finally, recent advancements have allowed for the targeted protein expression to the chloroplast, resulting in higher protein yields and stability (Holler, 2007).

Numerous valuable recombinant therapeutic proteins have already been expressed in tobacco (Table 2.1) and many are undergoing clinical trials. However, none have been approved by the US Food and Drug Administration (Holler, 2007). Two biotechnology companies that are actively pursuing tobacco as a host system are Planet Biotechnology and Meristem Therapeutics. In 2004 these were the only two companies to have plant-derived pharmaceuticals in phase-II clinical trials (Holler, 2007). While the expression of recombinant proteins in tobacco is well-studied, there are still many obstacles to overcome before tobacco can be used for the large-scale production of therapeutic proteins. Protein expression in many crops, such as corn and canola, is often targeted to the seed, which minimises interaction with

native plant components and also serves as a stable storage and transportation vessel (Holler, 2007). However, tobacco seeds are extremely small and would not be economical for the expression and production of recombinant proteins on a large scale.

For this reason, protein expression in tobacco is targeted to the leaves, which also enables the production of large amounts of biomass that can be easily scaled up (Holler, 2007). Unfortunately, expressing recombinant proteins in vegetative tissue creates challenging issues when it comes to the recovery and purification of the target protein. Tobacco leaves contain up to 30 mg/g dry weight of native phenolic compounds, which is an extremely high amount, as well as toxic alkaloids such as nicotine, that must be removed during the purification process (Holler, 2007). When the leaf material is processed by grinding or shearing, these compounds are released and can interfere with the downstream processing. This may include the formation of complexes with proteins in the aqueous extract (Twyman et al., 2003) or fouling the resin used during the adsorption processes, such as those used in chromatography (Holler, 2007). However, there are now some low-alkaloid cultivars that may be used for biopharmaceutical production (Twyman et al., 2003).

Watery leaf tissue will also contain higher levels of proteolytic and microbial activity relative to seed tissue, making the environment much less stable during the initial harvest and extraction of the target protein (Holler, 2007). Because of these components, fresh leaves should be processed immediately. However, drying, freeze-drying or freezing of the leaves immediately after harvest may provide extended storage for some proteins (Twyman et al., 2003).

### **1.12 *Agrobacterium*-mediated delivery**

*Agrobacterium* is a soil-borne bacterium that, in the presence of a wounded plant, moves toward it, attaches itself to the wound site and proceeds to transform the cell (Mokoena, 2010). The sugars and phenolic compounds exuded by the wounded plant not only signal the pathogenic opportunity to the bacterium, but also induce transcription of the virulence genes. These genes are located on a specific plasmid known as the tumour-inducing (Ti) plasmid, which also contains the transferred DNA (T-DNA). Virulence proteins have roles ranging from the transcriptional activation to T-DNA processing and export, with certain proteins also having a function in the host. One of the major contributions of research into *Agrobacterium*

to the field of plant research has been the use of T-DNA as a mutagen. To date, it has not been possible to target T-DNA to any particular locus in the genome with any great efficiency. This has the advantage that, in a DNA library, there is a high likelihood that there are T-DNA insertion in every open reading frame.

### **1.13 Downstream processing**

A major burden in the downstream processing of recombinant proteins from plants is the recovery and stability of the target protein in a plant extract (Wilken et al., 2012). For tobacco, the leaves are usually ground up or sheared and the proteins are released, or extracted, into an aqueous buffer. Equipment for tissue disruption includes blenders, ball-bead mills and homogenisers (Wilken et al., 2012). Factors such as pH, salt concentration and the temperature of the extraction buffer will affect the amount of protein extracted and protein stability. Steps should also be taken to minimise the effects of phenolics, protein oxidation and proteases during the extraction process. Free phenolics may bind to proteins in a solution and oxidative ‘tanning’ of proteins can cause the structural modification of proteins, both of which often result in the loss of activity or degradation. The addition of antioxidants (ascorbic acid), reducing agents (2-mercaptoethanol (BME); dithiothreitol (DTT) and phenolic-binding agents (polyvinylpolypyrrolidone, PVPP) to the extraction buffer may alleviate some of these interferences (Holler, 2007). To reduce the effects of proteases, the extraction buffer should always be kept ice cold during the extraction process and protease inhibitors (phenylmethylsulphonyl fluoride, PMSF) may be added to the extraction buffer.

Other additives, such as detergents (Triton X-100, *N*-lauroylsarcosine) may be necessary to solubilise membrane proteins. Chelating agents (ethylenediaminetetraacetic acid, EDTA) may be included to reduce the effects of divalent cations such as  $Mn^{2+}$ ,  $Co^{2+}$ ,  $Cu^{2+}$  and  $Zn^{2+}$ , which can inhibit a proteins’ biological activity (Wilken et al., 2012). It is recommended that a minimalist extraction buffer be selected as most additives will have marginal improvements on recoveries but will increase processing costs significantly (Holler, 2007). While the methods described above generally refer to the protein fractionation/recovery stage, the protein purification stage will usually include steps such as precipitation, filtration and column chromatography, among others. The physical characteristics of proteins can be used to select the appropriate separation step needed to recover a target protein. Size (molecular mass), shape (monomer, polymer), surface hydrophobicity and net charge are common protein

characteristics exploited for separation steps. The overall charge of a protein depends on the isoelectric point (pI) of a protein; this is the pH where the protein will have a net charge of zero. At a system pH above the isoelectric point, the protein is negatively charged and at a pH below the isoelectric point, the protein is positively charged. The system pH can be adjusted to change the overall net charge of protein. However, most proteins have a small, defined pH range in which they will remain biologically active. For plants expressing edible vaccines, extensive purification processes are not needed. However, this is not the case with tobacco (Holler, 2007).

Many recombinant proteins, especially biopharmaceuticals, must be purified to a highly purity (95% to 98% or greater) for safe use in clinical trials and for possible product formulation (Holler, 2007). As downstream processing dictates the major cost for protein production, it is necessary to develop economical and scalable initial purification steps to remove large amounts of impurities before more costly steps such as chromatography are used (Menkhaus et al., 2004). Generally, the components in a tobacco extract make it impractical to apply a crude extract directly onto a column because of resin fouling and column plugging over repeated use (Holler, 2007). It is also better to minimise the total number of purification steps used in an overall process as protein recovery generally decreases with the increased number of steps.

### **1.14 The development of expression vectors**

To increase protein yield, second generation *Agrobacterium* binary vectors have incorporated various elements to enhance transcription and translation. These improved vectors, used in conjunction with transient infiltration, have improved protein expression levels in plants. For instance, the transient expression of a human optimised HPV-16 L1 capsid protein gene using a specialised binary pTRA vector resulted in a yield of more than 0,5 g/kg of fresh leaf weight (17% total soluble protein) (Maclean et al., 2007). Significantly lower levels were obtained when the same protein was transgenically produced in tobacco and potato, resulting in the L1 protein accumulating to 0,5% and 0,2% of the total soluble protein respectively (Biemelt et al., 2003).

Further developments in vector systems have seen the merging of viral and binary vector technology to increase yields and address insert size restrictions, the retention of target genes

and containment issues. Icon Genetics GmbH (Halle, Germany) developed a deconstructed viral vector system initially based on TMV, in which target genes and different viral vector components are carried on several pro-module vectors (Marillonnet et al., 2004). In this system the viral coat protein has been removed to eliminate systemic spread. Instead, agro-infiltration provides the delivery of the modules to the plant cell and limits replication to the infiltrated area. In the cell, high-level expression is facilitated by an RNA- dependent RNA-polymerase. A site-specific recombinase facilitates the assembly of the modules into a DNA molecule that is transcribed and spliced into a functional transcript. The transcript moves to the cytosol where it is translated into the specified protein. Alternatively, target signals can be incorporated to direct proteins to specified subcellular compartments (Marillonnet et al., 2004). This system has been used to accumulate various proteins at over 4 g/kg plant-material levels (Bendandi et al., 2010).

One shortcoming of the initial Icon-system vectors was the inability to co-express more than one protein in the same spatial location (Giritch et al., 2006). This was problem as regards the production of multi-component proteins, such as immunoglobulins. A solution to this was the co-expression from two non-competing monopartite viral genomes such as TMV and PVX (Giritch et al., 2006). Alternatively, viral vectors derived from bi or tri-partite viral RNA genomes that do not seem to be competing and are able to co-function in the same area. The cowpea mosaic virus (CPMV) is a bipartite viral RNA genome from which two types of vector systems were developed. In the full-length system (wild type) the coding sequence for the protein of interest is fused to the C-terminus of the RNA-2 polypeptide that is co-translationally released via 2A-peptide mediated cleavage (Sainsbury and Lomonosoff, 2008). Replication is facilitated by the co-expression of RNA-1. The full-length version allows for local co-expression of two different proteins. However, segregation of the co-expressed proteins occurs with systemic movement (Sainsbury et al., 2008). A deleted CPMV version of RNA-1 (hypertranslatable, HT) was developed but lacked the property of systemic spread and was thus able to co-express more than one protein without the occurrence of segregation. Moreover, the deleted CPMV system obtained higher expression levels than the full-length version (Sainsbury et al., 2010).

Using this system, protein expression levels exceeded 0,3 g/kg protein (Sainsbury and Lomonosoff, 2008). Several pharmaceutically important molecules have been expressed in

plants using vectors based on the ssDNA geminivirus bean yellow dwarf virus (BeYDV) (Huang et al., 2010) have independently developed vector systems based on the DNA genome of the virus. The BeYDV system requires only two viral components for co-expressing heteromeric proteins. These are the long intergenic region (LIR) and the short intergenic region (SIR) control sequences, and the single, alternatively spliced gene for the replication-associated proteins Rep/RepA. In the system, non-competing co-expression can be achieved either from two replicons encoding different proteins or from a single replicon containing different proteins. In *N. benthamiana*, transient expression levels from the BeYDV vector were three to seven-fold more than for EGFP and HIV-1 p24 compared to levels obtained using a binary pTRA *A. tumefaciens* vector. Furthermore, expression with the BeYDV resulted in accumulation levels of 0,5 g/kg monoclonal antibody against Ebola virus GP1 (mAb 6D8) (Huang et al., 2010). It is anticipated that the system will be able to simultaneously produce as many as four different protein subunits. Several other geminiviruses and also the multicomponent ssDNA nanoviruses have been investigated for their potential as expression vectors. Their further development could greatly expand the range of plant species that can be used for the transient production of recombinant proteins (Rybicki and Martin, 2014).

### **1.15 Hypothesis**

This study aims to explore plant based-transient expression of *Epsilon* toxin *Clostridium*-type D *perfringens* antigen to demonstrate the feasibility and efficacy to produce a relevant developing-world Pulpy Kidney Disease Vaccine. I postulate that the EtxD protein could be transiently expressed efficiently in *Nicotiana benthamiana* plants via an Icon deconstructed vector, targeting the EtxD protein expression into the plant cell compartments - the apoplast or the cytosol.

## **Chapter 2**

# **TRANSIENT EXPRESSION OF *EPSILON* TOXIN IN *NICOTIANA BENTHAMIANA* LEAVES**

## ABSTRACT

*Clostridium perfringens* type D causes enterotoxaemia (commonly known as Pulpy Kidney Disease) in sheep and goats, causing mortality and heavy economic losses worldwide (for review, see Titball, 2009; Uzal et al., 2016). The disease has a mortality rate of between 10 and 30% in a non-vaccinated population. Because of the rapid progression of the disease after onset, the administration of antibiotics is of little value and prevention through vaccination is the only viable option. In South Africa, the vaccines currently available are based on formaldehyde-treated, whole-cell cultures in different formulations, which provide a good degree of protection in animals. However, the immunogenicity of the preparations is variable from batch to batch and vaccine breakdown can occur from time to time, which is a matter of concern. The *Epsilon* toxin produced by the organism is the major antigenic determinant and has been directly implicated in causing the disease.

This chapter reports on the expression feasibility and biochemical characterisation of a recombinant *Epsilon* toxin (EtxD) produced as soluble protein in *Nicotiana benthamiana* leaves. To achieve this, bioinformatics tools from NCBI and EMBL, and public databases were used to facilitate the design and construction of an appropriate formulation for the adoption of a plant-based transient expression approach in *N. benthamiana* leaves. The EtxD protein expression was analysed and measured at three, six and nine days post-infiltration by the Bradford assay, SDS-PAGE, Western Blot analysis and ELISA. The analysis results of the infiltrated tobacco leaf samples demonstrated the successful expression of a 34 kDa EtxD protein together with another tobacco specific band of about 25 kDa, which was analysed by mass spectrometry.

## 2 INTRODUCTION

### 2.1 Pulpy Kidney Disease

According to McClane et al. (2007), the *Epsilon* toxin (Etx) produced by *Clostridium perfringens* type B and D is responsible for a fatal *enterotoxemia* in economically vital livestock. *Enterotoxemia*, also known as Pulpy Kidney Disease, usually occurs in four-to-six-year-old lambs. However, they may be affected from as young as a few weeks and the disease can in some instances also occur in older sheep. The disease is caused by an anaerobic bacterium (*C. perfringens* type D) that commonly occurs in the intestinal tract. The organism forms resistant spores that persist in the soil. The *Epsilon* toxin is produced as an inactive protoxin. It becomes activated when trypsin removes a 13-amino acid residue at the N-terminal end of the polypeptide and 29 carboxy-terminal amino acids (Bokori-Brown et al., 2011). The toxin is known to increase intestinal permeability and can also cause liver damage, elevate blood pressure and cause an increase in vascular permeability. This can lead to vascular damage and oedema in many organs, including the brain, heart, lungs and kidneys. The mode of action of the *Epsilon* toxin is presently unknown, but recent work has indicated that the toxin remains on the outside of the cell, causing an efflux of intracellular  $K^+$ . This damages the cell membrane and eventually leads to cell death (Chandrand et al., 2010).

The disease is precipitated when sheep are fed a rich ration, such as green pastures, or if the diet is changed abruptly. The protein-rich material stimulates the organisms in the intestines to multiply rapidly and to produce lethal toxins. The *Staphylococcus aureus*  $\alpha$  toxin increases the permeability of the intestinal wall and it is consequently readily absorbed into the body (Goldstein et al., 2009; Fennessey et al., 2012). It is primarily a neurotoxin causing sudden death in sheep; symptoms are rarely observed. Farmers usually encounter a number of dead sheep in the field early in the morning (Titball, 2009; Uzal et al., 2016). During the early stages of the disease, animals lag behind the flock, have an unsteady gait and sometimes have diarrhoea. They gnash their teeth, fall over and die after lying prostrate for a short while (Titball, 2009). Frequently, a kicking movement can also be observed in cattle and sheep. Goats infected with *C. perfringens* type D often get diarrhoea (Titball, 2009; Uzal et al., 2016). Mortality is very high among lambs but is generally less severe in calves and goats, in which it causes a non-fatal sub-acute disease (Goldstein et al., 2009).

### ***2.1.1 Current production of and formulation methods for the Pulpy Kidney Disease vaccine***

The only practical means of controlling Pulpy Kidney Disease is by immunisation and avoiding conditions that are conducive to the occurrence of the disease. All currently available vaccines in South Africa are based on the formalinised toxoid of *C. perfringens* (Welchii) type D, either as an alum-precipitated or oil emulsion formulations of whole-cell culture or bacterial culture filtrates (Deepika, 2010; Jemal et al., 2016). Onderstepoort Biological Products (OBP) has been supplying formalinised vaccine formulations for 14 years. The *Epsilon* toxin is usually obtained from a *C. perfringens* type-D strain and has been purified either individually or in combination by methanol precipitation, ammonium sulphate precipitation, column chromatography, size exclusion and other forms of ion exchange chromatography.

Formalinised vaccines have several drawbacks. First, it is generally accepted that chemical inactivation with formalin is difficult to standardise. Second, classical methods of detoxification usually alter the overall protein structure in a random manner. Consequently, the immunogenicity of the vaccine is severely decreased. Third, there is a fine line between balancing the detoxification (the strength of formalin commonly used is 1% and the immunogenicity of the vaccine (Robertson et al., 2011). Because of these challenges, alternatives to formalin inactivation have been proposed, including ectopically expressing mutated toxoids in other gram-positive microorganisms. Plants provide a genuine alternative for expressing an immunogenic but non-toxic vaccine for the Pulpy Kidney Disease. The *C. perfringens Epsilon* type-D genes are available in the public domain, while patents that describe invention and methods for using the *C. perfringens Epsilon* type-D vaccine to protect animals against *Clostridial* diseases are also available (WO/1997/034001; US20060233825, among others). No patent cover South Africa and the Council for Scientific and Industrial Research (CSIR) in collaboration with OBP thus have freedom to operate.

### ***2.1.2 Veterinary medicine***

According to Floss et al. (2007), in veterinary medicine vaccinology addresses a wider spectrum of challenges. These include the development of cost-effective approaches to prevent and control infectious animal diseases with consideration for animal welfare and a focus on

decreasing the production costs of animals used as food. Furthermore, mass vaccination programmes have assisted to significantly lower the consumption of veterinary drugs, including antibiotics. Vaccines have also led to a reduced negative environmental impact by eliminating chemical residues in products such as milk, eggs and meat. Production losses caused by infection can be avoided. The development and improvement of vaccines are suitable ways to combat infectious disease in domestic animals. Current strategies use intact or inactivated pathogen strains to induce immunity and subunit vaccines that are commercially produced in bacteria, yeast or mammalian cell cultures.

### ***2.1.3 Plant-based for veterinary vaccines***

The main objectives of veterinary vaccines are to improve the health and welfare of companion animals; increase the production of livestock in a cost-effective manner, and prevent animal-to-human transmission from both domestic animals and wildlife (Sharma et al., 2012). These diverse aims have led to different approaches as regards the development of veterinary vaccines, including crude but effective whole-pathogen preparations to molecularly defined subunit vaccines, genetically engineered organisms or chimeras, vectored antigen formulations and naked DNA injections (Ling et al., 2014). The advantages of using plants as expression systems are well documented with several plant-expressed reagents already on the market.

The world's first regulatory opportunity for a plant-made vaccine for veterinary purposes occurred in early 2006. This was the Newcastle disease virus vaccine. It marked the potential transition of plant-made vaccine research into plant-made vaccine development (Claire *et al.*, 2011). The licensure of the Newcastle disease virus vaccine for chickens demonstrated that plant-made veterinary product technology had technical and industrial feasibility for application with animals (Claire et al., 2011; Ling et al., 2014;). Antigens from several veterinary pathogens have since been expressed in transgenic plants, including the rabies, Norwalk virus, anthrax, infectious disease virus, avian reovirus and avian influenza virus, and Hodgkin's lymphoma. The plant-made veterinary product can be easily stored and transported under limited refrigeration without degradation.

#### ***2.1.4 Advantages and challenges of plant-made veterinary products in South Africa***

There are several advantages to using plant-made vaccine antigens. These include –

1. proper protein folding when expressing other eukaryotic proteins;
2. a raw material cost that is relatively low;
3. a process that is highly scalable;
4. the ability to produce large amounts at relatively low cost; and
5. the possibility of producing multiple vaccines together.

However, the poor expression levels in transgenic plants and the complex regulatory problems surrounding plant-produced vaccines are major challenges. In addition, according to Rybicki and Martin (2014), the development of plant-based recombinant molecule expression technologies faces a number of hurdles in South Africa that range from a lack of financial support and manufacturing infrastructure to an uncertain regulatory and entrepreneurial environment for the commercial development of novel plant-made products. Most of these problems result from the fact that, while South Africa has a well-developed economy, it is still seen as a developing country with accompanying policy directions. Such a country tends to import rather than develop home-grown technologies.

#### ***2.1.5 Plant factories***

The need to find alternative methods to complement microbial and mammalian systems in the production of high-value products such as drugs, enzymes and antibodies has recently given birth to the concept of plant-made pharmaceuticals. The use of expression technologies has given momentum in the last five years to the development of products for human use, especially biosimilars (Rybicki, 2009) but also erythropoietin, insulin, interferon-beta, G-CSFs and others, in descending order (Claire et al., 2011). Plant-made expression systems for pharmaceuticals and vaccines for human use have received the most attention, but veterinary products could potentially receive the next biggest input owing to the less stringent regulatory burden that applies in this field (Penney et al., 2011). Table 2.1 shows some of the plant-made veterinary products that have been studied.

**Table 2.1: Plant-based vaccines for veterinary use**

Host	Pathogen	Antigen	Plant	Administration route	Treated animal	Reference
Chicken	Newcastle disease	Hemagglutinin neuraminidase	Tobacco suspension cells	Subcutaneous	Chicken	Vermijet et al. (2006). Approved by USDA
Chicken	Newcastle disease	F-protein	Maize	Oral	Chicken	Guerrero-Andrade et al. (2006)
Chicken	Newcastle disease	SI glycoprotein	Rice	Oral	Mice	Yang et al. (2007)
Chicken	IBVD	Fimbriae (F4)	Potato	Oral	Chicken	Zhou et al. (2004)
Pig	ETEC	Fimbriae	Tobacco (chloroplast)	N/D	Pig ( <i>in vitro</i> assay in intestines)	Wu et al. (2007)
Pig	ETEC	Cholera toxins B subunit	Alfalfa	Oral	Piglet	Kolotilin et al. (2012)
Pig	ETEC	Fimbriae (F4)	Rice	Oral	Pig	Joensuu et al. (2006)
Pig	ETEC	VPI	Barley	Subcutaneous	Mice	Takeyama et al. (2015)
Pig	Foot and mouth disease virus	<i>N. benthamiana</i>	<i>N. benthamiana</i>	Intramuscular	Pig	Joensuu et al. (2006)
Pig	TGEN	S protein	Tobacco	Intramuscular	Pig	Yang et al. (2007)
Cattle	Bovine Herpes virus	gD protein	Tobacco	Intramuscular and subcutaneous	Cattle	Tuboly et al. (2000)
Cattle	Bovine Viral Diarrhea	E2 protein	Alfalfa	Intramuscular	Cattle	Peréz Aguirreburualde et al. (2013)
Cattle	Rinderpest virus	Hemagglutinin	Peanuts	Oral	Cattle	Khandelwal et al. (2003)

Takeyama et al., 2015; IBVD: Infectious bursal disease virus; ETEC: Enterotoxigenic *Escherichia coli*; VPI: polyomavirus; TGEV: transmissible gastroenteritis

The view that plants are a major part of the future of biopharmaceutical production is supported by major investments in this technology by the South Africa government through its Technology Innovation Agency (Rybicki and Martin, 2011). The objective is to encourage and provide support for initiatives aimed at making high-value recombinant molecules in plants, including enzymes and other proteins for use as reagents, diagnostics and potential vaccines. According to Rybicki and Martin (2014), the main players in the field of plant expression are the University of Cape Town (UCT) and the CSIR, with the UCT leading in research outputs

such as publications and patents. Other institutions with potential in this field include the universities of Pretoria and Stellenbosch.

Different expression hosts, including crop plants such as *Nicotiana tabacum* (tobacco) and other *Nicotiana sp.*, alfalfa, rice, wheat, potato and soybeans, amongst others, are being considered (Takemaya et al., 2015). The expression systems include transient viral vector expressions and *Agrobacterium tumefaciens*-mediated transient expressions. The generation of stable transgenic plants or cultured plant cells expressing the protein are also of interest. The majority of plant-produced recombinant proteins have been obtained from transgenic plants, in many cases transplastomic plants (Takemaya et al., 2015). However, transient expression, including the deconstructed cucumber mosaic virus (CMV) and tobacco mosaic virus (TMV), appear to be the most viable alternative. Plant-made products have a short production cycle coupled with codon optimisation, suitable promoters and the help of silencing suppressors such as plant virus-derived p19 and NSs. This means that they can be scaled up to produce high protein yields in a very short time (Chakauya et al., 2006).

### ***2.1.6 Agroinfiltrated viral vectors***

Magniffection is a development of significant importance in recombinant protein production as it couples agroinfiltration with the delivery of cDNA encoding a deconstructed TMV-based vector (Gleba et al., 2005). In modular viral systems, viral components are split and inserted into *Agrobacterium* for co-inoculation; this reduces replicon size and increases vector stability. This modular system allows for other viral components to be retained and assembled in trans (Gleba et al., 2007). Magniffection was developed by Icon Genetics as MagnICON<sup>®</sup> viral vectors that are delivered into tobacco as pro-vectors via *Agrobacterium* and assemble in trans for transgene expression. These vectors are limited to tobacco as a host since they are based on a TMV virus. Alternatively, the host range is being addressed by using other plant viruses such as the turnip vein-clearing potyvirus and the PVX vectors, geminiviruses and nanoviruses. Other improvements include the use of a silencing suppressor protein, p19, and an effective in-plant activation technology (INPACT) that is an inducible system that allows amplified replicon-based transgenic expression. The inducible system is particularly useful for the expression of toxic molecules. MagnICON<sup>®</sup> viral vectors have been used to produce personalised single patient vaccines for non-Hodgkin lymphoma patients from 5 kg of *N.*

*benthamiana*, rescuing the novelty of personalised drug-care and the use of plant production systems in addressing the demand for functional recombinant proteins in most industries (Rybicki, 2010). In this study, MagnICON® viral vectors were used for the expression of recombinant codon optimised *C. perfringens* type-D vaccine candidate in the leaves of *N. benthamiana* via an agroinfiltration by vacuum infiltration. The aim of this section of the study was to investigate the feasibility of transiently expressing the plant-codon optimised *EtxD* gene in *N. benthamiana* leaves and biochemically characterising the recombinant protein.

## **2.2 Materials and method**

### ***2.2.1 Strains, chemical and non-chemical reagents***

All reagents used in the study were of analytical grade and were obtained from Sigma-Aldrich (South Africa) unless otherwise stated. Restriction digestion enzymes were obtained from Inqaba Biotech (Fermentas, Pretoria). Polyvinylidene difluoride (PVDF) membrane was obtained from Amersham Pharmacia Biotechnology (Johannesburg). A chemically synthesised, codon optimised *EtxD* gene for *Nicotiana sp.* was commercially produced by Geneart GmbH (Regensburg, Germany). The *E. coli* DH10B strain (Table 2.2) was used as the general host for cloning and plasmid propagation, while the *A. tumefaciens* cells were transformed with the expression vector modules and then infiltrated into the *N. benthamiana* leaves.

**Table 2.2: *E. coli* and *A. tumefaciens* strains**

<b>Bacterial strain</b>	<b>Description or genotype</b>
<i>Escherichia coli</i>	
DH10B	F <sup>-</sup> endA1 recA1 galE15 galK16 nupG rpsL ΔlacX74 Φ80lacZΔM15 araD139 Δ (ara,leu)7697 mcrA Δ (mrr-hsdRMS- mcrBC) λ <sup>-</sup>
<i>A. tumefaciens</i>	
GV3101::pMP90RK	MP90 (pTiC58ΔT-DNA) (Koncz and Schell, 1986)

### **2.2.2 Standards and kits**

Plasmid DNA was prepared from *E. coli* by using Zymogen Zypp Plasmid Miniprep kit as described by the manufacturer Zymogen (California, USA). T4 DNA ligase and DNA molecular markers were supplied by New England Biolabs (Hitchin, UK).

### **2.2.3 Nucleic acid manipulation**

Unless stated otherwise, all nucleic acid manipulations and cloning were as described by Sambrook and Russell (2000). These include restriction enzyme digestion and ligations.

### **2.2.4 Gene analytical work**

BLAST (Altschul et al., 1997) and ClustalX (Thompson et al., 1997) were used to identify and align proteins homologous to the EtxD protein toxin of *C. perfringens* type D. The homology between the sequences was investigated to view the differences among the EtxD protein strains that are found in other countries, paying particular attention to the structure. All gene and protein sequences of the *Epsilon* toxin from *C. perfringens* type D were obtained from the National Centre for Biotechnology Information (NCBI) data base (<http://www.ncbi.nlm.nih.gov>).

### **2.2.5 Phylogenetic relationship**

The amino acid sequence of the *Epsilon* toxin from *C. perfringens* type D (Accession number: AY858558 from China, because it was well reported in the literature) was retrieved from the NCBI data-base and was used to search for similar sequences using BLASTp2.2.21 (Altschul et al., 1997). Based on the protein sequences found, further searches were performed. Subsequently, these sequences were aligned to a sequenced South African isolate and sequence differences were investigated. The *Epsilon* sequence data of the South African isolate was obtained using a commercial company, Inqaba Biotech.

The protein sequences found in the NCBI database were aligned using ClustalX, implemented with MEGA 4 software (Tamura et al., 2007). The same program was used to infer the phylogenetic relationship between these sequences by neighbour-joining analyses (Saitou and Nei, 1987) based on the p-distance method. Statistical analysis for the nodes was determined using the 1 000 bootstrap replicates (Felsenstein, 1985).

### **2.2.6 Codon optimisation of the truncated EtxD**

The codon optimisation of the EtxD was undertaken as presented by GeneArt. Negative *cis*-acting sites (such as splice sites, poly (A) signals, TATA-boxes, etc.) that may negatively influence expression were eliminated wherever possible. The 44% GC content was adjusted to prolong mRNA half-life. Codon usage was adapted to the bias of *N. tabacum*, resulting in a codon adaptation index (CAI)\* value of 0,84, so that it would allow high expression. The optimised gene should therefore allow high and stable expression rates in *N. tabacum*.

### **2.2.7 Design and cloning of EtxD gene into the MagnICON vectors**

For this study, one expression vector system was tested to drive the transient expression of the *EtxD* gene in *N. benthamiana*. The Icon deconstructed viral vector system governs the

\* CAI: This parameter describes how well the codons match the codon usage preference of the target organism.

following: *EtxD* expression under the control of the Nos promoter and the *EtxD* targeted to the cytosol or apoplast. Combinations of different modules are recombined to give gene expression: the PhiC31 integrase module pICH14011, 3' module-cloning vector pICH11599 with the *Etx* ORF cloned into the multiple cloning site, and 5' module pICH17388 (apoplast protein targeting) and pICH17620 (cytosolic protein targeting). The modules are co-expressed and assembled in planta to express the protein (Figure 2.1).

The truncated form of the published *EtxD* gene sequence (GenBank: AY858558) was used in this study, but excluded the first 32 amino acids of the toxin to produce the toxoid only. The gene was codon-optimised for *Nicotiana sp.* expression and synthesised by GeneArt with *Nco*I at the 5' end and *Bam*HI at the 3' end (see Appendix 1 for the plasmid maps). These restriction sites were used for cloning into the MagIcon vector pICH11599 to generate the plasmid construct pICH11599-*EtxD* (Figure 2.1). The other plasmid construct (pMA-*EtxD*-1031994) containing the *EtxD* gene was purchased at GeneArt. It had *Kpn*I, *Eco*RI and *Hind* III restriction sites at the 5' end and *Xho*I, *Bam*HI and *Pst*I sites at the 3' end. The *EtxD* gene was digested with *Nco*I and *Bam*HI restriction enzymes, and after agarose electrophoresis the DNA fragment was purified with QIAamp DNA mini-kit (QIAGEN, SA), according to the manufacturer's instructions. The vector pICH11599 was also digested with *Nco*I and *Bam*HI restriction enzymes. Subsequently, the cut pICH11599 vector with the purified *EtxD* insert was carried out in a reaction mixture (25 µl) containing insert (*EtxD* gene), cut pICH11599 vector, 1 µl of ligase (Fermentas, SA) and 2,5 µl of ligase buffer. The reaction was incubated at 16 °C for 16 hours to facilitate ligation into the pICH11599 vector.

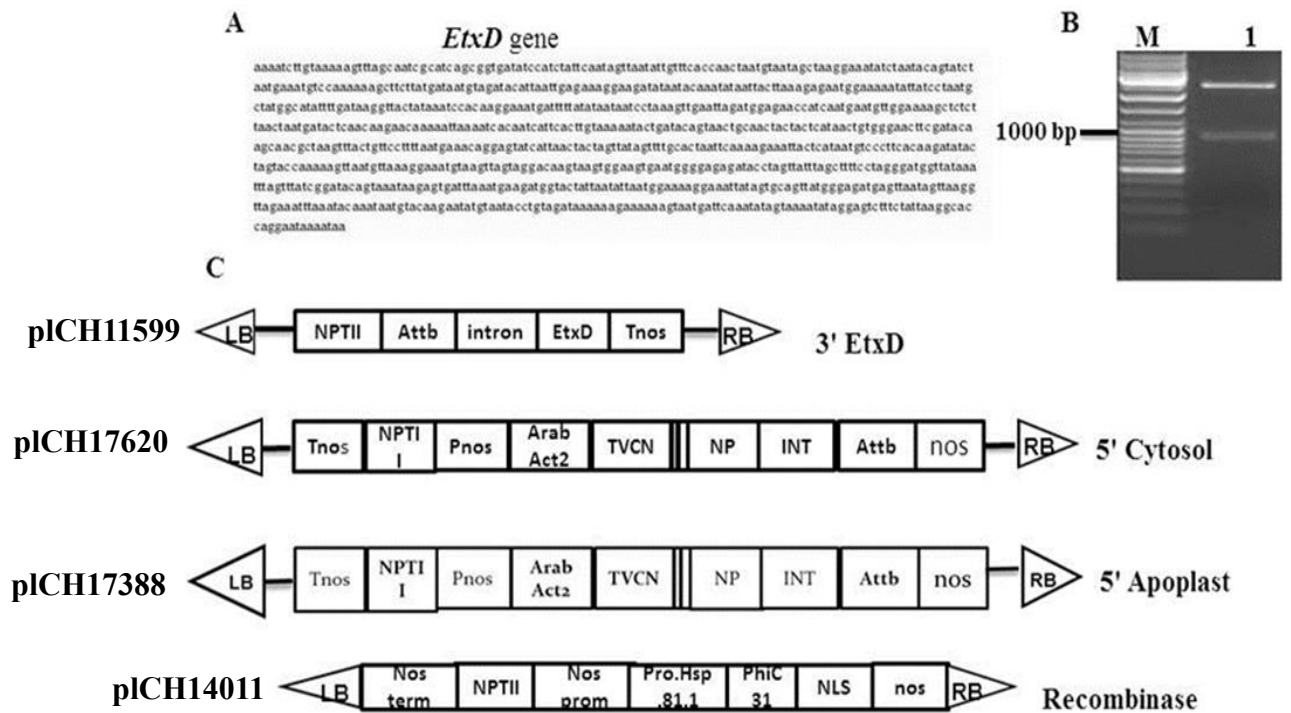


**Figure 2.1: Cloning of EtxD sequence into expression vectors.** (A) is the truncated gene sequence of the EtxD. (B) is the isolated *EtxD* (908 bp band) by enzyme digestion from the donor plasmid pMA-EtxD-1031994 (Geneart). Lane M represents the Thermo Scientific Generuler 1kb DNA ladder (SM0311) and Lane 1 the vector MA-EtxD-1031994 digested with *Bam*H1 and *Nco*I to release the EtxD gene. This was directly cloned into the pICH11599 vector. (C) is a schematic representation of the 3' Icon modules used in the transient expression of EtxD in *N. benthamiana* leaves. LB and RB, left and right borders of the T-DNA region, AttB, specific recombination site from phage PhiC31, NTR 3' non-translated region, Tnos, nopaline synthase terminator. *EtxD* was cloned into the 3' provector. The EtxD module can recombine with a 5' cytosol or apoplast targeting modules. The recombinase facilitates a combination of the different modules to affect the expression of any gene in the 3' module, in this case *EtxD*.

To transform the ligated plasmid into *E. coli*, an electroporation transformation procedure was used. Some commercially available competent *E. coli* cells supplied by Roche (Switzerland) were removed from the -80 °C freezer and placed on ice for 10 minutes to defrost. The competent cells (50 µl) were then mixed with 5 µl of the ligation reaction mixture and incubated on ice for 30 minutes before being exposed for 30 seconds to a 42°C heat-shocking treatment in the presence of 0,1 M CaCl<sub>2</sub>. This treatment results in the wounding of the bacterial membrane and allowing the uptake of the ligated DNA into the bacterial cells. After heat shocking, the cells were placed on ice for two minutes before 1 ml of SOC medium (20 g bactotryptone, 5 g bacto yeast, 0,5 NaCl and 20 ml of 1 M glucose solution) was added to the sample and shaken at 200 rpm at 37 °C for 60 minutes in a bench-top shaker. A cell suspension

(20 µl) was streaked out onto an LB plate containing 50 µg/ml carbenicillin and incubated overnight in a Memmert incubator set at 28°C. Transformed plasmids were then isolated using minipreps and subsequently quantified. The isolated plasmids were digested with *Nco*I and *Bam*HI restriction enzymes to confirm the presence of the *EtxD* gene.

### **2.2.8 Transformation of *A. tumefaciens***

The electroporation technique was used to transfer the isolated plasmid DNA into *Agrobacterium* cells. For transformation, 260 ng of the plasmid DNA was added to 40 µl of the GV3101::pMP90RK competent cells, the mixture was gently shaken, transferred to a plastic cuvette and placed on ice and electroporated at 140 Ω and a voltage of 1,44 kV. The plastic cuvette was placed into the electroporation chamber and a pulse of 5 milli-seconds was applied to transfer the DNA into the cells. Immediately after electroporation, 1 ml of YEP (10 g yeast extract, 10 g Bacto peptone, 5 g NaCl, pH 7,0) medium was added to the cuvette. The mixture was subsequently transferred to a 2 ml microfuge tube and the tube was incubated at room temperature for 60 minutes with agitation at 60 rpm. An aliquot was then plated onto an LB agar (10 g tryptone, 5 g yeast extract, 10 g NaCl, pH 7,0) plate containing the antibiotics kanamycin 50 µg/ml, rifampicin 50 µg/ml and carbenicillin 50 µg/ml for selection of the transformed *Agrobacterium* cells. The streaked plates were incubated at 28 °C for two days and the colonies that appeared were then selected for subsequent plasmid isolation and analysis.

### **2.2.9 General plant husbandry**

*N. benthamiana* (family: *Solanaceae*; subfamily: *Nicotianoideae*) seeds were obtained from the Forestry and Agricultural Biotechnology Institute at the University of Pretoria (South Africa) and sterilised using 70 ethanol. The ethanol was discarded, and the seeds were soaked for two minutes in 100% bleach. The bleach was discarded, and the seeds were rinsed thrice with sterile distilled water. The sterile seeds were then transferred into sterile bottles containing ½ MS (Murashige and Skoog macronutrients) (1,650 mg/l ammonium nitrate, 440 mg/l calcium chloride, 370 mg/l magnesium sulphate, 170 mg/l potassium phosphate and 190 mg/l potassium nitrate) and micronutrients (62 mg/l boric acid, 0.025 mg/l cobalt chloride, 0,025 cupric sulphate, 27,8 mg/l ferrous sulphate, 22,3 mg/l potassium iodide, 0,25 mg/l sodium and

37 mg/l Na<sub>2</sub>EDTA.2H<sub>2</sub>O) together with a kanamycin medium (30 µg/ml), sucrose (30 g/l), agar (8 g/l) and pH 5,8). The seeds were allowed to grow in a tissue culture laboratory under a 16-hour light/8-hour dark photoperiod and a temperature regime of 25°C day/20°C night. Three weeks after seeding, individual plantlets were selected out, transplanted into pots containing soil and left to grow in a tissue culture laboratory for five additional weeks under the same environmental conditions as stated above.

## **2.2.10 Infiltration of tobacco leaves with the pICH11599-EtxD vector**

### **2.2.10.1 Agrobacterium preparation for infiltration.**

Whole plants were inoculated with an *Agrobacteria* culture in LB media containing 50 µg/ml rifampicin, 50 µg/ml kanamycin and carbenicillin 50 µg/ml (pICH11599-EtxD, pICH14011 – Cre-integrase provector – with either pICH17388 (5' provector module for cytosolic targeting), or pICH17620 (5' provector module for apoplast targeting), and grown to an OD<sub>600</sub> of 1. The bacterial cells were pelleted in a centrifuge at 4 800 x g for 10 minutes and resuspended in two litres of infiltration buffer he10 mM 2-(N-morpholino) ethanesulfonic acid (MES) pH 5.5, 10 mM MgSO<sub>4</sub> to get a 10<sup>-1</sup> dilution. A beaker containing the infiltration solution was placed in the vacuum chamber.

**2.2.10.2 Infiltration of tobacco plants.** The tobacco plants of three to four weeks old were grown under tissue culture conditions with a 14-hour light period at 28 °C. Whole tobacco plants were inoculated as described by Marillonnet et al. (2004) in a 100 cm diameter vacuum chamber with the aerial parts of a plant dipped into the infiltration solution. The *Agrobacterium* containing the pICH11599-EtxD (3' provector module), pICH14011 (Cre-integrase provector) with either pICH17388 (5'-provector module for cytosolic target) or pICH17620 (5' provector module for apoplast targeting) were grown at 28°C for three days in a shaking incubator up to an approximate OD<sub>600</sub> of 1. The *Agrobacterium* containing the 3' module vector, cre-integrase vector module, and any one of the 5' module vectors were then mixed in 1:1:1 (v/v/v) and then pelleted at 4 800 x g for 10 minutes, resuspended in the infiltration medium (10 mM MES and 1 M MgCl<sub>2</sub> (pH 5.6) at OD<sub>600</sub> of 1. The whole *N. benthamiana* plant was immersed into the *Agrobacterium* mixture for one minute and then placed inside the vacuum chamber. Subsequent to that, the vacuum was applied for five minutes using a Type PM 16763-860.3

pump, with pressure ranging from 0,5 to 0,9 bar. The plants were returned to the greenhouse and grown at 22 °C under a 16 hour/8-hour light/dark cycle. The plants were subsequently harvested at three, six and nine days post-infiltration (dpi).

### ***2.2.11 Tobacco leaf protein extract***

The infiltrated tobacco leaves (1 g) were harvested and ground in liquid nitrogen and resuspended in 1 ml of extraction buffer containing 200 mM Tris-EDTA-Tween containing 1:10 volume of the protease inhibitor solution containing 1 mM PMSF (Phenylmethylsulphonyl flouride), 1 mM EDTA (Ethylenediaminetetraacetic acid), 10 µM trans-epoxysuccinyl-L-eucylamido (4-guanidino) butane (E-64) and 10 µM pepstatin A to block protease activity. The homogenate was centrifuge at 4 800 x g at 4°C for 10 minutes in an Eppendorf centrifuge (Eppendorf, Germany), The resulting supernatant was quantified by the Bradford assay (Bradford, 1976) and used for further analysis.

### ***2.2.12 Protein quantification***

The total soluble protein that was measured using the Bradford analysis (1976) as described in the manufacturer's manual. Absorbance was measured at 595 nm using a Power Wave HT spectrophotometer (BioTek). A Bovine Serum Albumin (BSA, catalogue number 500-0206, BIO-RAD) was used as the standard in concentrations of 0, 100, 200, 400, 600 and 800 µg/ml. To check the purity of the proteins, the protein samples were separated on a 12% SDS-PAGE gel as described by Laemmli (1970).

### ***2.2.13 Protein identification using mass spectrometry***

The protein bands of interest that were visualised on an SDS-PAGE gel were excised and subsequently treated as described by Webster and Oxley (2005). Briefly, samples were digested overnight with porcine trypsin (Promega, Madison, USA). MALDI-TOF-MS was performed using a QSTAR® Elite mass spectrometer (Applied Biosystems, Ontario, Canada). The generated PMF data was searched against a SWISS-PROT/TrEMBL release 29, using a Protein

Probe (Micromass), or against a non-redundant database maintained by the NCBI using the Mascot (Matrix Science, Boston, MA, USA) search engine (Helsens et al., 2007).

### **2.2.14 Immuno-blotting**

Exactly 8 µg of the supernatant protein samples were added to an equal volume of a 2x sample loading dye (90 mM Tris-HCl, pH 6,8, 20% glycerol, 2% SDS, 55 (v/v) β-mercaptoethanol and 0,2% bromophenol blue) and boiled for four minutes. The boiled protein extracts were separated on a 12% (w/v) SDS-PAGE according to Laemmli (1970). The proteins separated on SDS-PAGE gels were electro-blotted onto a hybond<sup>TM</sup> membrane (Amersham, UK) at 13 V for one hour at room temperature in a trans-blot SD machine. The membrane was blocked overnight at room temperature with gentle shaking in a solution of 5% (w/v) low-fat milk powder in Tris-buffered saline containing 0,1% Tween-20 (TBS-T). The membrane was then incubated for one hour with gentle shaking in primary blood antiserum from guinea pig (for detection of EtxD protein) diluted to 1:5000 in TBS-T. The membranes were then washed three times in TBS-T containing 0,5% low-fat milk. This was followed by a one-hour incubation in rabbit anti-guinea pig IgG–HRP (horseradish peroxidase) (Amersham, UK) conjugated as the secondary antibody (1:1 0000 dilutions) in PBST buffer for one hour at room temperature. Detection of the labelled proteins was undertaken by chemiluminescence using an ECL<sup>TM</sup>-plus kit (Amersham, UK) and according to the manufacturer's instructions.

### **2.2.15 ELISA**

#### **2.2.15.1 Development of the standard curve for ELISA.**

The EtxD protein concentrations derived from the non-formulated OBP control *C. perfringens* type-D protein for the standard curve were diluted in 0,05 M sodium bicarbonate (NaHCO<sub>3</sub>), pH 9,6, to a stock concentration of 1 000 ng/ml and serially diluted in Eppendorf tubes to two-fold dilutions in the sodium bicarbonate buffer to a starting concentration of 15,625 ng/ml. The starting concentration was diluted to five, two-fold concentrations (15,625–0,488 ng/ml), which resulted in a linear graph (Figure 2.2).

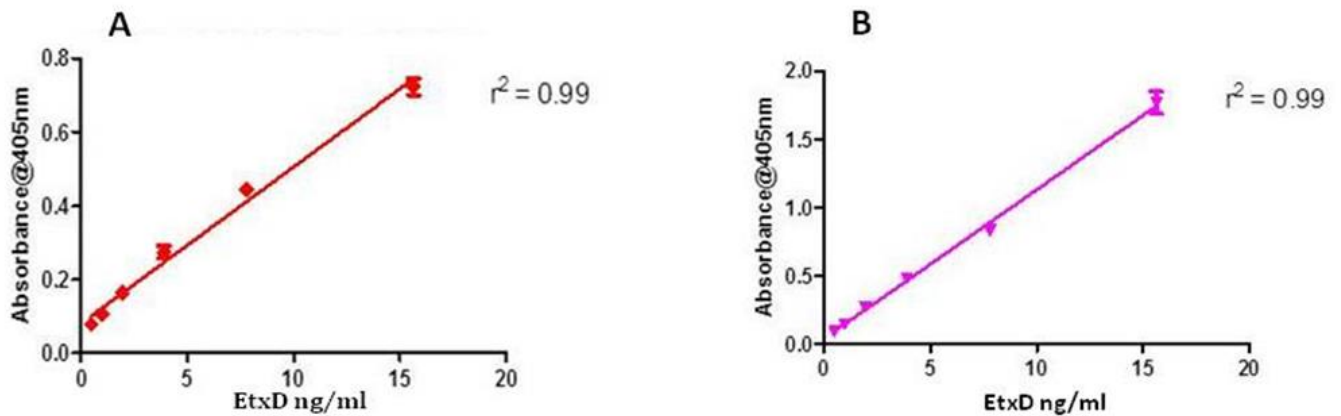


**Figure 2.2: Optimisation of sample standard for ELISA analysis.** (A) ELISA standard curve from EtxD sample adsorbed at 37 °C. (B) ELISA standard curve from EtxD sample adsorbed at 4 °C overnight.

Figure 2.2(A) shows an ELISA standard curve derived from the absorbance of 495 nm of recombinant EtxD protein in ng/ml, which was detected by the direct ELISA and allowed to adsorb to the ELISA plate at 37 °C EtxD protein for one hour. The correlation coefficient of this graph was 0,99, showing the best data fit. Experiments were conducted to determine the optimal temperature and time for the EtxD protein incubation. It was observed that when the EtxD was adsorbed to the ELISA plates overnight at 4 °C, more EtxD adsorbed to the plate – Figure 2.2(B). The correlation coefficient here was also 0,99, showing the best fit. Therefore, Figure 2.2(B) was used to perform the sample quantification.

The EtxD protein dilutions were loaded at 100 µl/well in triplicates in a 96-well microtiter plate (Nunc A62219) and incubated overnight at 4 °C to 5 °C. Sodium bicarbonate in PBS ( $\text{Na}_2\text{HPO}_4 \cdot 2\text{H}_2\text{O}$ ; 2,4  $\text{KH}_2\text{PO}_4$ , 80 g NaCl and 2 g KCl, pH 7,5) was used as a blank BSA as the negative control. The plate was washed three times (200 µl/well), with the washing buffer (PBS with 0,1% Tween 20) and the wells blocked with 200 µl/well of 5% non-fat milk in PBS for one hour at 37 °C. The plate was washed as before and the 100 µl/well blood serum from guinea pig was added and incubated for one hour at 37 °C. After another wash, 100 µl/well of secondary polyclonal antibody ((Rb pAb to Gpig, IgG (HRP), cat # ab6771, lotGR20285-2)) was added and the plate was incubated for one hour at 37 °C, washed and a 100 µl/well ABTS (2,2'-Azinobis [3-ethylbenzothiazoline-6-sulfonic acid]-diammonium salt) substrate added. After 20 minutes, a 100 µl/well stopping solution of 2% SDS (sodium dodecyl sulphate) was added. ABTS yields a green end-product upon reaction with peroxidase that was quantitated

by reading the absorbance at 405 nm using a multi-well spectrophotometer (Tecan Infinite 500). Thus, the green end-product levels are dependent on the secondary HRP antibody bound to the EtxD antibody in the serum, which in turn is an indication of the EtxD concentration. The absorbance was plotted against the EtxD concentrations from which the unknown concentration of the EtxD protein from the tobacco extracts were then derived using a GraphPad Prism software.

**2.2.15.2 Quantification of EtxD by ELISA.** For an indirect ELISA, 96-well microtitre plates ((Nunc A62219) were loaded with the 100 µl of the serial two-fold dilutions of the crude extracts and the PLK1102 standard (non-formulated Etx *C. perfringens* type-D control protein from OBP) and then incubated at 4 °C overnight. Each plate was then washed three times with PBS-T (Na<sub>2</sub>HPO<sub>4</sub>.2H<sub>2</sub>O; 2.4 KH<sub>2</sub>PO<sub>4</sub>, 80 g NaCl and 2 g KCl, pH 7,5) containing 0,1% Tween-20 buffer and then blocked for one hour at 37 °C with PBST containing 5% skim-milk powder. After the blocking period, the plate was washed three times with 1x PBST buffer. Next 100 µl of the 1:5 000 dilution of guinea pig-blood serum in the PBST buffer and then subsequently incubated for one hour at 37 °C, agitating at 60 rpm. The plate was again washed three times with PBST buffer. Subsequently, the plate wells were loaded with 100 µl of 1:5 000 of the rabbit anti-guinea pig IgG-HRP conjugated secondary polyclonal antibody in PBST buffer and incubated for one hour at 37 °C and shaking at 60 rpm. Subsequently, the plates were washed three times with PBST buffer and the plates were treated with 100 µl of ABTS [2, 2-azinobis-(3-ethylbenzthiazoline-6-sulfonate) (Calbiochem, San Diego, California, USA)] as a peroxidase substrate. The colour reaction was stopped with 100 µl of 2% SDS. The absorbance was measured at 405 nm by using a universal microplate reader F500 (Tecan, Infinite F500). The calculation of the data was performed by using Excel 2007 software (Microsoft, Redmond, Washington, USA).

## 2.3 Results

### 2.3.1 Bioinformatics analysis of *EtxD* gene

To establish the relationship between the *EtxD* gene sequences from different countries, a desktop study analysis of the different *EtxD* genes and proteins from published sources was carried out of the five multiple sequences identified from NCBI using BLAST and Clustal1W alignment. The identified *EtxD* gene, accession number (AY858558) genetic region from NCBI and EMBL database was targeted for this study as it is well reported. The *EtxD* protein sequence BLAST revealed that three other protein sequences of the same species had been determined in China, Japan, Belgium and USA (Table 2.3). When these protein sequences were aligned, the results revealed that the protein sequences from the four countries were identical. The four proteins were then compared with the translated *EtxD* protein found in South Africa (the non-formulated OBP control protein) to view sequence similarity. The results revealed that the protein found in South Africa was 99% identical to those produced in the other countries. It only differed with one amino acid at position five of the leading sequence. The USA protein sequence differed with only one amino acid at position 317 with the proteins from the other countries (Table 2.3). Because of this, the *EtxD* gene sequence from China (accession number AY85855) was used as a template for the synthetic gene.

**Table 2.3: Gene bank sequences of EtxD proteins from different countries**

<b>Gene Bank/EMBL Ac. No.</b>	<b>Country</b>
M95206,1	USA
BAG75487,1	Japan
AAW47580,1	China
CAA43104	Belgium
EtxD not submitted	South Africa

### ***2.3.2 Codon optimisation of the truncated EtxD***

To select the best method for the cloning strategy, the first task was to choose the target protein component to be used. This was achieved by first reviewing the data published on the EtxD gene primary structure and its pathogenesis. From the published data, it was then established that the leading sequence gets cut off during pathogenesis. By taking this into consideration, it was decided not to use the full sequence but to remove the first 32 amino acids of the leading sequence to produce the EtxD as a toxoid. The EtxD toxoid was therefore plant-codon optimised to enhance its expression and synthesised in such a way that it was devoid of the first 32 amino acids of the leading sequence of the *C. perfringens*. It also incorporated three restriction sites, namely *Nco*1, *Eco*R1 and *Kpn*1, at the 5' and *Bam*H1, *Xho*1 and *Sac*1 at the 3' end for ease of cloning into the p1CH11599 vector (Figure 2.1). The protein alignment shown in Figure 2.3 and the resulting dendrogram (Figure 2.4) revealed that only the removal of the leading sequence produced a truncated *EtxD* gene from the AY858558.

Subsequent to the codon optimisation of the truncated *C. perfringens EtxD* gene for expression in the *N. benthamiana*, a multiple nucleic sequence alignment was performed. To compare the

sequence of the original truncated *C. perfringens* *EtxD* gene with the codon optimised sequence and to understand or view the location where the 44% GC shift took place to prolong the mRNA half-life for enhancing the *EtxD* gene expression in *N. benthamiana* plant, Figure 2.5.

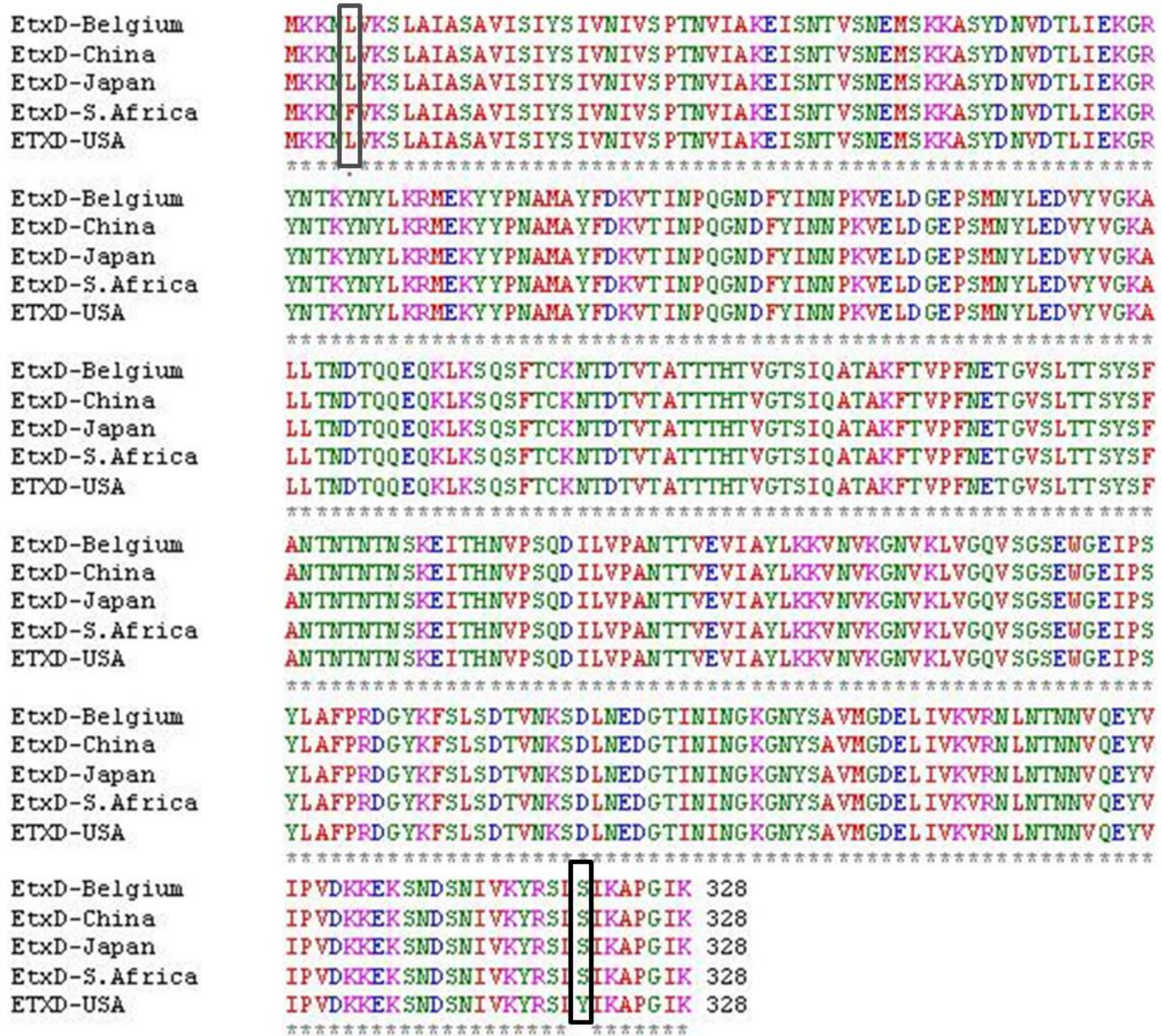
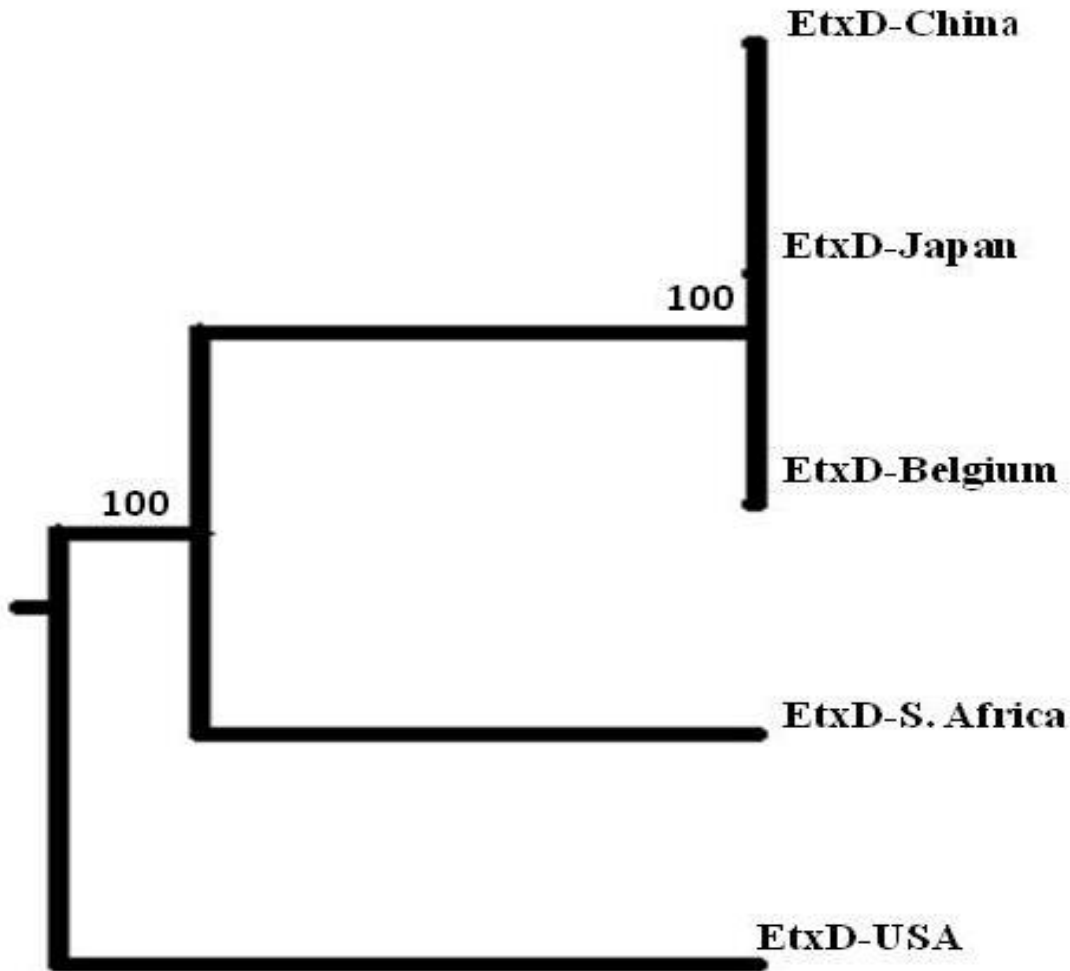


Figure 2.3: Multiple amino acid sequence alignment of the different *C. perfringens* *EtxD* protein found in other countries with the *EtxD* protein found in the South African isolate. Black block shows the amino sequences that are different.



**Figure 2.4:** Dendrogram based on a neighbour-joining algorithm showing the phylogenetic relationships among the protein sequence of the five *C. perfringens* type-D *Epsilon* toxins. The tree was constructed using the p-distance method. Bootstrap values are shown next to branches. The accession numbers of *C. perfringens* toxins obtained from the NCBI database are shown in Table 2.3

```

>AY858558      AAAATCTTGTAAAAAGTTTACGAATCGCAAA TGTCCAAAAAGCTTCTTATGATAATGTA 60
>GeneArtAY858558 GGTACCCCTG-----CAGACCCGTA TGTCTAAGAAAGCTTCTACGATAATGTG 48
      * * * * *
>AY858558      GATACATTAATTGACAAAGCGAAGATAAATACAAAATATAATTACTTAAAGAGAA TGGAA 120
>GeneArtAY858558 CATACTCTCATTGACAAGCGCAGCTACAACA CTAAGTACAAC TACCTCAAGAGGA TGGAA 108
      * * * * *
>AY858558      AAAATATTATCCTAATGCTATGGCATATTTTGATAAGGTTACTATAAATCCACAAGGAAAT 180
>GeneArtAY858558 AAGTACTACCCAAACGCTATGGCTTACTTCGATAAGGTGACAA TCAACCCACAGGGCAAC 168
      * * * * *
>AY858558      GATTTTTATATTAATAATCCTAAAGTTGAATTAGATGGAGAACCATCAA TGAATTATCTT 240
>GeneArtAY858558 GATTTCTACATCAACAATCCAAAGTGGAC TCGATGGTGAGCCATCTA TGAATTACCTT 228
      * * * * *
>AY858558      GAAGATGTTTATGTTGAAAAGCTCTCTTAACTAATGATACTCAACAGAACAAAATTA 300
>GeneArtAY858558 CAGGATGTGTACGTGGAAAAGCTCTTTTGA CTAACGATACTCAGCAAGAGCAGAACTT 288
      * * * * *
>AY858558      AAAATCACAAATCATTCACTTGTAAAAATACTGATACAGTAACTGCAACTACTACTCATACT 360
>GeneArtAY858558 AAGTCTCAGTCTTTCACTTCAAGAACTGATACTGTGACTGCTACTACTACTCACA CT 348
      * * * * *
>AY858558      GTGGGAACCTTCGATACAAGCAACTGCTAAGTTACTGTTCCCTTTAATGAAAACAGGAGTA 420
>GeneArtAY858558 GTGGGAACCTTCTATTAGGCTACTGCTAAGT TCACTGTCCCAT TCAATGAGACTGGTGTG 408
      * * * * *
>AY858558      TCATTAAC TACTAGTTATAGTTTTCGAAATA CAAATA CAAATA CTAATTCAAAAGAAAT 480
>GeneArtAY858558 TCTCTTACTACTTCTACTCTTCGCTAACACTAACACAAACACTA ACTCCAAAAGAGATC 468
      * * * * *
>AY858558      ACTCATAATGTCCCTTCACAAAGATA TACTAGTACCAGCTAATACTACTGTAGAAGTAATA 540
>GeneArtAY858558 ACTCACAAACGTTCCATCCCAGGATA TTCTTGTTCCAGCTAACACTACTGTGAGGTGATC 528
      * * * * *
>AY858558      GCATATTTTAAAAAAGTTAATGTTAAAGGAAATGTAAAGT TAGTAGGAC AAGTAA GTGGA 600
>GeneArtAY858558 GCTTACCTCAAGAGGTTAAGCTTAAAGGAAACGTGAAGCTTGTGACAGCTTT CAGGA 588
      * * * * *
>AY858558      AGTGAATGGGAGAGATACCTAGTTATTAGCTTTTCCCTAGGGATGGTTATAAATTTAGT 660
>GeneArtAY858558 TCTGAATGGGAGAGATTCCTATTTACCTTTCCTTTC CAAAGGATGGATACAAGTCTCT 648
      * * * * *
>AY858558      TTATCGGATACAGTAAATAACAGTCAATTAATGAAAGATGGTACTATTAATATTAATGGA 720
>GeneArtAY858558 CTCTCCGATACGTGCAACAAGTCTGATCTTAAAGGAGATGGCACTATCAACATCAACGGA 708
      * * * * *
>AY858558      AAAAGGAAATTATAGTGCAGTTATGGGAGATGAGTTAATAGTTAAGGTTA GAAATTAAT 780
>GeneArtAY858558 AAGGGAAACTACTCTGCTGTTATCGGAGATGAGCTTAATG TGAAGGTGAGGAACCTCAAC 768
      * * * * *
>AY858558      ACAAAATAATGTACAAGAATATGTAATACCTGTAGATAAAAAAGAAAAA GTAATGATTCA 840
>GeneArtAY858558 ACTAACCAACGTGC AAGAGTACGTTATCCAGTGGATAAGCAAAGCAACTCCAACGATTCC 828
      * * * * *
>AY858558      AATATAGTAAAATATAGGAGTCTTTCTATTAAGGCACCAGGAA TAAAAT AA----- 891
>GeneArtAY858558 AACATCGTCAAGTACCGTTCTTCTATTAAGGCTCCAGGCA TCAAGTCACTCGAGCCA 888
      * * * * *
>AY858558      -----
>GeneArtAY858558 TGGGGATCCTCTAGAGCTC 907

```

**Figure 2.5: Multiple nucleic acid sequence alignment comparing the sequence of the targeted *C. perfringens* EtxD protein with the codon optimised *EtxD* gene. The data shows a 44% GC shift on the plant codon optimised gene sequence between the two gene sequences.**

### 2.3.3 Vector design and construction

#### 2.3.3.1 *EtxD* isolation.

The plant codon optimised truncated *EtxD* gene was commercially produced. For verification, it was isolated with *Nco1* and *BamH1* enzyme digests from the donor plasmid pMA1031994 and generated a restriction product of 908 bp fragment that is the same size as the *EtxD* gene

(Figure 2.3.4A). The codon optimised truncated *EtxD* gene was then directly cloned into the plant expression vector pICH11599, as described in the materials and methods to make a pICH11599–*EtxD* construct. The construct was then confirmed by restriction enzyme digestion. The construct was then transformed into an *A. tumefaciens* GV3101 strain and this was subsequently confirmed by enzyme digestion and by retransforming it back into the *E. coli* (Figure 2.1B).

### **2.3.4 Expression analysis**

To validate that the Icon provector modules were working, *GFP* gene was cloned into the pICH11599 vector and used as a positive control (Figure 2.3.4). Subsequently, the construct was transformed into an *A. tumefaciens* GV3101 strain. Co-infiltration of this clone pICH11599–*GFP* with pICH17388 or pICH17620, respectively, together with the pICH14011 (integrase) led to *GFP* expression in amounts such that the leaves (Figure 2.6) showed a gradual increase in *GFP* activity of green spots from three to nine days post-infiltration. These results confirmed that the Icon provectors were viable for transiently expressing the *EtxD* recombinantly in tobacco leaves and that there would be a gradual increase in spots and spatial distribution on the *EtxD* infiltrated leaves over three to nine days.

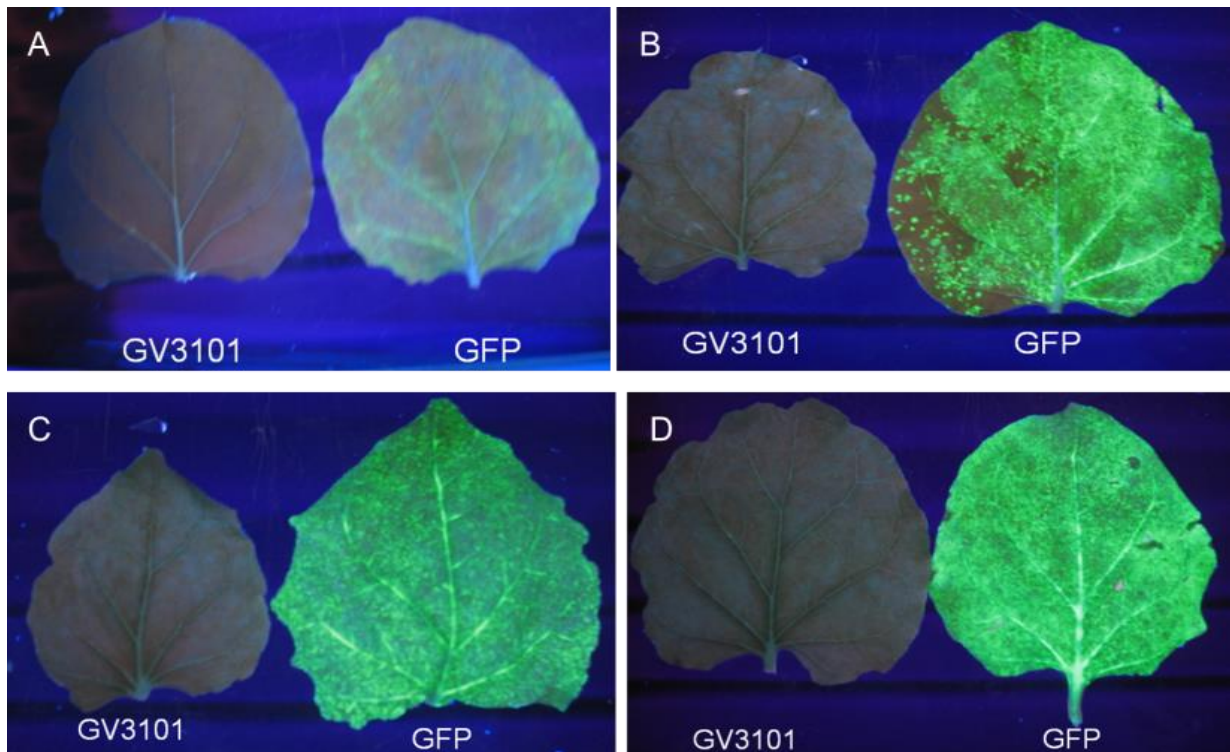


**Figure 2.6: Transient expression of the GFP protein in the leaves of *N. benthamiana*.** The leaves were collected at zero, three, six and nine days after infiltration and photographed under UV light. (A) represents zero days post infiltration (dpi) leaves, (B) three dpi leaves, (C) six dpi leaves and (D) nine dpi leaves.

### ***2.3.5 Effect of the EtxD protein on leaf phenotype***

The physical traits of a leaf change post-infiltration and when the EtxD protein is directed to the cytosol is shown in Figure 2.7(I) and (II), respectively. At 3 dpi, the leaf shows yellow spots distributed throughout the leaf, which could be an indication of the beginning of necrosis process. At day six, the colour of a leaf appears to be a darker green, which could be due to pigment changes. The leaf is dehydrated and brittle, indicating cell death because of a lack of nutrients. Visual observation indicates a similar result on day nine.

The physical traits of the leaf also change post infection (Figure 2.7(II)) when the EtxD protein has been directed into the apoplast. At day three, the leaf looks healthy with minor yellow spots. However, at day six, the leaf is dark green with yellow spots distributed across the leaf. At day nine, the leaf changes colour from dark green to light green with the yellow spots becoming more prominent. This could result from stress or incorrect nutrient levels and because some of the pigments are associated with proteins (Armstrong, 1996). Most likely, the

changes in the physical traits of the leaf result from the toxic effects of the gene product. The results shown in Figure 2.7 indicate that targeting the *EtxD* gene with the Icon system to either apoplastic or cytosolic space is severely harmful to the leaf and results in cell death.

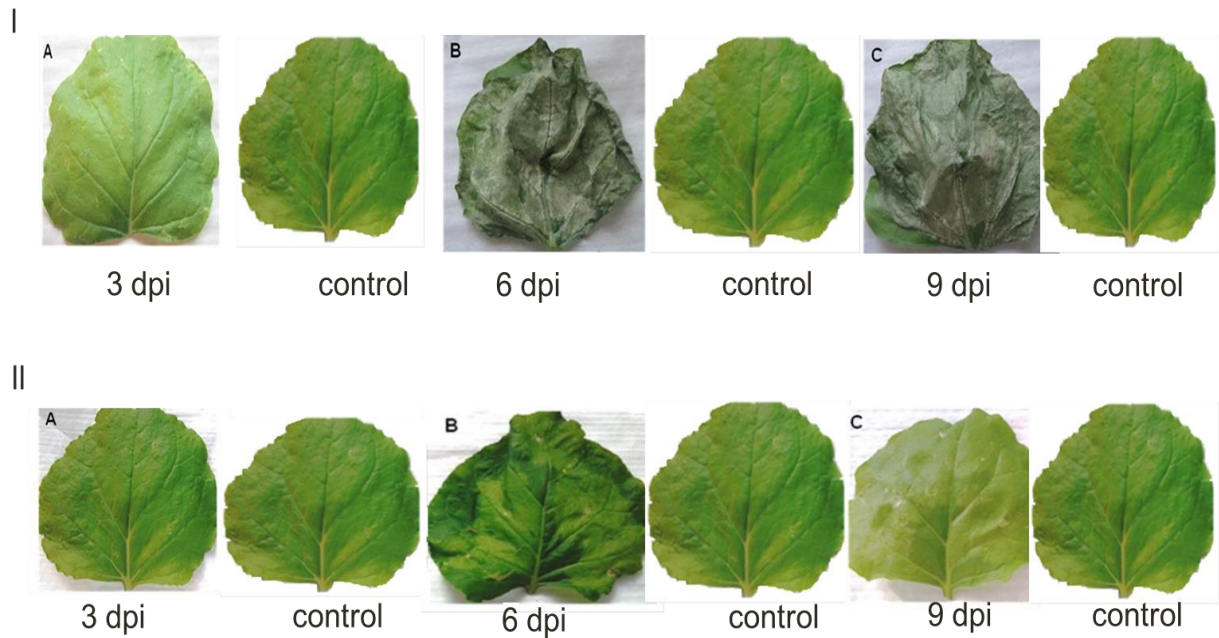


**Figure 2.7: Images of *N. benthamiana* leaves after agroinfiltration with the recombinant EtxD gene directed to the cytosol.** (I) Samples were collected three, six and nine days post-infiltration (dpi). (A) represents 3 dpi, (B) 6 dpi and (C) 9 dpi. (II) Images of *N. benthamiana* leaves post-agroinfiltration with the EtxD gene directed to the apoplast and collected at three, six and nine days post-infiltration (dpi). (A) represents 3 dpi, (B) 6 dpi and (C) represents 9 dpi.

### 2.3.6 Recombinant *EtxD* expression

The total protein supernatant was collected at three, six and nine days post-infiltration intervals and electrophoresed on a 12% SDS-PAGE gel (Figure 2.8). This was to visually confirm the expression of the EtxD protein in the agroinfiltrated *N. benthamiana* leaves. The OBP positive control (EtxD culture) appears in lane C and gave a band of 34 kDa, which corresponds to the predicted size of the EtxD protein in published data. The *N. benthamiana* negative control showed a highly abundant band around 55 kDa, which correspond to the protein Rubisco. However, no protein band corresponded to 34 kDa, as per the positive control. Day three post-infiltration of the cytosol directed samples showed a  $\pm 32$  kDa band similar to that of the OBP positive control. However, on days six and nine, the  $\pm 32$  kDa showed decreasing levels of this protein, which is indicative of the necrosis process as seen in Figure 2.7(I). The apoplast

directed samples at 3 dpi showed a presence of a 34 kDa protein that corresponded to that of the positive control. However, it would appear to be expressed at a lower level when compared to the day three dpi sample from the cytosol. The six and nine dpi-sample levels of the 34 kDa protein appeared to be increasing, which is in contrast to the decreasing concentration seen in the cytosol. These results indicate that a protein band was seen on a PAGE gel corresponding to the size of the EtxD protein from OPB.

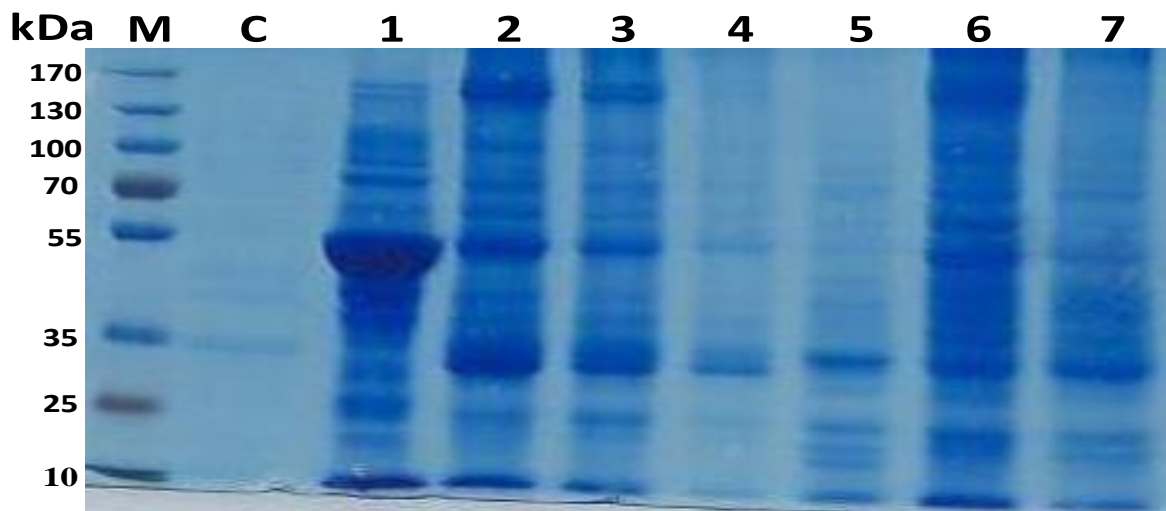


**Figure 2.8: An SDS-PAGE (12%) gel analysis of the agroinfiltrated recombinant EtxD protein.** Total leaf protein supernatant sample was collected at three, six and nine days after post-infiltration. Lane M represents a PageRuler-stained multi-colour broad-range protein ladder (Fermentas, SM1841). Lane C is the OPB EtxD positive control, with the band corresponding to 34 kDa of the OPB EtxD control. Lane 1 represents a wild type and Lanes 2, 3 and 4 represent, respectively, 3 dpi, 6 dpi and 9 dpi of the agroinfiltrated *EtxD* gene directed into the cytosol. Lanes 5, 6 and 7 represent, respectively, 3 dpi, 6 dpi and 9 dpi of the agroinfiltrated EtxD protein directed into the apoplast.

### ***2.3.8 Cross-reaction detections of the blood serum and the secondary antibody***

Although there is a commercial available ELISA kit for *Epsilon* toxin, it could not be purchased from Germany because of biosafety concerns. Therefore, an ELISA assay was developed using the available antibodies. As there is no commercial EtxD antibody on the market, the commercial vaccines (alum precipitate Pulpy Kidney Disease vaccine) were used to optimise the Western Blot technique. Initially, the cross-reaction between the guinea-pig blood serum and the secondary antibody was tested by spotting different amounts of the blood serum onto the nylon membrane. Detection was by colour production using a TMB (3, 3', 5, 5' tetramethyl

benzidine) substrate (Figure 2.9). The optimal secondary antibody dilution was 1:1 000 as this gave low background activity compared to the other dilutions. The dilution was used to test for the presence of the EtxD protein in the agroinfiltrated leaf extracts.

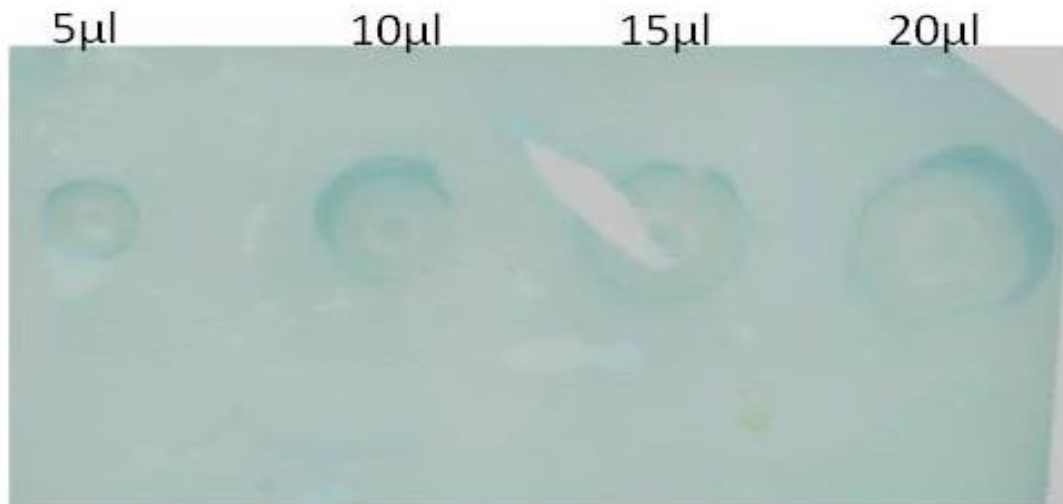


**Figure 2.9: Characterisation of the guinea-pig blood serum and the secondary antibody for cross-reaction.** Varying amounts of guinea-pig blood serum were spotted on nylon membrane and analysed by a rabbit anti-guinea pig IgG-HRP conjugate using TMB (3, 3', 5, 5' tetramethyl benzidine) substrate for colour detection.

### ***2.3.7 Validation of the EtxD protein***

The plant extracts (Figure 2.8) targeted to the apoplast have a detectable protein band of the same size (34 kDa) as the positive control 34 kDa protein. While the plant extract targeted to the cytosol have  $\pm 32$  kDa, this band was not visible in the crude plant extract from the wild-type sample. This demonstrates that the plant is producing sufficient levels of the EtxD protein in the leaves to be detectable using an SDS-PAGE gel stained with Coomassie Brilliant blue. The recombinant *EtxD* gene plant extract was probed with HRP-conjugated polyclonal anti-guinea pig antibody by the Western Blot technique (Figure 2.10) to further characterise the plant expressed EtxD protein. The non-formulated OBP EtxD protein was used as a positive control for the Western Blot analysis. The blood serum from guinea pig was used as the primary antibody. Two bands were detectable in the positive control corresponding to the 28 kDa and 34 kDa EtxD protein. In the different plant extracts harvested on three, six and nine days, the protein band corresponding to the 28 kDa OBP control sample was clearly visible.

This is not surprising as bands ranging from 26 to 32 kDa have been detected before even from the *C. perfringens* extracts and *E. coli* made EtxD protein (Knapp et al., 2009). Since a polyclonal primary antibody was used there were other bands at higher molecular weight that were detectable. Based on the Western Blot data it could be concluded that the plant-made EtxD protein cross-reacts with the serum raised against the EtxD protein and can thus be used as a recombinant Pulpy Kidney Disease vaccine in animal trials.

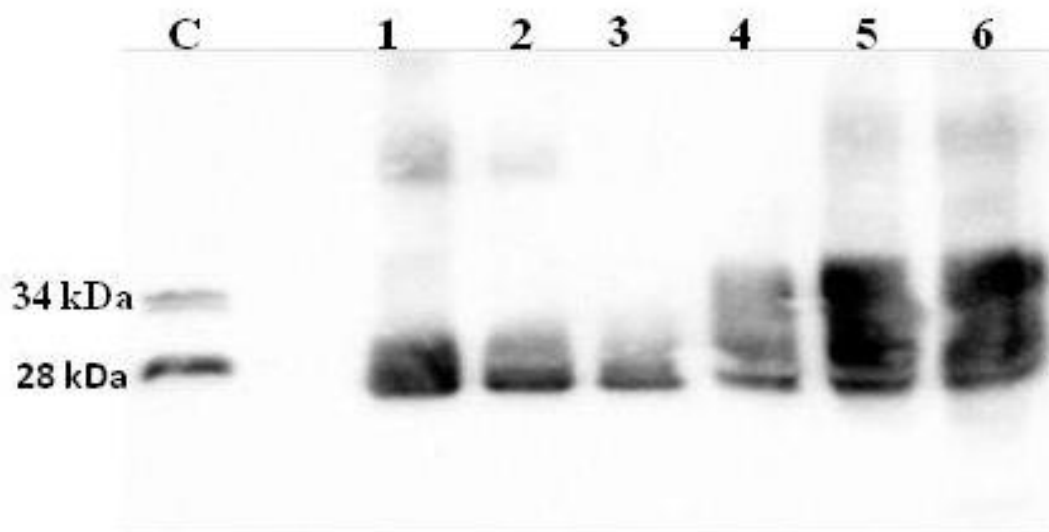


**Figure 2.10: Western Blot analysis of the EtxD protein expressed in tobacco leaves.** The protein was separated on a 12% SDS-PAGE gradient gel and probed with a polyclonal guinea-pig anti-EtxD antibody. The total leaf protein supernatant samples were from three, six and nine dpi samples. Lane M is a PageRuler-stained protein ladder (Fermentas) and Lane C the OBP EtxD protein control. Lane 1 represents the tobacco wild type, Lanes 1 to 3 represents the agroinfiltrated leaf samples with EtxD directed to the cytosol, and Lanes 4 to 6 the agroinfiltrated EtxD protein directed to the apoplast.

### 2.3.9 Protein identification using mass spectrometry

After validation of EtxD expression using the Western Blot analysis and the identification of three expressed bands, namely 34 kDa of OBP positive standard, 34 kDa plant-derived protein, and 32 kDa that coexpressed with the 34 kDa plant-derived protein in Figure 2.8 were established by being excised from an SDS-PAGE gel and sequenced by LC MALDI (Liquid chromatography Matrix-Assisted Laser Desorption/Ionisation). Table 2.4 shows the sequencing results, including the sequence coverage for the three bands. Protein band 1 (34 kDa) from the OBP is the positive control and was confirmed to be *Epsilon* toxin from *C.*

*perfringens* with a 65% protein coverage. The next most abundant protein was Trypsin, which is used in the peptide digestion during sequencing. This confirms that the protein sample being formulated by OBP is predominantly the *Epsilon* toxin. Sequencing results of the corresponding protein band migrating at the same size as the positive control was confirmed to be that of the plant derived *Epsilon*-toxin from *C. perfringens* at 68% sequence coverage.

Sequencing of the 32 kDa protein that co-expresses with the 34 kDa plant-derived protein was confirmed as the stress-related protein from the tobacco extract of Glucan *endo*-1, 3-*beta*-*glucanase* at 55% and 54% sequence coverage. In summary, the sequencing results confirmed that the *Epsilon* toxin protein was expressed in the crude plant extract at levels detectable by SDS-PAGE and Western Blot analysis and that the second band, migrating at 32 kDa, was a stress-related protein glucan *endo*-1, 3-*beta*-*glucanase* that further confirmed the stress shown by the agroinfiltrated leaves. All the expressed protein sequences with the highest coverage from the agroinfiltrated tobacco leaf crude extracts were then downloaded from the database and are listed in Figure 2.11

**Table 2.4: Sequencing data for the putative *Epsilon* protein bands from SDS-PAGE proteins** with the highest coverage are represented in bold type. Protein band 1–34 kDa positive control from OBP, protein band 2–34 kDa from the plant extract, Band 3–32 kDa band that co-express with the 34 kDa band in the plant sample.

<b>Band ID</b>	<b>% Coverage</b>	<b>Accession</b>	<b>Name of Protein</b>	<b>Species</b>	<b>Peptide (95%)</b>
<b>1</b>	<b>65</b>	<b>S27536</b>	<b><i>Epsilon-toxin-C. perfringens</i></b>	<b><i>C. perfringens</i></b>	<b>25</b>
1	26	TRPGTR	Trypsin (EC 3.2.21.4) precursor-pig	Pig	5
1	8	T07140	Glycan-endo - 1,3 <i>beta</i> -D- <i>glucanase</i> (EC 3.2.1.3)	Potato	2
<b>2</b>	<b>68</b>	<b>S27536</b>	<b><i>Epsilon-toxin-C. perfringens</i></b>	<b><i>C. perfringens</i></b>	<b>28</b>
2	54	D38257	Glycan-endo - 1,3 <i>beta</i> -D- <i>glucanase</i> (EC 3.2.1.3)	Common tobacco	10
2	52	B38257	Glycan-endo - 1,3 <i>beta</i> -D- <i>glucanase</i> (EC 3.2.1.3)	Common tobacco	10
3	55	B34801	Pathogenesis-related protein Q precursor-common tobacco	Common tobacco	14
3	25	B38J14	Triose phosphate isomerase cytosolic isoform-like <i>Solanum tuberosum</i>	<i>Solanum tuberosum</i>	5
3	21	TRPGTR	Trypsin (EC 3.2.21.4) precursor-pig	Pig	5

**A**

MTLCTKNGFLAAALVVLVGLLICSIQMIGA**QSIGV****CYGK**HANNLPSDQDVINLYNANGIRKMR**IYNPDTNV**FNA  
 LRGSNEIHLDVPLQDLQSLTDPSRANGWVQDNIIHFPDVKFKYIAVGNEVSPGNNGQYAPFVAPAMQNV  
**YNALAAAGLQDQIKV**STATYSGILANTYPPKDSIFRGEFNSFEN**PIIQFLVQHNL**PLLANVVPYFGHIFNTADV  
 LSYALFTQQEANPAGYQNLFDALLDSMYFAVEK**AGGQNVEHV**SESGWPSEGNSAATIENAQTYVENLINHV  
 KSGAGTPKKPGKAIETY**LFAMFDEN**KEGDITEK**HFGLFSPDQRAKYQLN**FN

**B**

MEFSGSPMALFCCVFFLFLTGSLA**QGIGSIVTSDLFNEMLK**NRNDGRCPANGFYTYDAFIAAANSFP**GFGT**  
**GDDTARRKEIAAFFGQTS**HEITGGSLSAEPFTGGYCFVRQNDQSDRYYGRGPIQLTNRNNYEKAGTAIGQ  
**ELVNNPDLVATDATISFK**TAIWFWMTFQDNKPSHSDVIIWRWTPSAADQAANR**VPGYGVITNI**NGGIECGIGR  
 NDAVEDRIGYYRRY**CGMLNVAPGENLDCYNQR**NFGQG

**C**

MKKNLVKSLAIASAVISIYSIVNIVSPTNVIAKEISNTVSNEMSK**KASYDNVD**TLIEKGRYNTKYNYLKRMEKY  
**YPNAMAYFDKVTINPQGNDFYINNPKVELDGEPSMNYLE**DVYV**GKALLTNDTQQEQK**LKSQSFTCKNTD  
 TVIAITHTVGTISIQATAKFTVPFNETGVSLTTSYFANTNTNNSKEITHNVPSQDILVPANTTVEVIAYL  
**KKVNVKGNVKLVGGQVSGSEWGEIPS**YLA**FP**RDGYK**FSLSDTVNKSDLNE**DGTININGKGNYS**AVM**GDELI  
**VKVRNLNTNNVQEYVIPVDK**KEKSNDSNIVKYRSLYIKAPGIK

**Figure 2.11: Peptide sequencing of plant-produced proteins by mass spectrometer.** (A) The sequence analysis of the glucan endo-1, 3-*beta*-glucanase expressed on the tobacco leaves crude extract. The green letters represent 95% confidence, the grey letters 0% peptide confidence, the red letters greater than 0 and less than 50% peptide confidence, and yellow letters 50% but less than 95% peptide confidence. (B) The sequence analysis of the pathogenesis-related protein identified on the tobacco crude extract. The colours represent the same information as under (A). (C) This shows the sequence analysis of the *Epsilon* toxin-*C. perfringens* identified from the agroinfiltrated tobacco leaf crude extracts. The colours represent the information as under (A).

### 2.3.10 ELISA analysis

The expression level of the EtxD protein in plants was quantified alongside the standard curve. The ELISA results in Figure 2.12 shows that the EtxD protein directed to the cytosol compartment was most highly expressed at three dpi. EtxD protein levels decrease from this point onwards until no EtxD protein could be detected at nine dpi. The EtxD protein directed into the apoplast showed protein levels increasing with time from 25 to 380 mg/kg between three and nine dpi. The EtxD protein-expression levels directed to the apoplast was chosen for further experiments for the production of the EtxD protein in *N. benthamiana*. This expression profile correlates with the Western Blot analysis (Figure 2.10) at day six and nine, when no

EtxD protein could be detected. This could be because of the necrosis process observed in Figure 2.7.

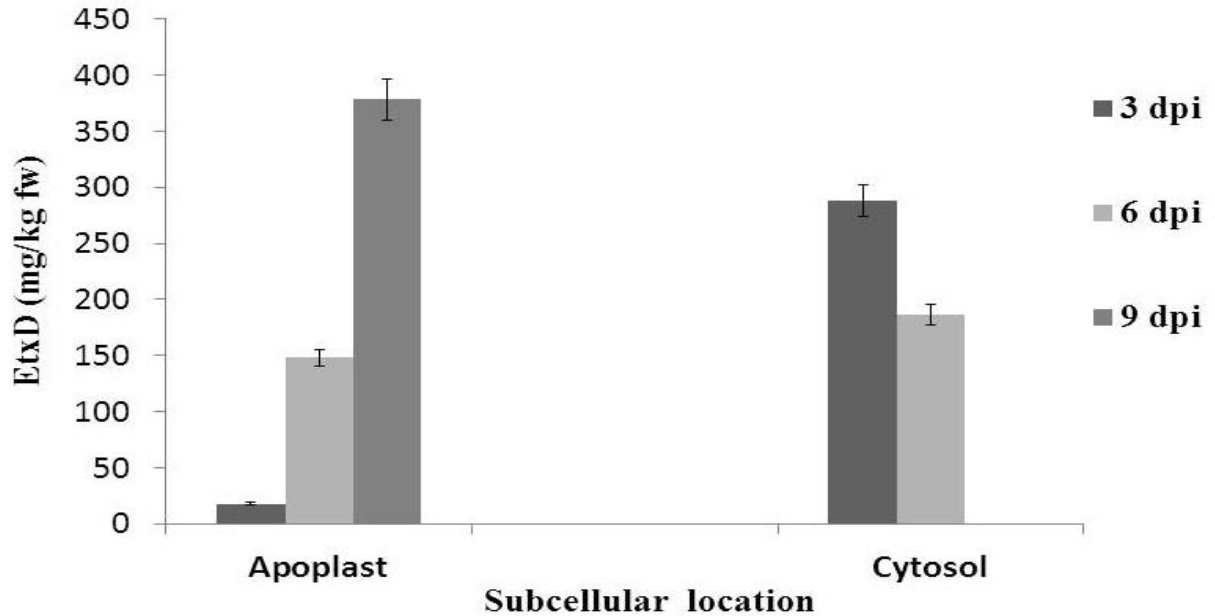


**Figure 2.12: Expression levels of EtxD protein targeted to different subcellular compartments as measured by ELISA.** The expression was quantified at three, six and nine dpi respectively in wild-type EtxD infiltrated *N. benthamiana* leaves, apoplast and cytosol directed recombinant expression.

The ELISA results in Figure 2.12 shows the EtxD protein expression directed to the cytosol and the apoplast compartments at three, six and nine dpi respectively. The apoplast results show that at three dpi the EtxD protein level was about 25 mg/kg fw, at six dpi it increased to 150 mg/kg fw and at nine dpi the level increased to 380 mg/kg fw, which is more than doubled the six-dpi level. The rate of increase in the apoplast is almost a linear increase. For the cytosol results, the data shows that at three dpi the EtxD level was about 300 mg/kg fw, at six dpi the level decreased to 200 mg/kg fw and at nine dpi it decreased to 10 mg/kg fw.

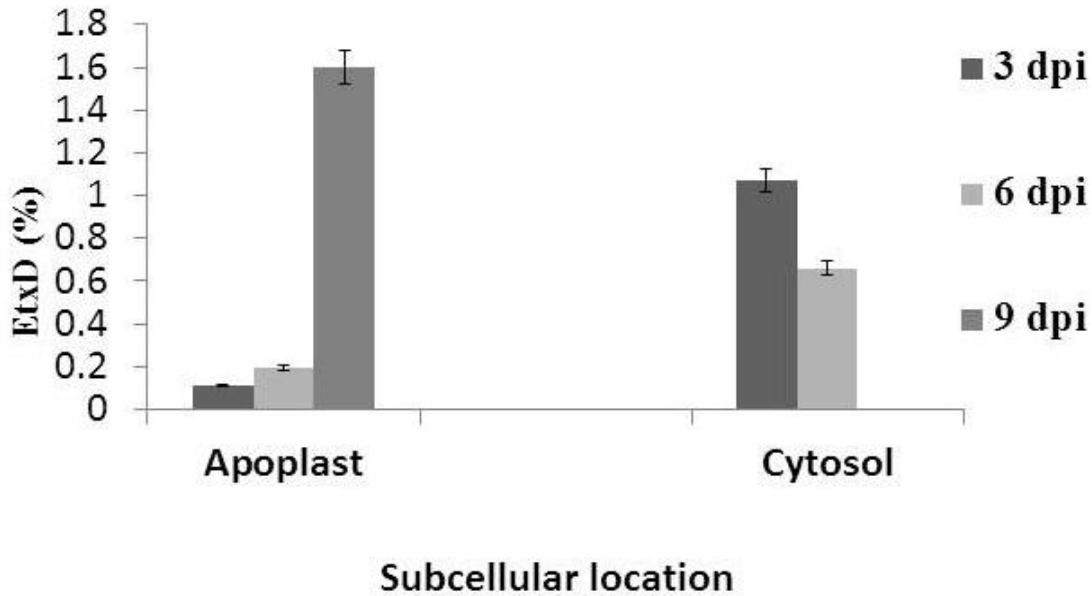


**Figure 2.13: EtxD protein in different subcellular compartments as a percentage of total soluble protein from *N. benthamiana* leaves.**

The total soluble protein in the leaf tissue of each sample was determined using the Bradford assay with a BSA standard curve. The percentage of the expressed EtxD protein was calculated as part of the total soluble protein as is shown in Figure 2.13. This was undertaken to determine the percentage of the protein expressed in the cytosol and the apoplast compartments of the *N. benthamiana* leaves at each day point. The results show that in the apoplast compartment, the levels of the EtxD protein at three dpi is 0,1% of the total protein produced. This increased to 0,2% at day six and then to 1,6% at day nine. In the cytosol, the results show that the level of the EtxD protein at day three was 1,0% of the total protein produced. This decreased to 0,6% at day six and then to almost zero at day nine. The trend of increasing percentages of EtxD within the apoplast fraction over the nine days and its decline in the cytosol are consistent with the expression data shown in Figure 2.12.

## 2.4 Discussion

The specific aim of this study was to evaluate tobacco as a production system for a recombinant EtxD protein with the potential to be used as a vaccine for Pulpy Kidney Disease. The study further compares the influence of targeting the recombinant EtxD protein to the apoplast and

cytosol with respect to the accumulation of the EtxD protein. Lastly, the feasibility of producing sufficient quantities of the recombinant EtxD protein via agroinfiltration for purification and biochemical analysis were also investigated.

Bioinformatic tools and public databases were used to facilitate the design and construction of appropriate expression vectors for the adoption of an expression transient approach in *N. benthamiana* leaves. Tobacco is considered a relatively safe crop for recombinant protein production. Like all other plants, tobacco does not harbour human pathogens, eliminating the threat of transmissible diseases. It is also a non-food and non-feed crop, and the threat of food or feed supply contamination is thus minimised (Twyman et al., 2008).

The identified *EtxD* (AY858558) gene from the NCBI and EMBL databases was targeted in this study. The targeted EtxD protein sequence blasting research indicated three other EtxD proteins that are produced in Japan, the USA, Belgium and China. The EtxD proteins from these countries, were aligned with the sequenced and translated EtxD protein from South Africa. The aim was to view the diversity among the EtxD protein from the different countries (Figure 2.3). The results revealed that the South African EtxD protein is 99% identical to those produced in Belgium, China and Japan, only differing with one amino acid on the fifth amino acid on the leading sequence. The USA protein sequence differs from the other countries with only one amino acid at position 317 (Table 2.3). This difference could be as a result of evolutionary processes and geographic specificity. The phylogenetic tree (Figure 2.4) revealed that the EtxD proteins produced in the different countries are from the same ancestor, with the EtxD proteins from Japan, China and Belgium being identical. The cladogram also reveals that the EtxD protein isolated from South Africa and the USA are closely related when compared to the other three EtxD proteins, which could be the result of evolution and geographic specificity. Since the *EtxD* gene from China (AY85855) is well studied and published, and is 99% similar to the South African EtxD protein, it was decided to use this gene sequence as a template for the study's synthetic gene. In general, rare codons such as AU-rich destabilising sequences, and putative polyadenylation and splicing signals, may contribute to rapid mRNA decay, thus limiting the expression of foreign genes in plants.

The CAI value is considered to be a measure of the expression levels of a given gene in different organisms (Laguia-Becher et al., 2010). It is believed that increasing the CAI of a foreign gene

results in a high expression level of those proteins (Laguia-Becher et al., 2010). However, increasing the CAI value brings about an increase in the A+T content. This could decrease mRNA stability and reduce the protein expression level (Geyer et al., 2007). Sou et al. (2007) have shown that constructs carrying optimised sequences, where the A+T content is higher than 50%, present a protein expression level significantly lower than the native protein, although the mRNA level by RT-PCR is similar in all constructs. The usage of plant codon-optimised gene expresses better than the native gene produced in *N. benthamiana* leaves (Maclean et al., 2007).

The highest expression of a protein is correlated with the lowest A+T content, resulting in better transcription and RNA processing. Finally, in the codon-optimised PyMSP4/5 antigen from *Plasmodium*, the A+T content is reduced from 67% to 53% and the AT-rich regions are disrupted (Wang et al., 2008). The constructs that express a reduced A+T gene version were more efficient in antigen production than the native versions, thus, supporting the view that increasing the A+T content may decrease mRNA stability and reduce the protein expression level (Wang et al., 2008; Webster et al., 2009). In this study, codon optimisation adjusted the CAI value to 0,84 (the codon usage was adapted to the codon bias of *N. tabacum* genes) so that it would allow high expression and G+C content to prolong mRNA half-life. The multiple nucleotide alignment (Figure 2.5) compares targeted EtxD sequences against the GeneArt codon optimised sequences. The results show the differences among the sequences and also a shift of 44% GC content of the optimised sequence. Based on the results obtained in this study, it is possible to infer that plant codon optimisation may have positively affected the EtxD expression, with the yield of the optimised EtxD protein being high compared to the plant codon-optimised gene (SYNL1) that did not generate detectable L1 protein (Maclean et al., 2010).

The truncated EtxD plant codon-optimised gene was successfully cloned into an Icon deconstructed viral vector system that governed the following: i) EtxD expression was under the control of the nopaline synthase (Nos) promoter, and ii) EtxD expression targeted to cytosol or apoplast into an *A. tumefaciens* GV3101 strain for agroinfiltration into tobacco plants. To illustrate that the MagIcon pro-vectors work with other genes, the *N. benthamiana* leaves that were agroinfiltrated with pICH11599-GFP after three days post-infiltration, were clearly distinguishable from the non-GFP-infiltrated control leaves (Figure 2.6). This was observed by

the fluorescence of GFP in infiltrated leaves versus the non-GFP infiltrated leaves when observed under UV illumination. According to Lagui-Becher et al., (2010), the technique of subcellular targeting can markedly improve the expression yield.

With regard to the biochemical analysis of the EtxD protein in tobacco leaves directed into the apoplast and cytosol subcellular location, the quantification of EtxD in agroinfiltrated leaves was measured at three, six and nine days post-infiltration. SDS-PAGE (Figure 2.7) and the Western Blot analysis (Figure 2.10) showed that the infiltrated samples successfully expressed the 34 kDa EtxD protein together with another tobacco-specific band of about 25 kDa. This band was identified by mass spectrometry to be a *glucan endo-1, 3-beta-glucanase* that is a plant pathogen-related protein (Figure 2.11). *A. tumefaciens*-mediated transient expression induces physiological and regulatory changes in plant cells that lead to the induction of pathogenesis-related (PR) proteins. This then triggers the plant signal transduction pathways that lead to defence associated cell death (Pruss et al., 2008).

The 34 kDa protein EtxD bound with the rabbit anti-guinea pig IgG-HRP conjugated secondary polyclonal antibodies, as shown by the Western Blot analysis. The dramatic decrease of the EtxD protein accumulation in the cytosol is probably the result of cell death beyond the three-day post-infiltration period (Figure 2.7). According to Soosaar et al. (2005), resistance genes in plants confer resistance to a particular virus by triggering localised cell death around the infected areas. It is thus assumed that the cell was not able to produce the protein, hence the observed decline in the EtxD protein. However, with the expression of the EtxD protein into the apoplast, the EtxD protein levels seemed to increase with time (Figure 2.7(II)), which may be the result of recombinant proteins in plants being secreted into the apoplast and becoming trapped into the apoplastic space (Pham et al., 2012). Hence the increase of the EtxD protein levels with time. The EtxD protein expression levels expressed as total soluble protein showed the apoplast-derived EtxD at nine days post-infiltration to be 1,6%, against 1,2% at day three. The ELISA results showed that the highest yields of the EtxD protein were achieved by an apoplast targeting construct and for this reason this construct was chosen for the production of the EtxD recombinant protein in *N. benthamiana*.

## 2.5 Conclusion

Concerning the development of a plant expression system for the production of the EtxD vaccine, it was investigated whether the EtxD protein can be expressed in tobacco plants. To do so, two targeting strategies were adopted and compared: the EtxD protein was directed to the apoplast and cytosol, respectively. EtxD protein expression was measured at three, six and nine days post-infiltration by ELISA from three independent *Agrobacterium* infiltrations. These results achieved are in agreement with Chakauya et al. (2006), namely that subcellular targeting of transient expressed proteins in *N. benthamiana* yields a significant amount of recombinant proteins. The ELISA results of the infiltrated tobacco leaf samples demonstrated the successful expression of the 34 kDa EtxD together with a *glucan-endo-1, 3-beta-glucanase* band of about 25 kDa. The highest yield of 380 mg/kg fw in the transient leaves were achieved by the apoplast targeting strategy. The cytosol generated the lowest EtxD protein production at 300, 200 and 10 mg kg fw three, six and nine dpi respectively. For the large scale-production of EtxD protein, transient expression targeted to the apoplast is preferable because of the high yield per fresh weight achieved in this study. The study has also demonstrated that tobacco is a suitable host for the production of the EtxD protein.

## **Chapter 3**

# **PURIFICATION OF THE ETXD PROTEIN EXPRESSED RECOMBINANTLY IN *NICOTIANA BENTHAMIANA* LEAVES**

## ABSTRACT

Numerous recombinant proteins, including enzymes, antibodies and vaccines, have been expressed in tobacco (Genetic Engineering and Biotechnology News, 2013). Because of this, various methods have been studied to recover and purify these recombinant proteins, as well as some native tobacco proteins. Generally, the purification processes involve one or more affinity steps that offer high selectivity and specificity to the target protein. The objective of this part of the study was to investigate methods of purification to recover and purify the *Epsilon* toxin (EtxD) that was transiently expressed recombinantly in *Nicotiana benthamiana* leaves. Pure EtxD was obtained by employing two purification methods, namely the ion-exchange chromatograph and the size-exclusion chromatograph. The ion-exchange chromatograph results on SDS-PAGE indicated partial purification of the EtxD protein collected in the flow-through. The size-exclusion chromatograph was then employed to further purify the sample. The size-exclusion results on SDS-PAGE displayed a single band corresponding to the 34 kDa size of the EtxD protein. This band was further confirmed by the Western Blot analysis. Almost 50%, or 49,85% to be exact, of the EtxD protein could be recovered after the final step of purification.

## 3.1 Introduction

### 3.1.1 Protein purification from tobacco

In this study, the highest-level expression of the *Epsilon* toxin (EtxD) protein was found to be accumulated in the apoplast of the *Nicotiana benthamiana* leaves, as described in Chapter 2. Next, it was necessary to explore methods that would recover and purify the plant-derived EtxD protein. Unlike proteins expressed in yeast or bacteria, the purification of recombinant proteins is difficult (Abdoli-Nasab et al., 2016). According to the *Genetic Engineering and Biotechnology News* (2013), numerous recombinant proteins, including enzymes, antibodies and vaccines have been expressed in tobacco, and various methods have been studied to recover and purify these recombinant proteins, as well as some native tobacco proteins.

Generally, the purification processes involve one or more affinity steps that offer high selectivity and specificity to the target protein. In one study, a GUS protein with a calmodulin (CaM) affinity tag was purified in a phenothiazine affinity column to 20-fold purification and 85% yield following ammonium sulphate precipitation, dialysis and concentration of the extract (Desai et al., 2002). Similarly, histidine (His) tags have been used to purify recombinant proteins from tobacco using immobilised metal affinity chromatography (IMAC). Cationic peanut peroxidase (CPRX) with the addition of a His-tag to the C-terminal was purified from tobacco using one step of the IMAC. Attachment of a His<sub>6</sub>-tag to lactate dehydrogenase and purification in a Zn<sup>2+</sup>-IMAC column increased yield from 7% to 55% and the purification factor from 21 to 82 (Desai et al., 2002; Bornhorst and Falke, 2015). Ricin, a plant protein toxin, was also purified 288-fold on a lactose-agarose affinity column with 72% recovery (Holler, 2007).

Most studies involve a molecular modification of the target protein and expensive affinity chromatography processes, which may not be feasible in the case of large-scale production of proteins in human therapeutics. There have been a few reports on more generic processes having been used to purify proteins from tobacco leaves or cell suspensions, although most researchers still rely on affinity steps or molecular modification. Recombinant trichosanthin, a basic ribosome-inactivating protein, was purified from tobacco extract by several steps of chromatography, including gel filtration, anion exchange and cation-exchange, but purity and recovery data was not reported (Holler, 2007). A combination of anion exchange (DEAE) and

size-exclusion chromatography (Sephacryl S-200) was used to purify a native tobacco protein, anionic peroxidase (MW 36 kDa, pI 3.5), to a single band on SDS-PAGE with 80% recovery (Holler, 2007). Green fluorescence protein (GFP) fusion proteins were purified from tobacco cell cultures in three main steps (Holler, 2007). Precipitation by ammonium sulphate at 30% (v/v) was first performed to remove particulate matter and aggregated material while maintaining the solubility of GFP (Gutiérrez et al., 2013; Murayama and Kobayashi, 2014). Hydrophobic interaction chromatography was performed next to remove background proteins and to elute the GFP and fusions in a low salt buffer that could then be applied to DEAE chromatography. Secreted alkaline phosphatase (SEAP) and granulocyte-macrophage colony stimulating factor (GM-CSF), both as GFP fusions, as well as GFP itself, were all recovered with yields greater than 70% and estimated purities over 80%.

### **3.1.2 FPLC chromatography**

One or more chromatographic steps are almost always needed to obtain a high level of purity for recombinant protein purification. Chromatographic processes are highly selective, and provide high resolving and separation power. However, these processes are more expensive than other methods and have several limitations (Senstad and Mattiasson, 1989). One limitation is the slow and limited binding capacity owing to diffusion limitations and steric hindrance when the molecules compete for interaction with the stationary phase. Second is the inability to handle crude or viscous extracts that contain impurities and can cause column plugging, column fouling or reduced flow rates. A third limitation is the uncertainty of scale-up as bead deformation changes with higher pressure drops. Fast-performance liquid chromatography (FPLC) is used to purify proteins in most cases as the columns can generally be scaled up for commercial use. There are many different types of chromatography used in FPLC, but the most common ones are the ion exchange, hydrophobic interaction, gel filtration and affinity (FPLC).

Each method has a unique separation principle based on some physical characteristic of the target protein. Ion-exchange chromatography separates proteins based on the overall net charge and charge distribution of the protein. Elution is accomplished by increasing the salt concentration in the buffer, which displaces the bound proteins from the functional ligands of the resin beads (Shen, 2014). Hydrophobic-interaction chromatography separates proteins based on the strength of the interaction between the hydrophobic patches located on the surface

of the protein, and the hydrophobic ligands of the stationary phase. Elution is accomplished by decreasing the chaotropic salt concentration in the buffer, which disrupts the hydrophobic interactions between the bound protein and the stationary phase (Holler, 2007). Gel-filtration or size-exclusion chromatography separates proteins based on their molecular weight, with larger molecules eluted prior to smaller molecules. Affinity chromatography separates proteins on the basis of the interaction with specially designed ligands specific to the target protein, such as antigen-antibody interactions (Holler, 2007). Out of all these methods, affinity chromatography is the most expensive due to the specificity of the designed stationary phases (Holler, 2007).

## **3.2 Materials and methods**

### ***3.2.1 Tobacco leaf protein extract***

About 200 g of agroinfiltrated tobacco leaf and 200 ml, pH 5,4 of extraction buffer containing 200 mM Tris-EDTA-Tween and 20  $\mu$ l of the protease inhibitor (Sigma-Aldrich) comprising 1 mM PMSF (phenylmethylsulphonyl flouride), 1 mM EDTA (ethylenediaminetetraacetic acid), 10  $\mu$ M trans-epoxysuccinyl-L-eucylamido (4-guanidino) butane (E-64) and 10  $\mu$ M pepstatin A to block protease activity, were homogenised in the blender and then filtered through double cheesecloth to remove debris. Subsequently, the homogenate was centrifuged at 13 000 g at 4 °C for ten minutes in the corning 50 ml centrifuge tubes (Merck, South Africa). The resulting supernatant was quantified and stored at 4 °C for further purification.

### ***3.2.2 Protein quantification***

Protein concentration of the leaf-sample supernatant was determined by the Bradford assay (1976) using BIO-RAD protein dye reagent, according to the manufacturer's instructions. Absorbance was measured at 595 nm using the Power Wave HT (BioTek). Bovine serum albumin (Roche, Mannheim, Germany) was used as a standard. To check the purity of the assessed proteins, the purified protein samples were analysed on a 12% SDS-PAGE gel as described by Laemmli (1970).

### ***3.2.3 Ion exchange chromatography***

All chromatographic runs were performed using an AKTA avant 150 (GE Healthcare, South Africa) FPLC system controlled via Unicorn 6.0 software. For anion-exchange experiments, 20 ml Cpto™ Q resin (GE Healthcare, South Africa) packed in an XK16 glass column was used. The flow rate was 5 ml/min and various fraction sizes for different phases were collected in the 15 ml and 50 ml tubes. Fractions collected were then analysed for the presence of the EtxD and other proteins. The column was equilibrated with three column volumes (CV) of buffer A (50 mM diethanolamine, pH 9,5), after which a total of 50 ml of the agroinfiltrated tobacco extract was loaded to the column. This typically corresponded to about 229 mg/ml of crude extract. The flow through was collected in 15 ml fractions. After the sample was loaded, the column was washed with three CV of buffer A to remove unbound proteins. Bound proteins were eluted with a linear gradient of increasing Buffer B (50 mM diethanolamine + 1.0 M NaCl, pH 9,5). The gradient was programmed to span a total of 10 CV. After analysis by SDS-PAGE, fractions containing the protein of interest were pooled.

### ***3.2.4 Size exclusion chromatography***

Size-exclusion chromatography was conducted to further purify the partially purified EtxD protein from the ion exchange chromatography process. Pre-packed Superdex 200 Prep Grade column (GE Healthcare, South Africa) was used for gel infiltration. Fractions containing the EtxD from the ion exchange process were concentrated using a centrifugal ultrafiltration in 15 ml vivaspin tubes (10 000 molecular weight cut-off (MWCO)). The concentrated sample of the partially pure EtxD was injected onto the gel filtration column using a 2 ml capillary loop. The run was conducted in 50 mM diethanolamine buffer, pH 9,5 at a flowrate of 1 ml/min. Then, 2 ml of protein flow-through was collected using a 96-well microtitre plate. Fractions were collected and analysed for EtxD.

### ***3.2.5 Immuno-blotting (Western Blot)***

Proteins were added to an equal volume of a 2x sample loading buffer (90 mM Tris-HCL, pH 6,8, 20% glycerol, 2% SDS, 55 (v/v)  $\beta$ -mercaptoethanol and 0,2% bromophenol blue) and boiled for four minutes. Boiled protein extracts were separated on a 12% (w/v) SDS-PAGE,

according to Laemmli (1970). The proteins separated on SDS-PAGE gels were electroblotted onto a hybond™ membrane (Amersham, UK) at 13 V for one hour at room temperature, using a trans-blot SD machine (Bio-Rad, SA). The membrane was blocked overnight at room temperature with gentle shaking in a solution of 5% (w/v) low-fat milk powder in Tris-buffered saline (TBS-T) containing 0,1% Tween-20. The membrane was then incubated for one hour with gentle shaking in a primary blood antiserum from guinea pig (for detection of EtxD), diluted to 1:5000 in TBS-T, whereupon membranes were washed three times in TBS-T containing 0,5% low-fat milk. This was followed by a one-hour incubation in an anti-goat IgG as the secondary antibody (1:10 000 dilutions) conjugated to horseradish peroxidase (Amersham, UK) in PBST buffer for one hour at room temperature. This was followed by three washes of 10 minutes each in TBS-T containing 0,5% low-fat milk. Detection of labelled proteins was then done by chemiluminescence using an ECL™-plus kit (Amersham, UK) and according to the manufacturer's instructions.

### **3.3 Results**

#### ***3.3.1 Anion exchange chromatography***

The transiently expressed recombinant EtxD protein in *N. benthamiana* leaves showed a high expression profile of the EtxD by ELISA analysis (see Chapter 2). The plants were selected for purification trials. Capto Q ion exchange chromatography was initially selected for the trials. A total of 50 ml extract was loaded into the Capto Q column at the flow rate of 5 ml/min. The chromatogram showing the separation regimes of the proteins appears in Figure 3.1. The agroinfiltrated tobacco extract was eluted in three major peaks indicated by a blue line. The third peak was achieved during a simple linear salt-gradient elution. The flow-through fractions were collected and analysed for purity of the EtxD protein. The accompanying SDS-PAGE gel in Figure 3.2 was performed for the analysis of the selected fractions from all the peaks in the chromatogram.

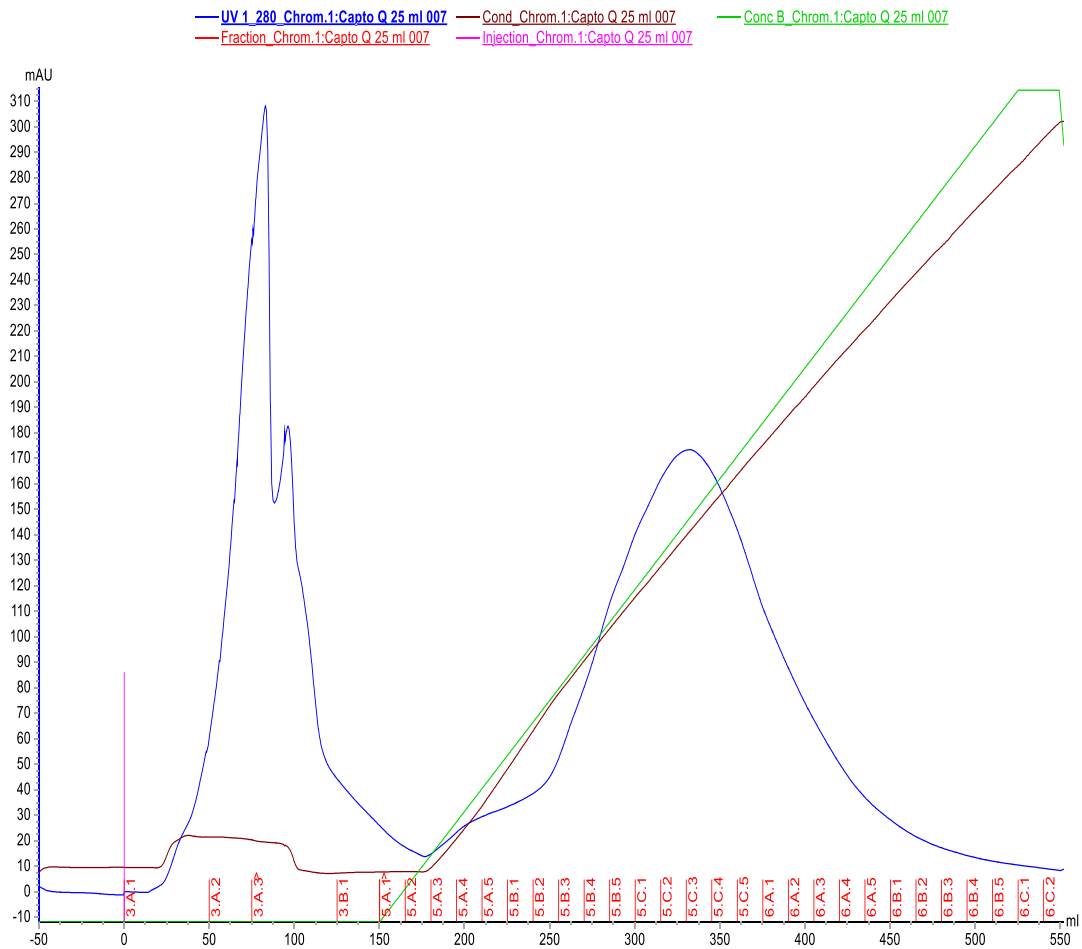


**Figure 3.1: Capto Q anion-exchange chromatography of the agroinfiltrated tobacco leaf extract and corresponding fraction analysis of plant-derived EtxD protein activity.** Results were identical for all the three replicates.

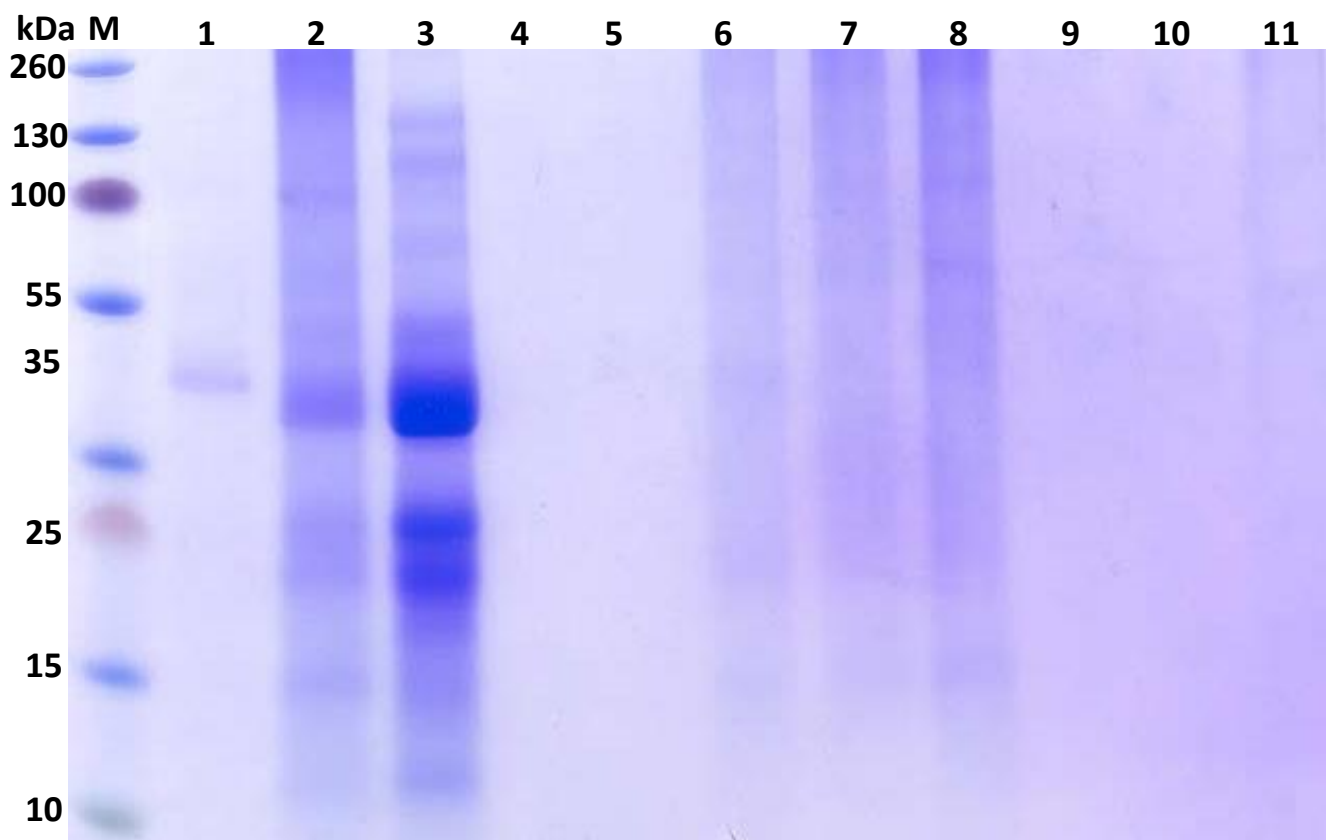


**Figure 3.2: SDS-PAGE analysis of the partially purified EtxD transiently expressed in *N. benthamiana* leaves.** The fractions derived from the major UV peaks from ion exchange chromatography were analysed on a 12% SDS-PAGE gel stained with Coomassie brilliant blue for EtxD purity. Lane M is the PageRuler-stained protein ladder (Fermentas), 1 is the OBP EtxD protein control, 2 is the crude extract, 3 is the flow through (1 A1 in the chromatogram), 4 to 5 represents 3 A1 and 3 A4 in the chromatogram), 6 to 8 represents 5 B5, 5 C1,5 C3, and 9 to 11, 6 A1, 6 A2 and 6 A3.

The Capto Q anion exchange chromatography was carried out to recover the purified EtxD protein from the agroinfiltrated tobacco extracts. Fractions collected from the major peaks were analysed by electrophoresis on 12% SDS-PAGE gel. The OBP EtxD control in lane 1 gave a band of 34 kDa and corresponds to the correct size of the EtxD protein. Lane 2 represents the buffer exchanged crude extract with the transiently expressed 34 kDa protein accompanied by other *N. benthamiana* proteins. Lane 3 represents fraction 1 A1 in Figure 3.1 and corresponds to the flow-through fractions during ion exchange. The result indicated that the greatest part of the EtxD protein in the tobacco extract that was loaded did not bind to the Capto Q column, but was literally eluted in the flow-through with partial purification. Lanes 4 and 5 represent the first peak in Figure 3.1 (fraction 3 A1 and 3 A4). The SDS-PAGE gel shows that there is no EtxD protein activity taking place. Lanes 6 to 8 represents the major peak during a simple

linear salt gradient elution, fractions 5 B5, 5 C1 and 5 C3. The SDS-PAGE gel shows that a few proteins still appear and may likely be other negatively-charged native tobacco proteins. Lanes 9 to 11 in Figure 3.1 represents the fractions after the peak 6 A1 to 6 A3; the SDS-PAGE gel shows no protein bands. It is clear from the SDS-PAGE that the greatest part of the EtxD protein was in the flow-through and that partial purification only had occurred.

### 3.3.2 Size-exclusion chromatography

As the EtxD protein sample was not purified and could not be separated from other tobacco native proteins such as the RuBisCO (55 kDa on the SDS-polyacrylamide gel) with the ion-exchange chromatograph, 90 ml of the flow-through was concentrated down to 5 ml and size-exclusion chromatography (Superdex) was employed as a second process to remove the contaminating proteins on the sample. The chromatogram in Figure 3.3 shows the results of the size-exclusion chromatography.

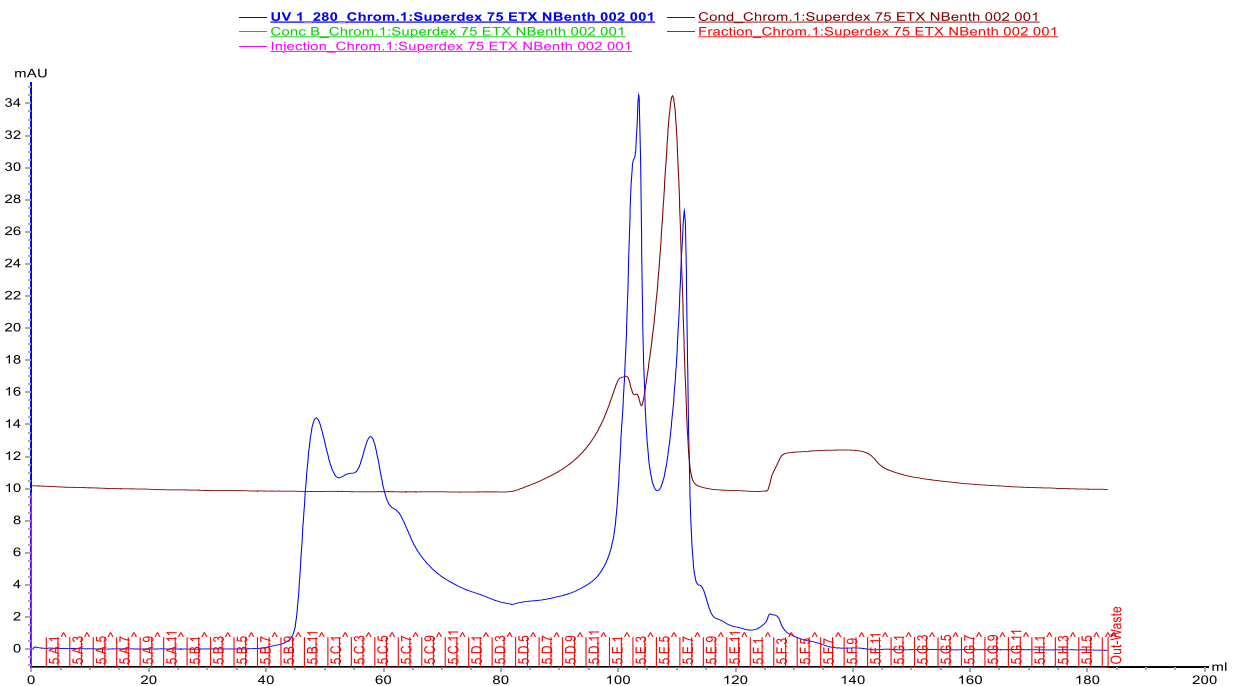


**Figure 3.3: Chromatogram of Superdex 75 gel-filtration chromatography of the unpurified EtxD sample.**

The EtxD sample fractions were collected from the size exclusion chromatogram and run on an SDS PAGE to confirm the presence of EtxD as seen in Figure 3.4 below.

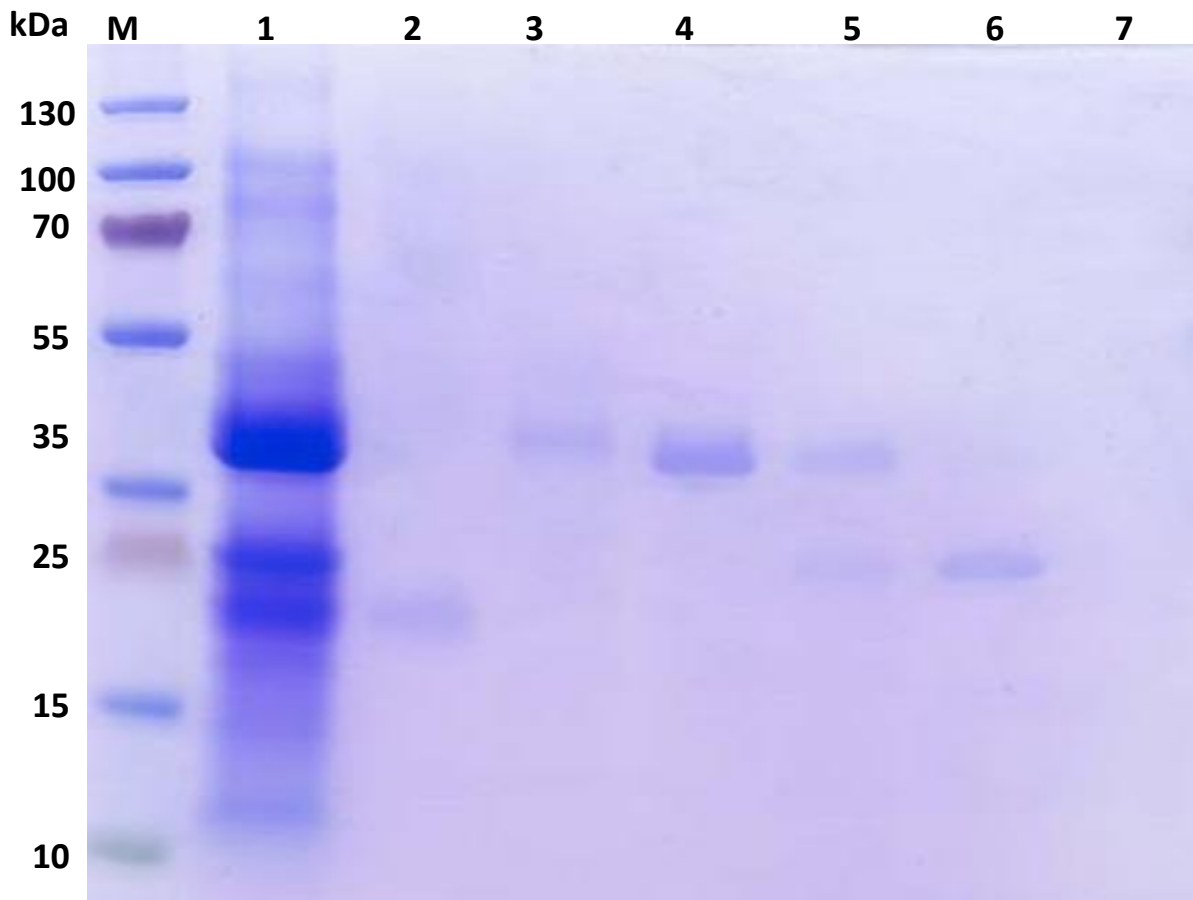


**Figure 3.4: SDS-PAGE analysis of the purified EtxD transiently expressed in *N. benthamiana* leaves purified with a gel filtration.** The purified EtxD was analysed on a 12% SDS-PAGE gel stained with Coomassie Brilliant Blue. Lane M represents the PageRuler-stained protein ladder (Fermentas), Lane 1 represents the concentrated flow through collected from the previous ion exchange chromatography processes, Lane 2 represents 5 B11 in the chromatogram, Lanes 3 to 5 the first peak, and lanes 6 to 7 the second peak indicated with the blue line in the chromatogram.

The SDS-PAGE gel in Figure 3.4 was performed for the analysis of the partially purified samples that were further purified by Superdex size-exclusion chromatograph. The partially purified concentrated sample in lane 1 shows the band of interest at 34 kDa, which corresponds to the correct size of the EtxD protein but is still accompanied by some tobacco native proteins. Lane 2 (5 B11 in the chromatogram) and 3 represents the first peak in the chromatogram shown in Figure 3.3. According to the SDS-PAGE, fraction 5 B11 only shows a single band that is less than 34 kDa. Lanes 3 to 5 represent the fractions from the second peak. Lanes 3 (5 C4 in the chromatogram) and 4 (5 C8 in the chromatogram) show a single band that corresponds to the 34 kDa of the partially purified sample. The 34 kDa protein in lane 4 is fatter than the one

in lane 3, which could be the result of 5 C8 being on top of the peak. Lane 5 (fraction 5C9 on the chromatogram) shows two bands, with the top band size corresponding to the EtxD protein. The lower band accompanying the EtxD protein could arise from the overlapping of peaks. Lane 6 (fraction E3 on the chromatogram) represents the third peak. It only shows a single band that does not correspond to the size of the EtxD. Lane 7 (fraction E7 in the chromatogram), represents the fourth peak, which does not show any band or activity on the SDS-PAGE. Based on the SDS-PAGE results, individual fractions from the second peak (C3 to C8) on the chromatogram were then pooled and run together with buffer-exchanged crude extract and the Capto Q ion exchange unpurified sample on the SDS-PAGE in Figure 35 below.

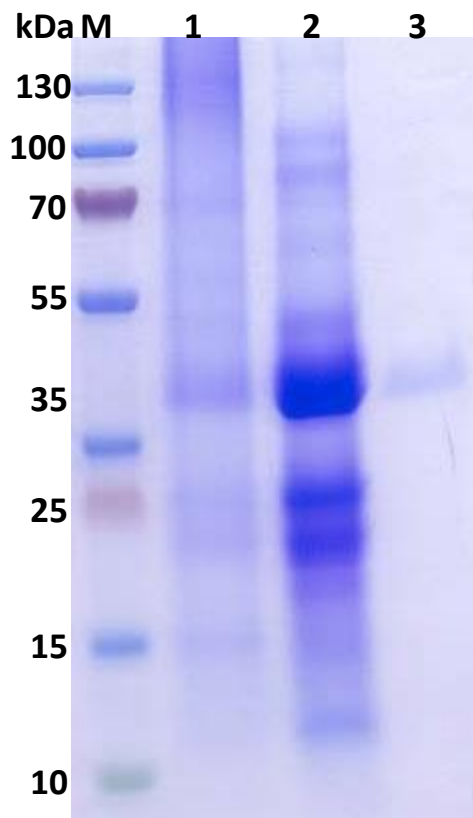


**Figure 3.5: SDS-PAGE (12%) analysis of the purified EtxD protein fractions pooled together.** M represents the PageRuler-stained protein ladder (Fermentas), lane 1 the tobacco crude extract, lane 2 the concentrated unpurified sample via the ion exchange chromatography, and lane 3 the purified fractions via the gel infiltration chromatography that were pooled together.

The SDS-PAGE in Figure 3.5 shows the results of the two-step purification required to purify the transient-expressed EtxD protein from the crude *N. benthamiana* leaves extract. Lane 1 represents the crude extract, with the band corresponding to 34 kDa of the EtxD protein that

was buffer exchanged with 50 mM ethanol diamine, pH 9,5. Lane 2 represents the partially purified sample via Capto Q ion exchange chromatograph and lane 3 the purified EtxD protein via Superdex gel infiltration chromatograph. The purified EtxD protein was later trypsinated and confirmed by the Western Blot analysis (Figure 3.6).

### 3.3.4 Confirmation of the purified protein

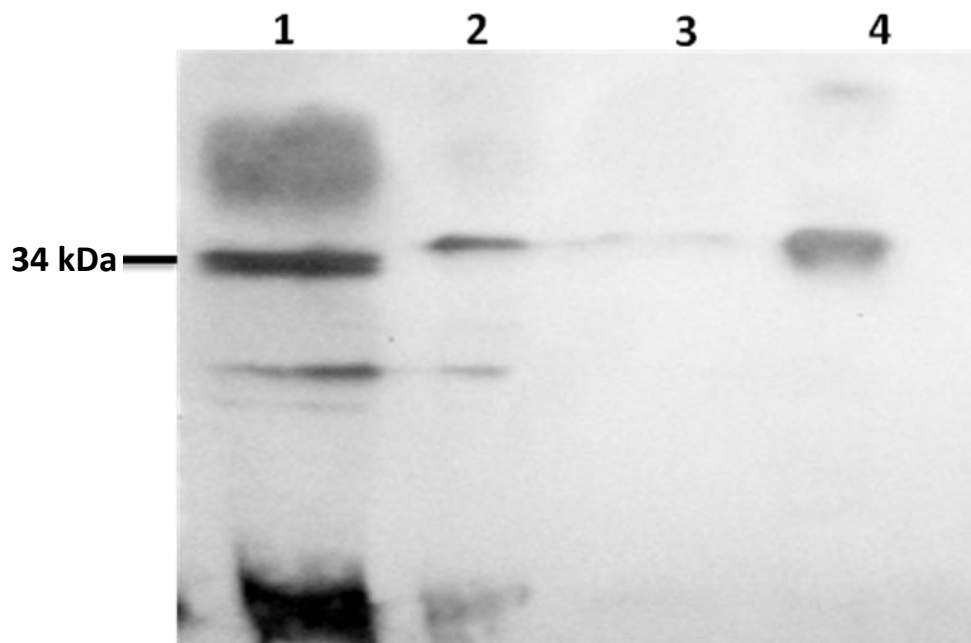


**Figure 3.6: The Western Blot analysis of the EtxD.** The recombinant gene was expressed in tobacco leaves and separated by SDS-PAGE on a 12% polyacrylamide gradient gel and probed with an anti-guinea pig polyclonal antibody. Lane 1 represents the OBP EtxD protein control showing the band of interest at 34 kDa, the other numbers are depicted on top of the gel image Lanes 2 to 4 correspond to the following: 2 is the trypsinated OBP EtxD protein, 3 is the trypsinated purified sample via gel filtration chromatography and 4 is the purified sample via gel filtration chromatography.

The EtxD protein was detected by the Western Blot analysis (Figure 3.6). The levels of recovery and confirmation of the identity of the protein produced were further investigated with the Western Blot analysis and the Bradford Assay. The fractions were pooled and then separated using SDS-PAGE alongside the OBP sample standard. After this they were electroblotted onto a hybond<sup>TM</sup> membrane (Amersham, UK) and then detected by chemiluminescence using an ECL. The OBP standard showed one major band of approximately 28 kDa and a faint band at slightly bigger molecular weight between 32 kDa

and 35 kDa, as expected by OBP. The plant purified extract via Capto Q and Superdex gel filtration had a single detectable protein band at the same size as the positive control at 34 kDa corresponding to the size of EtxD protein. To report the efficiency of the EtxD protein purification, it was important to calculate the protein recovery after the Capto Q ion-exchange and the Superdex size-exclusion chromatography methods employed for purification. Therefore, protein recovery was calculated by dividing the protein concentration in the sample by the protein concentration in the original sample. Table 3.1 shows the percentage protein recovery.

**Table 3.1: The protein efficiency recovery for the EtxD**

<b>Protein</b>	<b>Volume</b>	<b>Original total protein</b>	<b>Total protein after ion-exchange purification</b>	<b>Total protein after gel filtration purification</b>	<b>Recovery protein</b>
EtxD	50	229 mg/ml	110 mg/ml	55 mg/ml	49,56%

The protein recovery table indicates that 49,56% of the EtxD protein was recovered after purification. It also shows that almost half of the protein is lost during buffer exchange.

### **3.4 Discussion**

The apoplast directed sample that showed a high ELISA expression of the EtxD protein was then selected for purification via the Capto Q ion-exchange chromatography. The Capto Q anion exchange and size exclusion (Superdex 200-pg) chromatography were employed to optimise the purification of the EtxD protein that was transiently expressed in *N. benthamiana* leaf extracts. With the Capto Q anion exchange chromatograph, the EtxD sample showed a partial purification on the SDS-PAGE (Figure 3.2), most likely because of a significant reduction in native proteins such as RuBisCO. Tobacco leaves contain an extremely high amount of native phenolic compounds, up to 30 mg/g dry weight, and toxic alkaloids, such as nicotine, that must be removed during the purification process (Moloney, 1995). According to Moloney, the overall charge of a protein depends on the protein's isoelectric point (pI), which is the pH where the protein will have a net charge of zero. At a system pH above the isoelectric point, the protein is negatively charged and at a pH below the isoelectric point the protein is

positively charged. The system pH could be adjusted to change the protein's overall net charge. However, most proteins have a small, defined pH range in which they will remain biologically active.

According to Deepika et al. (2010), the isoelectric pH for the native EtxD toxin is 5,4. Therefore, in this study, the extraction of protein was still carried out at pH 7,5, which is an optimal pH for extracting proteins from tobacco samples. Subsequently, the sample was buffer exchanged from 200 mM Tris-EDTA-Tween pH 7,5 to 50 mM ethanoldiamine pH 9,5 at 4 °C and then eluted on the Capto Q anion exchange chromatography. The chromatography results in Figure 3.3 were analysed on the SDS-PAGE gel to obtain the analysis shown in Figure 3.4. This showed a single band the same size as the OBP control at 34 kDa, and was subsequently confirmed on the Western Blot analysis (Figure 3.6) as the EtxD protein. This protein, at pH 9,5, showed instability by precipitating. To prevent protein degradation, it was decided that immediately after size exclusion purification, to buffer exchange to 200 mM Tris-EDTA-Tween pH 7,5, where the protein shows stability. The SDS-PAGE and Western Blot analysis results in Figure 3.6 clearly shown that the purification was achieved, and that the recovery was almost 50%.

### **3.5 Conclusion**

It has been shown in this study that a transiently expressed EtxD protein can be efficiently purified from tobacco to a high standard and yield in just two main steps after the initial extraction. A 50% product yield, based on the initial recombinant EtxD protein concentration, was obtained after the final step, while achieving purity as judged by the Coomassie stained SDS-PAGE. The results suggest that the transiently expressed EtxD protein may be efficiently purified from *N. benthamiana* extract. The purification steps incorporated in this study suggest that the purification method has the potential of being scaled up for large scale production.

## **Chapter 4**

# **CYTOTOXICITY AND EFFICACY OF THE PLANT-DERIVED EtxD ANTIGEN**

## ABSTRACT

The objectives of the study were to investigate the suitability of the plant-derived purified EtxD as an antigen for the Pulpy Kidney Disease vaccine production, evaluate the toxicity of the plant-derived EtxD and test the efficacy of the plant-derived EtxD. To achieve this, both *in vitro* and *in vivo* studies were conducted. The LD<sub>50</sub> studies on mice revealed that the plant-derived EtxD is slightly toxic, which correlated with the IC<sub>50</sub> results on the Mandin-Darby Canine Kidney (MDCK) cells. For the animal challenge results, two formulations of vaccines were prepared from the recombinant antigens EtxD and administered to the mice. Onderstepoort Biological Products (OBP) Pulpy Kidney Disease vaccine and Pulpyvax (Intervet) were used as positive controls. Saline was used as a negative control. The mice that received the negative control were killed when challenged with *Epsilon* toxin, proving the toxicity of the toxin, as well as demonstrating the need of a viable antigen to protect the mice being treated with the active *Epsilon* toxin. The formulations that contained the plant-derived EtxD that was not activated by trypsin were unable to protect mice against the *Epsilon* toxin challenge, indicating that the toxin in the purified plant extract was not immunogenic. When the plant-derived EtxD was treated with trypsin, inactivated with formalin and formulated with the adjuvant, alum, it was still not protective. However, the formulation containing plant-derived EtxD and the DCA-immune stimulant, was protective. These findings indicated that the plant-derived *Epsilon* toxin is a viable recombinant antigenic vaccine when formulated with the immunostimulant DCA. It is now necessary to evaluate the plant-derived vaccine in larger animal studies to define a dosage regime.

## 4. INTRODUCTION

### 4.1 Current production and formulation methods of the Pulpy Kidney Disease vaccine

The *Epsilon*-toxin (Etx) is produced by *Clostridium perfringens* types B and D and represents the major pathogenicity factor of these bacteria. EtxD is one of the most potent clostridial toxins after botulinum and tetanus neurotoxins (Jemal et al., 2016). It is responsible for the pathogenesis of the fatal enterotoxaemia in sheep, goats, calves and other domestic animals (Payne et al.; Jemal et al., 2016; Bath et al., 2016). Absorption of the toxin through the intestinal mucosa and its spread into all the organs by the bloodstream induces blood pressure elevations and edema in various organs (Goldstein et al., 2009; Jemal et al., 2016). EtxD can also cross the blood-brain barrier, causing perivascular edemas, neuronal damage and the excessive release of glutamate from the hippo-campus neurons (Miyamoto et al., 2000). The inactive protoxin is encoded by the *etx* gene and must be activated after secretion by protease cleavage of the 13 and 29 residues at the N and C-termini, respectively (Minami et al., 1997). Activation normally occurs in the gut of the infected animals by the action of trypsin,  $\alpha$ -chymotrypsin or *C. perfringens* lambda protease, but activation can also occur in vitro. Cleavage of the C-terminal residues is essential for the biological activity and the ability to form large sodium dodecyl sulphate (SDS) resistant heptameric complexes in rat synaptosomal membranes (Miyata et al. 2001). EtxD acts on MDCK cells (Miyata et al. 2001), where it causes a decrease in intracellular  $K^+$ , while increasing in  $Cl^-$  and  $Na^+$  (Bokori-Brown, 2011). The toxin preferentially binds to isolated detergent resistant microdomains (DRMs), suggesting that a putative receptor located in the DRMs is responsible for the toxin binding and its subsequent heptamerisation.

#### 4.1.1 Pulpy Kidney Disease vaccine

A number of commercially available vaccines exist for the prevention of *C. perfringens* enterotoxaemia, which have been used extensively over the past decades to prevent diseases in domesticated livestock. The vaccines are typically prepared by treating *C. perfringens* type-D culture filtrate with formaldehyde to toxoid components. Since relatively crude culture filtrates are used, the vaccines are likely to contain additional proteins other than the *Epsilon* toxoid. The typical immunisation regimens involve an initial course of two doses of vaccine, two to

six weeks apart. Sheep are boosted annually, whereas goats are boosted after every three to four months (Bokori-Brown et al., 2011). Adjuvants, such as aluminium hydroxide, are often used. These vaccines confer protection in animals if they induce antibody titres equivalent to five international units (IU) of antitoxin. However, these vaccines have several drawbacks. The immunogenicity of the *Epsilon* toxoid in some vaccine preparations has been reported to be poor or variable (Lobato et al., 2010; Bokori-Brown et al., 2011), and inflammatory responses following vaccination have been reported to lead to reduced food consumption (Stokka et al., 1994; Bokori-Brown et al., 2011).

Attempts to improve vaccine efficacy using a liposome formulation have reportedly not been successful (Uzal et al., 1999; Bokori-Brown et al., 2011) together with the use of formalin to lower the toxic level of the Etx. First, it is generally accepted that chemical inactivation with formalin is difficult to standardise and second, classical methods of detoxification usually alter the overall protein structure in a random manner. Consequently, the immunogenicity of the vaccine is severely decreased. Third, there is a narrow band to balance the detoxification (strength of formalin used from the commonly used 1%) and the immunogenicity of the vaccine (Robertson et al., 2011). Because of these difficulties, alternatives to formalin inactivation have been proposed, including ectopically expressing mutated toxoids in other gram-positive microorganisms. A method for the reliable production of *Epsilon* toxoid vaccines remains one of the challenges facing the veterinary vaccine industry. One approach to solving this problem would involve using genetic engineering to produce the toxin and then use this recombinant protein for toxoiding. For this reason, this study proposed to produce a less toxic *Epsilon* toxoid vaccine recombinantly in plants.

There has been significant interest in the potential value of antibodies against *Epsilon* toxin for the prevention of enterotoxaemia caused by the  $\epsilon$ -toxin. The passive transfer of polyclonal antisera against the toxin into new-born lambs has reportedly been achieved either by injection (Odendaal and Astruc, 1989; Bokori-Brown et al., 2011) or by feeding the animals colostrum that contains antibodies reactive with the *Epsilon* toxin (Bokori-Brown et al., 2011).

The objectives of this part of the study were to –

1. Investigate the suitability of the plant-derived EtxD as an antigen for Pulpy Kidney Disease vaccine production;
2. Evaluate the toxicity of the plant-derived EtxD; and
3. Test the efficacy of the plant-derived EtxD.

The only practical means of control of the disease is by immunisation and avoiding circumstances that are conducive to the occurrence of the disease. All currently available Pulpy Kidney Disease vaccines in South Africa are based on the formalinised toxoids of the *C. perfringens* (Welchii) type D, either as an alum-precipitated or oil emulsion formulation of the whole cell culture or bacterial culture filtrates (Deepika, 2010). OBP has been supplying these vaccine formulations for some time. The *Epsilon* toxin is usually obtained from a *C. perfringens* type-D strain and has been purified either individually or in combination by methanol precipitation, ammonium sulphate precipitation, column chromatography, size exclusion and various other forms of ion-exchange chromatography. Traditionally, the activity of the purified *Epsilon* toxin has been determined in mouse lethality tests (Deepika, 2010).

## **4.2 Materials and methods**

### ***4.2.1. Reagents and cultures***

The mammalian MDCK cell line used was a gift from CSIR Biosciences in Pretoria. The chemicals and growth media used to maintain cell growth were purchased from Sigma-Aldrich (St. Louis, Mo.). These materials include the Dulbecco's Modified Eagle's Medium (DMEM), Fetal Bovine Serum (10%), 0,05 mg/ml of gentamycin, trypsin/EDTA and phosphate-buffered saline (PBS). Trypan-blue stain and emetine were also purchased from Sigma-Aldrich, while a CellTiter 96® AQueous Non-Radioactive Cell Proliferation Assay kit was purchased from Promega (Madison, USA).

### ***4.2.2 Trypsin-activation and formalin treatment of antigens***

The EtxD plant-derived partial-purified sample was treated with EtxD (trypsin-activated) + aluminium phosphate and EtxD (trypsin-activated) + DCA immune stimulant.

## **4.3 Methodology**

### ***4.3.1 Tobacco leaf protein extract***

The leaf protein from the agroinfiltrated *N. benthamiana* leaves transiently expressing the EtxD protein was extracted as described in section 2.2.11.

### ***4.3.2 Protein quantification***

Protein concentration of 100 µg/ml of the leaf-derived sample supernatant was determined by the Bradford assay (1976), as described in section 2.2.12

### ***4.3.3 Ion exchange and size exclusion chromatograph***

Chromatography experiments were performed using an AKTA Explorer 100 (GE Healthcare, SA) fast-performance liquid chromatography (FPLC) system-controlled by Unicorn software, as described in section 3.3.

### ***4.3.4 Immuno-blotting***

The protein was resolved using SDS-PAGE and were electro-transferred onto a nitrocellulose membrane, whereafter it was immunoblotted with antiserum from guinea pig as the primary antibody and rabbit anti-guinea pig IGg-HRP (horseradish peroxidase) (Amersham, UK), conjugated as the secondary antibody.

### ***4.3.5 Preparation of trypsin for activation of Epsilon toxin***

Trypsin (Biochrom Trypsin/EDTA solution, Cat. no. L2163, supplied by the Scientific Group) was prepared by allowing the trypsin solution to melt and mixing it well by swirling. The trypsin solution (1 ml) was transferred to a 1,5 ml microcentrifuge tube before 0,7 µl of a 1 M MgSO<sub>4</sub> or MgCl<sub>2</sub> was added. After mixing well by inversion, the Mg-treated trypsin solution was aliquoted in 100 µl volumes into microcentrifuge tubes and stored at -20°C.

### ***4.3.6 MDCK cells in vitro cytotoxin***

#### ***4.3.6.1 The trypan-blue exclusion method:***

This method was used to test the toxicity of the EtxD protein onto the MDCK cell line. The reactivity of trypan blue is results from the fact that the chromophore is negatively charged and does not interact with the cell unless the membrane is damaged. In other words, live cells with intact cell membranes do not take up trypan blue and therefore do not get coloured. All the cells that exclude the dye are thus considered viable. Dead cells with damaged cell membranes are clearly visible under light microscopy because of their distinctive blue colour.

Mammalian cells (MDCK) were seeded in 100 mm tissue-culture dishes with 10 ml culture media at a density of  $1 \times 10^5$  cells/cm<sup>2</sup> and grown for 24 h in DMEM to allow the cells to express their characteristic morphologies. The cells were washed three times with PBS and treated with 20 µM of the EtxD protein for 24 hours. As a control, selected dishes containing MDCK cells were not treated with the trypsin-EtxD. After the 24-hour period, the cells were detached from the surface area with 1 ml trypsin/EDTA and neutralised with the culturing media. Cell viability was determined as described above. To count the cells after the trypsinisation step, the cells were pelleted by centrifugation at 3 000 g at 4 °C for five minutes. The supernatant was carefully discarded so as not to disturb the pellet. The same amount of PBS was added to wash the cells and again subjected to centrifugation at 3 000 g at 4 °C for five minutes. The supernatant was discarded and a small quantity of cells in the pellet was transferred into a sterile 15 ml centrifuge tube. An adequate amount of DMEM was added and mixed well to disperse the cells and form a suspension consisting of single cells (i.e. not agglomerates of cells).

About 0,1 ml of the cell suspension was aliquoted into a 1 ml sample tube and 0,1 ml of 0,4% trypan-blue stain solution was added and mixed thoroughly and allowed to stand for two minutes. With a cover-slip in place, a small quantity of trypan-blue cell suspension was transferred to a chamber of a haemocytometer. This was achieved by carefully touching the edge of the cover-slip with the pipette tip and allowing the chamber to fill by capillary action. Cells were enumerated microscopically using a light microscope (Carl Zeiss, USA). As only live cells do not take up the trypan-blue dye, this allows the calculation of the percentage of viable cells.

#### ***4.3.7 MTS assay method***

A quantitative colorimetric method for mammalian cell survival and proliferation, the CellTiter 96® AQueous non-radioactive cell proliferation assay was used to determine cell viability in the presence of the EtxD protein. This method is composed of solutions of a novel tetrazolium compound (3-(4,5-dimethylthiazol-2-yl)-5-(3-carboxymethoxyphenyl)-2-(4-sulfophenyl)-2H-tetrazolium, inner salt) (MTS), an electron coupling reagent (phenazine methosulfate; PMS) (Vistica, 1991). The MTS assay is based on the reduction of the yellow colour of MTS by mitochondrial dehydrogenase enzymes of metabolically active cells to a soluble blue formazan (Mosmann, 1983). The quantity of the bioreduced MTS product (formazan) is measurable by absorbance at a wavelength of 490 nm. This quantity is directly proportional to the number of living cells in a culture. Emetine was used as a positive control as it is known to inhibit eukaryotic protein synthesis. This antiprotozoal agent inhibits protein synthesis by blocking translocation of the peptidyl-tRNA in the ribosome and thereby causing cell death (Noriss and Ravdin, 1990).

MDCK cells were seeded in 96 well plates in 200 µl of culture medium at a density of 1 x 10<sup>4</sup> cells/well. They were grown for 24 hours in a DMEM culturing medium to allow cells to adhere and retain their characteristic morphology. The cells were then washed three times with PBS and the dispersions of PLGA were prepared in DMEM. The MDCK cells were thereafter treated with 100 µl of 0,14, 1,23, 11,11 and 100,00 µM suspensions of the EtxD protein at 37 °C, 5% CO<sub>2</sub> and 90% humidity conditions for 24 hours. After this, 20 µl of a 20:1 mixture of MTS and PMS was added into each of the 96 test wells without removing any medium. The

plate was then incubated for another three hours. The wells were then measured by reading the absorbance at 490 nm in a spectrophotometric microtiterplate reader (Tecan Infinite F500, Männedorf, Switzerland) against blank wells (wells with only DMEM). The background absorbance at 690 nm was subtracted. Cells incubated with DMEM alone were used as a control. The cell viability was then expressed as a percentage using a 3 000 rpm at 4 °C for five minutes, as shown in the equation:

$$\text{Cell Viability (\%)} = (\text{OD sample}/\text{OD control}) \times 100$$

Where:

OD sample = optical density of a test compound

OD control = optical density of the control (untreated wells)

#### ***4.3.8 Mice in vivo cytotoxicity***

Items that were tested in vivo included the EtxD (200 µg/ml) derived recombinant *Epsilon* toxin from *C. perfringens* and the natural *Epsilon* toxin supplied by OBP. Culture supernatants of *C. perfringens* type D were supplied by Disease Control Africa.

**4.3.8.1 Controls:** The controls were test substances not treated with trypsin. The buffer in which the test substances were supplied was TBS pH10.

#### ***4.3.9 Trypsin treatment of the recombinant Epsilon toxin (activation)***

Each sample was treated with 100 µl of the prepared trypsin for 30 minutes at 37 °C. Subsequently, 10<sup>-1</sup>, 10<sup>-2</sup> and 10<sup>-3</sup> dilutions of the 100 µg/ml were made and then stored at 4 °C. Two mice were used for each dilution and 200 µl of the trypsinated samples were administered intravenously via the tail vein within 60 minutes. The remaining samples were stored at -20°C. The mice were observed twice daily for morbidity and mortality. Animals in extremis were terminated humanely and considered to have died as a result of the toxicity of the samples. The test samples were then analysed by the Western Blot analysis.

#### ***4.3.10 Preparation of the plant-derived EtxD antigen***

The EtxD plant-derived antigen (3 ml) was trypsinated with 300 µl of the Mg-trypsin solution at 37 °C for 30 minutes. The trypsinated EtxD antigen was then equilibrated at room temperature for 10 minutes. Subsequently 9,9 µl of formalin was added and then incubated overnight at 37 °C to inactivate the trypsin activity.

#### ***4.3.11 Adsorption of the trypsin-activated and formalin-treated antigen into aluminium phosphate***

The EtxD plant-derived antigen was removed from the 37 °C incubating temperature and equilibrated at room temperature for 10 minutes. A 1,6 ml aliquot of the trypsin-activated and formalin-treated preparations were then transferred to a 5 ml tube and the remaining sample stored at -20°C. The aluminium phosphate preparation was resuspended by gently shaking the bottle. Then, 1,6 ml of aluminium phosphate was added to the EtxD plant-derived antigen and stored at 4 °C. The remaining EtxD plant-derived antigen was removed from -20°C and allowed to thaw, after which 1,6 ml of the EtxD antigen was transferred to a clean tube. The aluminium phosphate preparation was resuspended by gentle shaking. Then 1,6 ml of the aluminium phosphate was added to 1,6 ml of the EtxD plant-derived antigen and mixed well. The mixture was incubated on the shaker at 60 rpm for two hours and then stored at 4 °C.

#### ***4.3.12 Preparation of the EtxD (trypsin activated) + DCA immune stimulant***

The trypsin-activated and formalin-treated samples were removed from the incubator and equilibrated at room temperature for 10 minutes. Subsequently, 1,6 ml of the trypsin-activated and formalin-treated preparations were transferred to 5 ml tubes and 1.6 ml of saline added. Subsequently, 2 µg/ml of the DCA immune stimulant was added, mixed well and stored at 4 °C.

#### ***4.3.13 Vaccination and challenge of experimental animals***

Six animals (Balb/C mice (6 to 8 weeks of age, mass about 20 +/-2g/animal) were used for each vaccination. Different dilutions of 100 µg/ml of the vaccine formulation were administered to each mouse, see Table 4.1. The mice were vaccinated two times with various preparations of the recombinant *Epsilon* toxin. The vaccine administration was subcutaneously undertaken in the neck area. The booster dose was administered 21 days after the first dose was given. The mice were observed twice daily for morbidity and mortality. Animals in extremis were terminated humanely and regarded to have died as a result of the toxicity of the sample.

#### ***4.3.14 Collection of the blood from mice***

At the termination of the experiment, blood was collected from the animals by bleeding them from the heart. The blood was allowed to clot, and the serum was separated and stored at below 0 °C.

#### ***4.3.15 Ethical considerations***

All experiments were approved by the necessary ethics committees at the Council of Science and Industrial Research (CSIR) and Onderstepoort Biological Products (OBP).

### **4.4 Results**

#### ***4.4.1 In vitro studies of the plant-derived EtxD on MDCK cells***

The cytotoxicity of the plant-derived trypsin activated *Epsilon* toxin was determined using the MDCK cells. For this, a quantitative calorimetric method for mammalian cell survival and proliferation (CellTiter 96® Aqueous non-radioactive cell proliferation assay (Promega)) was used to determine the cell viability. Microscopic observation was carried out as indicators for cell viability. MDCK cells were quantified spectrophotometrically to determine the toxicity of the plant-derived trypsinated EtxD compared with the emetine (Figure 4.1). To determine the dose of the Epsilon-toxin needed to kill 50% of the MDCK cells (IC<sub>50</sub>), the cells were incubated

with serial dilutions (0,001-0,1  $\mu\text{g/ml}$ ) of the trypsin-treated *Epsilon*-prototoxin and emetine (Figure 4.2).

The  $\text{IC}_{50}$  graph (Figure 4.1A) represents the MDCK cells that were treated with the purified plant-derived trypsin activated EtxD. The  $\text{IC}_{50}$  graph (Figure 4.1B) represent the MDCK cells that were treated with the emetine. The  $\text{IC}_{50}$  was calculated by nonlinear regression analysis of the data presented in Figure 4.1. According to the  $\text{IC}_{50}$  results the plant-derived EtxD induces the 50% inhibitory concentration at 27  $\mu\text{g/ml}$ . While the emetine induces the 50% inhibitory concentration at 0.95  $\mu\text{g/ml}$ . Furthermore, the  $\text{IC}_{50}$  results reveals that the plant-derived EtxD is less toxic than emetine at the same concentration of 100  $\mu\text{g/ml}$ .

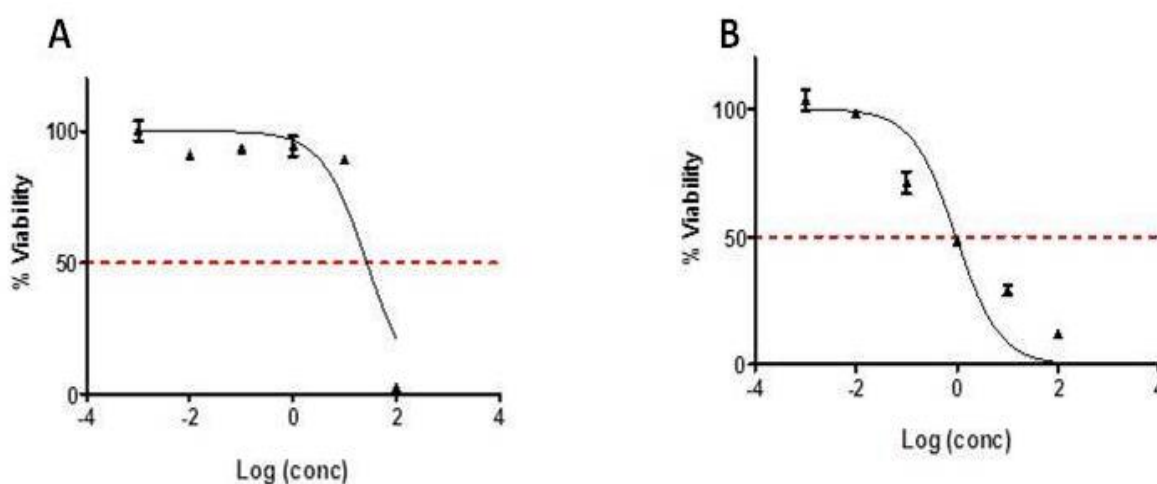


**Figure 4.1: Graphs showing the determination of  $\text{IC}_{50}$  of the EtxD protein.** Cell viability of the MDCK cells ( $4 \times 10^5$  cells/ml) treated with the EtxD was measured by MTS assay and is expressed relative to the untreated cells (control). The MDCK cells that were incubated for a 24 h period with serial dilutions of 100  $\mu\text{g/ml}$  EtxD (0,001–0,1  $\mu\text{g/ml}$ ) at 37  $^{\circ}\text{C}$ . Each data point represents the mean and the standard deviation of three different independent experiments conducted in triplicates. (A) represents the MDCK cells that were treated with the purified plant-derived trypsin activated EtxD and (B) represent the MDCK cells that were treated with the emetine.

Subsequently, the cytotoxic activity of the purified EtxD was assessed by observing its effects onto the MDCK cells, which correlates well with the standard mouse lethality tests. The purified plant-derived-trypsin activated EtxD-induced morphological changes, including an elongation of cells, the formation of membrane blebs and a clumping and detachment of cells

from the substratum. The changes were very rapid, ultimately leading to cell death, indicating that the EtxD was biologically active (Figure 4.2).

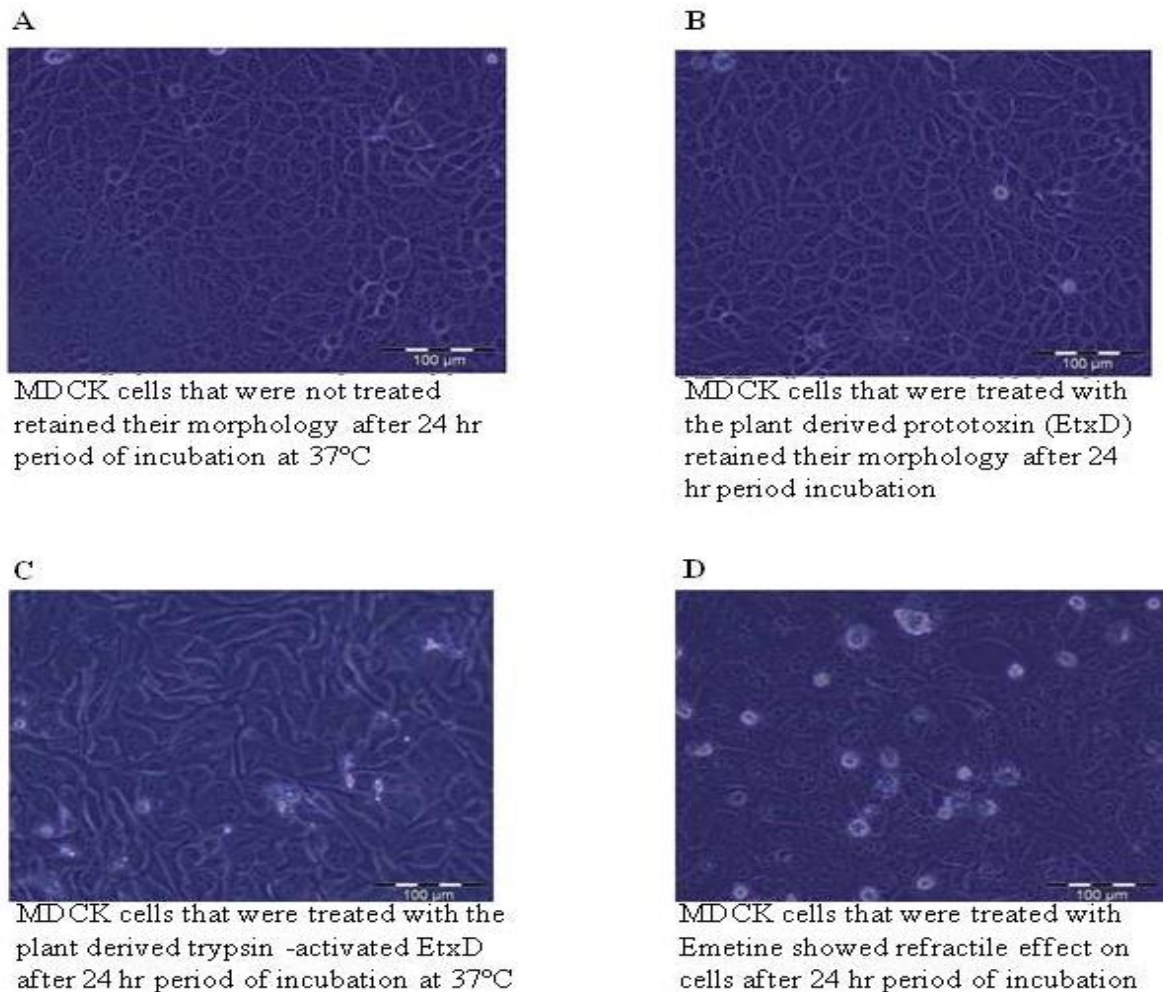


**Figure 4.2: Microscopy images showing the biological activity of the plant-derived-purified EtxD.** (A) MDCK cells that were not treated with EtxD protein. (B) MDCK cells that were treated with non-trypsinated EtxD protein. (C) Effect of the EtxD in MDCK cells. (D) Effect of the emetine on MDCK cells. Images ( $\times 40$ ) showing morphological changes in the MDCK cells treated with the EtxD (30  $\mu\text{g}/\text{ml}$ ) for a 24-hour period.

An MTS assay of cells treated with the same EtxD concentration as the standard (emetine), revealed the plant-derived EtxD to be cytotoxic. Light microscopic examination showed a layer of well-spread, adhering cells after a 24-hour period of incubation in the MDCK culture cells that were not treated (Figure 4.2A). For the MDCK culture cells that were treated with the non-trypsinated EtxD protein, the light microscopic examination showed no change or effect (Figure 4.2B). The cells retained their morphology as in the non-treated MDCK cells, which could be because the plant-derived prototoxin (EtxD) is not toxic. Proportionally, larger and

poorly adhering cells with elongated or spiderlike appearance were observed in the MDCK cells that were treated with the trypsinated EtxD protein (Figure 4.2C). This effect could be due to the toxic character of the plant-derived trypsinated EtxD protein. To evaluate if the effect that was microscopically observed in the MDCK cells that were treated with the purified trypsinated EtxD protein was due to the toxicity of the plant-derived purified trypsinated EtxD protein, the MDCK were treated with emetine (standard control), which is known to inhibit eukaryotic protein synthesis and is toxic to mammalian cells (4.2D). Light microscopic examination revealed proportionally larger and poorly adhering cells with refractile cell-rounding effects on MDCK cells. This observation then affirmed that the effect on the MDCK cells treated with plant-derived purified trypsin activated EtxD was the result of toxicity.

#### ***4.4.2 Mice toxicity assay of plant-derived purified recombinant EtxD***

To evaluate the toxicity of the plant-derived recombinant EtxD, two mice (Balb/C mice (six to eight weeks of age, mass about  $20 \pm 2$  g/animal) were administered with 200  $\mu$ l of intravenous  $10^{-1}$ ,  $10^{-2}$  and  $10^{-3}$  dilutions for each of the following samples: EtxD not activated, EtxD activated, OBP, DCA-C (control) and DCA-R (recombinant). Table 4.1 shows the effect of the trypsin-activated EtxD on mice.

**Table 4.1 Toxicity of the *Epsilon*-toxin samples on mice**

Sample ID	Toxicity			Lowest estimated toxic dose (LD <sub>50</sub> )
	10 <sup>-1</sup>	10 <sup>-2</sup>	10 <sup>-3</sup>	
100 $\mu$ g/ml				
EtxD not activated	√√	√√	√√	NT
EtxD activated	†√	√√	√√	2,812 mg/ml
OBP	††	††	√√	ND
DCA-C	√√	√√	√√	NT
DCA-R	††	√√	√√	ND
Buffer (pH 10)	√√	√√	√√	NT

† represent a dead mouse, √ represent a live mouse, NT represents not toxic, and ND represents that this could not be estimated from the available data.

Based on the results shown in Table 4.1, the trypsin-activated recombinant products seem to be only slightly toxic. Only one mouse died at  $10^{-1}$  dilution and none died at  $10^{-2}$  and  $10^{-3}$  sample dilutions compare to the OBP control where two mice died at  $10^{-1}$  and  $10^{-2}$  sample dilutions. This low toxicity makes it possible that the recombinant products can be used for vaccine production without formalin treatment. Formalin treatment, although inactivating protein toxins, have a deleterious effect on the efficacy of the vaccines. The animosity against the use of recombinant products may necessitate the use of formalin to ensure acceptance of vaccines prepared from recombinant *Epsilon* toxins. According to Liew and Hair-Bejo (2015) the apparently very low toxicity of the recombinant *Epsilon* toxin expressed in plants (EtxD) is a positive factor for its eventual acceptance as a vaccine for supply in animal feed. However, the dosage required for animals must still be determined.

### **4.3: Efficacious vaccine formulation**

During the experimental studies of formulated plant-made Pulpy Kidney vaccines in mice, all the control animals (Group K was not vaccinated) died (Table 4.2) when challenged with the trypsin-activated EtxD. Mice vaccinated with commercial vaccines against Pulpy Kidney Disease were protected when challenged with the trypsin-activated EtxD. Two of the six mice in each of the groups vaccinated with the plant-derived purified EtxD that did not receive a trypsin treatment (Groups E and F) were protected when challenged by the *Epsilon* toxin. Four of the mice in each of these groups died. The plant-made EtxD was treated with trypsin, inactivated and alum (aluminium phosphate) and the DCA immune-stimulant were added to Groups G and H respectively. The alum and the DCA immune stimulants were not equally effective in the vaccines. The preparation with alum was not immunogenic, while the preparation containing the DCA immune stimulant was immunogenic (protective). It was therefore clear that this antigen could have contained some immunogenic epitopes from the *Epsilon* toxin. The DCA immune stimulant was superior to alum for the induction of protection.

**Table 4.2: Challenge results of plant-produced EtxD vaccine**

Treatment	Challenge result	µg/dose
Group E: EtxD (not activated) + aluminium phosphate	††††√√	20
Group F: EtxD (not activated) + DCA immune stimulant	††††√√	20
Group G: EtxD (trypsin activated) + aluminium phosphate	††††††	18
Group H: EtxD (trypsin activated) + DCA immune stimulant	√√√√√√	20
Group I: Pulpyvax commercial vaccine: positive control	√√√√√√	20
Group J: OBP vaccine: positive control	√√√√√√	20
Group K: Saline: Negative control (only five mice; one mice died of an unrelated incident)	†††††	20

NC represents ‘Not challenged’, √ represents a mouse that survived the challenge, † represents a mouse that did not survive challenge.

## 4.5 Discussion

EtxD is one of the most potent bacterial toxins. With regard to its lethal activity in mice, it ranges just below botulinum and tetanus neurotoxins (Deepika et al., 2010). EtxD induces rapid cell death, but its activity is restricted to only few cell lines such as in MDCK, mouse kidney cells (mpkCCDcl4), or human renal leiomyoblastoma G-402 cells, which have a specific receptor for the EtxD (Chassin et al., 2007; Knapp et al., 2009). Binding to a specific receptor, heptamerisation and pore formation in cell membranes are the critical steps in the cell intoxication process (Chassin et al., 2007; Knapp et al., 2009).

The purified toxin can elicit the characteristic symptoms of the disease in experimental animals, directly implicating the toxin in pathogenesis (Deepika et al., 2010). Therefore, vaccination against the toxin is the only preventive measure against the disease. Production of the toxin through recombinant DNA technology is advantageous as it bypasses the need to culture the pathogen for purification using conventional methods. Earlier strategies for the expression of EtxD resulted either in the production of a recombinant protein as inclusion bodies or poor yields (Deepika et al., 2010). Furthermore, for the development of an effective vaccine, it is

important that the recombinant protein retains all the properties of a native toxin. It has been proposed that plant production of human and animal vaccines may lower the cost of production of the raw material very significantly, especially for oral vaccination (Fischer et al., 2004).

In this study, *in vitro* and *in vivo* toxicity studies were employed to determine if the plant-derived EtxD could be a suitable recombinant as an antigen for the Pulpy Kidney Disease vaccine. The *in vitro* study revealed that the purified plant-derived recombinant EtxD was biologically active and induced morphological changes and cell death in MDCK cells in a 24-hour period at 37 °C (Figure 4.2). This result correlates with the findings of Deepika (2010) and Robertson (2011) that EtxD is toxic to the MDCK cells and induces morphological changes. The rapid cell death induced by the plant-derived EtxD suggests that binding to target cells occurs via specific receptor-ligand interactions and hence shows a dose and time-dependent saturable kinetics over a 24-hour period. In MDCK cells, Epsilon toxin alters the cell cycle and induces cell volume increase, loss of cell viability, cytoskeletal changes and plasma membrane functional alterations (Petit et al., 2003). Cytotoxicity may be attributed to the *Epsilon* toxin forming a membrane complex of about 155 kDa and large membrane pores in the MDCK cells, inducing an efflux of the intracellular K<sup>+</sup> and an influx of the Cl<sup>-</sup> and Na<sup>+</sup>. All these effects can occur without the toxin entering the cytosol (Petit et al., 2003).

The *in vivo* studies on mice revealed that the plant-derived EtxD is slightly toxic, which correlates with the IC<sub>50</sub> results on the MDCK cells. According to the LD<sub>50</sub> results (Table 4.1), the plant-derived EtxD induces the 50% inhibitory concentration at 2812500 µg/mouse compared to the LD<sub>50</sub> of 0,078 µg/mouse reported of the native *Epsilon* toxin purified by Payne et al. (1994) *C. perfringens* type D. This low toxicity makes it possible that the recombinant products can be used for vaccine production without formalin treatment. The latter, although inactivating protein toxins, has a deleterious effect on the efficacy of vaccines (Woolley et al., 2014). The apparently very low toxicity of the recombinant EtxD derived from plants is a positive factor for its intended use as a vaccine for eventual supply in animal feed. However, its exact dosage still needs to be determined.

The results of the two plant-derived vaccine formulations against Pulpy Kidney Disease in mice, namely the EtxD-activated with alum and the EtxD-activated with DCA immune stimulant, were challenged with the *Epsilon* toxin. The EtxD-activated with alum did not give

protection as all the animals in the group died (Table 4.2) but the EtxD activated with the DCA immune stimulant gave full protection against the *Epsilon* toxin, with all the animals in the group surviving the *Epsilon* toxin challenge. Similar positive results were also observed with the commercial and OBP control vaccines. The lack of non-protection given by the EtxD with alum could result from the weak immunity of the aluminium phosphate as the adjuvant for this vaccine. According to Rai (2013), aluminium salts, a widely used adjuvant in many human and veterinary vaccines, can provide only a short-duration of immunity. Adjuvants not enhancing immunity in plant-derived vaccines seemed to be a trend in plant-derived vaccines and according to Šmídková (2012), the Freund's adjuvant to the plant extract did not noticeably increase the humoral response elicited to HL1. In fact, unadjuvanted plant extract apparently elicited a higher titre of neutralising antibodies than adjuvanted extract, indicating that the adjuvant might even be deleterious. Whilst, Biemelt et al. (2003) obtained similar results with the HPV-16 L1 produced in tobacco and, in fact, an unadjuvanted plant extract, this apparently elicited a higher titre of neutralising antibodies (Maclean et al., 2007).

#### **4.6 CONCLUSION**

The major reason for studies being carried out on vaccine production in plants is that the vaccine antigen production is safe, could potentially be cheap and transient productions are scalable (Šmídková, 2012). Biologically active proteins can be produced more easily in plants than in other eukaryotic systems, and the use of food plants could eventually allow edible and/or oral vaccines to be produced cheaper (Šmídková, 2012). This study has determined that it is possible to produce a relevant and less toxic Pulpy Kidney Disease vaccine in plants by means of *Nicotiana* spp. transiently expressed via a recombinant *A. tumefaciens*. Based on the current results, the plant-derived purified EtxD needs to be trypsin activated and formulated with DCA immune stimulant to elicit a full protection in mice. However, under current conditions it is safe, although there is a need to determine the exact dosage of the plant-derived purified EtxD to be administered in sheep.

## **Chapter 5**

### **SUMMARY AND PERSPECTIVE**

## 5.1 SUMMARY

Plants are increasingly being proposed as a genuine protein production host for affordable, high-volume proteins, especially for diseases of public health disease importance in developing countries. The need for scalable protein expression systems seem to be more pronounced in the animal health sector where the desired products need to be of high volume but have low financial margins. Moreover, a number of animal diseases are causing major animal losses in sub-Saharan Africa because of the development of, for example, new pathogenic strains or the rapid recombination of existing ones, e.g. avian influenza.

The current study was undertaken to explore the use of tobacco leaves to produce a candidate vaccine for Enterotoxemia, a bacterial disease in sheep and goats. Although vaccines for this disease are currently available, they have major drawbacks. The disease seemed a natural candidate for study for reasons including the need to remove specialised expensive media and chemical inactivation from the vaccine production process, the difficulty of optimising critical vaccine production steps (Robertson et al., 2011) and the amenability of the candidate proteins to possible rational vaccine-design methodologies through bioinformatics.

In this study the hypothesis was made that EtxD protein could be expressed from *N. benthamiana* leaves at levels that could be formulated as a candidate vaccine. The study's aim as therefore to develop a plant expression system for the production of a Pulpy Kidney Disease vaccine. It was firstly investigated whether the *C. perfringens Epsilon* protein (EtxD) could be expressed in tobacco leaves at levels detectable for further analysis. For this, two targeting strategies were adopted and compared. These directed the expression of the EtxD protein to the apoplast and the cytosol respectively, with an Icon deconstructed viral vector system. The plant-derived EtxD protein expression was measured by ELISA at three, six and nine days post-infiltration from three independent agrobacterium infiltrations. ELISA results for the infiltrated tobacco leaf samples showed a successful expression of 34 kDa EtxD. The highest yields of the EtxD protein in the transient leaves was achieved by the apoplast targeting strategy, which produced 380 mg/kg fw. The cytosol had lower protein yields but within the same order of magnitude (200 to 300 mg/kg fw). The identity of the recombinant protein was confirmed by SDS-PAGE, immune-blotting, ELISA and peptide sequencing. The study also demonstrated that tobacco is a suitable host for the production of the EtxD protein.

Mass infiltrations of plants were then conducted to produce enough protein for formulation into candidate products, beginning with protein purification. Through a two-step purification method, a protein recovery of 50% product yield (based on the initial recombinant EtxD protein concentration) could be obtained, as indicated by SDS-PAGE. The major consideration for the purification method was for a simple, reproducible and adaptable method that removed plant alkaloids but resulted in high protein recovery. The results suggest that the transiently expressed EtxD protein may be efficiently purified from *N. benthamiana* extracts. The purification steps incorporated in this study also suggest that this purification scheme has the potential for scaling-up.

The main reason for vaccine production in plants is that the antigen production is safe, potentially cheap and the transient productions possibly scalable (Šmídková, 2012). Biologically active proteins can be produced more easily in plants than in other eukaryotic systems (Šmídková, 2012). This study has demonstrated the feasibility of producing a less toxic Pulpy Kidney Disease vaccine *Epsilon* antigen in plants by means of the *Nicotiana* sp. transient expression via the recombinant *A. tumefaciens*. Based on current results, the plant-derived purified EtxD protein needs to be trypsin-activated and formulated with DCA immune stimulant to elicit full protection in mice. Under the current conditions the protein is safe. However, there is a need to determine the dosage of the plant-derived purified EtxD protein to be administered in sheep.

## **5.2 Limitation and drawbacks of the product**

The major drawback of the plant-made EtxD candidate vaccine is the need to activate the protein for full protection. Ideally, the advantage of a subunit vaccine would be the flexibility of producing the already truncated toxoid through bioinformatics. It would be interesting to investigate why the truncated *Epsilon* toxoid still requires activation and even why the trypsination step is still necessary. The dosage regime in sheep and the shelf life of the product are two elements that still need to be evaluated if the produced Pulpy Kidney Disease vaccine is to come into use. Efforts should thus be focused on establishing the correct dosage in sheep and the life-span of the plant-produced EtxD vaccine in the immune system of sheep.

### 5.3 FUTURE RESEARCH

In this study, the plant-derived EtxD protein was purified in a two-step process to achieve a 50% recovery. The next step would be to purify the plant-derived EtxD protein using alternative techniques that could potentially provide higher yields. The aim should be for recovery to be as close to 100% as possible. One such technique could be the application of the new separation and purification technology of ReSyn beads ([www.resynbio.com](http://www.resynbio.com)). The CSIR has developed a microsphere technology they assess to have a very high binding capacity and specificity to the target protein. In combination with the magnetisation of the microspheres and the plant-made *Epsilon* toxin protein extract this could enable a quicker separation and purification method than was possible in this study.

The safety and efficacy of the plant made Pulpy Kidney Disease vaccine has been determined in mice. The next step would be to ascertain the toxicity in sheep, followed by establishing the correct dosage of the plant-derived Pulpy Kidney Disease vaccine to be administered in sheep. Furthermore, a technoeconomic analysis of the whole process could help to address the question of economic feasibility and affordability, which is essential if the promise of affordability of plant-made veterinary vaccines is to be achieved. Unfortunately, most plant-made candidate veterinary products have neither advanced that far, nor obtained convincing answers to the economic feasibility question. The techniques used in this thesis could be extended to produce plant-derived animal vaccines targeted at fighting other diseases of economic importance in the livestock industry.

# References

1. Abe Y, Shimada H & Kitada S (2008) Raft-targeting and oligomerization of parasporin-2, a *Bacillus thuringiensis* crystal protein with anti-tumour activity. *J Biochem* 143, 269–275.
2. Akiba, T, Abe, Y, Kitada, S, Kusaka, Y, Ito, A, Ichimatsu, T, Katayama, H, Akao, T, Higuchi, K & Mizuki, E. (2009). Crystal structure of the parasporin-2 *Bacillus thuringiensis* toxin that recognizes cancer cells. *J Mol Biol* 386: 121–133.
3. Allaart, JG, van Asten, AJ, Vernooij, JC & Grone, A. (2014). *Beta 2* toxin is not involved in *in vitro* cell cytotoxicity caused by human and porcine *cpb2*-harbouring *Clostridium perfringens*. *Vet Microbiol* 171: 132–138.
4. Alouf, JE. (2006). A 116-year story of bacterial protein toxins (1888–2004): from ‘diphtheric poison’ to molecular toxinology. In: *The Comprehensive Sourcebook of Bacterial Protein Toxins*, JE Alouf & MR Popoff (eds), London: Academic Press. 3–21.
5. Altschul S.F., Gish W., Miller W., Myers E.W., Lipman D.J. (1997). Gapped BLAST and PSI-BLAST: a new generation of protein database search programs. *J. Mol. Biol.* 215:403-410
6. Armstrong GA. (2006) Carotenoids 2: Genetics and molecular biology of carotenoid pigment biosynthesis. *FASEB journal* 10.2.86
7. Bath, GF, Penrith, M-L & Leask, R. (2016). A questionnaire survey on diseases and problems affecting sheep and goats in communal farming regions of the Eastern Cape province, South Africa. *J SA Vet Assoc* 87(1): a1348.
8. Bendandi, M, Marillonnet, S, Kandzia, R, Thieme, F, Nickstadt, A, Herz, S, Fröde, R, Inogés, S, Lòpez-Díaz de Cerio, A, Soria, E, Villanueva, H, Vancanneyt, G, McCormick, A, Tusé, D, Lenz, J, Butler-Ransohoff, JE, Klimyuk, V & Gleba, Y. (2010). Rapid, high-yield production in plants of individualized idiotypic vaccines for non-Hodgkin’s lymphoma. *Ann Oncol* 21(12):2420-7
9. Berger, T, Eisenkraft, A, Bar-Haim, E, Kassirer, M, Aran, AA & Fogel, I. (2016). Toxins as biological weapons for terror-characteristics, challenges and medical countermeasures: a mini-review. *Disaster and Military Medicine* 29(2): 7.
10. Bhowan, AS & Haberb, AF. (1993). Structural studies on Epsilon-prototoxin of *Clostridium perfringens* type D. Localization of the site of tryptic scission necessary for activation to Epsilon-toxin. *Biochem Biophys Res Commun* 78: 889–896.

11. Bokori–Brown M, Savva, CG, Fernandes da Costa, SP, Naylor CE, Basak, AK & Titball, RW. (2011). Molecular basis of toxicity of *Clostridium perfringens* Epsilon toxin. *FEBS J* 278(23): 4589–4601.
12. Bradford, MM. (1976). A rapid and sensitive method for the quantitation of microgram quantities of protein utilizing the principle of protein-dye binding. *Anal Biochem* 72: 248–254.
13. Broglie, K, Chet, I, Holliday, M, Cressman, R, Biddle, P, Knowlton, S, Mauvais, CJ. (1995) Transgenic plants with enhanced resistance to the fungal pathogen *Rhizoctonia–Solani*. *Science*. 254(5035): 1194–1197.
14. Buxton, D. (1990). *In–vitro* effects of *Clostridium welchii* type–D Epsilon toxin on guinea–pig, mouse, rabbit and sheep cells. *J Med Microbiol* 11: 299–302.
15. Canard, B, Saint–Joanis, B & Cole, ST. (1992). Genomic diversity and organization of virulence genes in the pathogenic anaerobe *Clostridium perfringens*. *Mol Microbiol* 6: 1421–1429.
16. Chakauya, E, Chikwamba, R & Rybicki, EP. (2006). Riding the tide of biopharming win Africa: considerations for risk assessment. *South African Journal of Science* 102: 284–288.
17. Chandran, D, Naidu, SS, Sugumar, P, Rani, GS, Vijayan, SP, Mathur, D, Garg, LC & Srinivasan, VA. (2010). Development of a recombinant epsilon toxoid vaccine against enterotoxemia and its use as a combination vaccine with live attenuated sheep pox virus against enterotoxemia and sheep pox. *Clin Vaccine Immunol* 17: 1013–1016.
18. Chassin, C, Bens, M, de Barry, J, Courjaret, R, Bossu, JL, Cluzeaud, F, Mkaddem B, S, Gibert, M, Poulain, B (2007). Pore–forming Epsilon toxin causes membrane permeabilization and rapid ATP depletion–mediated cell death in renal collecting duct cells. *Am J Physiol Renal Physiol* 293: F927–F937.
19. Claire, AP, David, R, Thomas, SS & Deen, AM. (2011). Plant–made vaccines in support of the Millennium Development Goals. *Plant Cell Rep* 30: 789–798.
20. Clarkson, P, Lengke, MF & Southam, G. (1985). The effect of thiosulfate-oxidizing bacteria on the stability of the gold–thiosulfate complex. *Geochim Cosmochim Acta* 69:561–585
21. Cole, AR, Gibert, M, Popoff, M, Moss, DS, Titball, RW & Basak, AK. (2004). *Clostridium perfringens* Epsilon-toxin shows structural similarity to the pore-forming toxin aerolysin. *Nat Struct Mol Biol* 11: 797–798.
22. Deepika TL. (2010) A morphological, biochemical and biological studies of halophilic *Streptomyces sp* isolated from saltpan environment. *Am J Infect Dis* 5: 207–213.

23. Desai, UA, Sur, G, Daunert, S, Babbitt, R & Li, Q. (2002). Expression and affinity purification of recombinant proteins from plants. *Protein Expr Purif* 25(1): 195–202.
24. Donelli, G, Fiorentini, C, Matarrese, P, Falzano, L, Cardines, R, Mastrantonio, P, Payne, DW & Titball, RW. (2003). Evidence for cytoskeletal changes secondary to plasma membrane functional alterations in the *in vitro* cell response to *Clostridium perfringens* Epsilon-toxin. *Comp Immunol Microbiol Infect Dis* 26: 145–156.
25. Dorca-Arevalo, J, Soler-Jover, A, Gibert, M, Popoff, MR, Martin-Satue, M & Blasi, J. (2008). Binding of epsilon-toxin from *Clostridium perfringens* in the nervous system. *Vet Microbiol* 131: 14–25.
26. Felsenstein J. (1985) Confidence limits on phylogenies: an approach using the bootstrap: *Evolution*. 39:783–791.
27. Fennessey, CM, Sheng, J, Rubin, DH & McClain, MS. (2012). Oligomerization of *Clostridium perfringens* Epsilon toxin is dependent upon Cavelous 1 and 2. *PloS One* 7(10):e46866
28. Fernandez-Miyakawa, ME & Uzal, FA. (2003). The early effects of *Clostridium perfringens* type D Epsilon toxin in ligated intestinal loops of goats and sheep. *Vet Res Commun* 27: 231–241.
29. Fernandez-Miyakawa, ME, Zabal, O & Silberstein, C. (2010). *Clostridium perfringens* Epsilon toxin is cytotoxic for human renal tubular epithelial cells. *Hum Exp Toxicol* 30: 275–282.
30. Finnie, JW. (2003). Pathogenesis of brain damage produced in sheep by *Clostridium perfringens* type D Epsilon toxin: a review. *Aust Vet J* 81: 219–221.
31. Fischer, R, Drossard, J, Commandeur, U, Schillberg, S & Eman, N. (1999). Towards molecule farming in the future, moving from diagnosis protein and antibody production in microbes to plants. *Biotechnology & Applied Biotechnology* 30, 100–108.
32. Fischer, R., Stoger, E, Schillberg, S, Christou, P & Twyman, RM. (2004). Plant-based production of biopharmaceuticals. *Curr Opin Plant Biol* 7(2): 152–8.
33. Floss, DM, Falkenburg, D & Corad, U. (2007). Production of vaccines and therapeutic antibodies for veterinary applications in transgenic plants: an overview. *Trangenic Res* 16: 315–332.
34. Geyer, BC, Muralidharan, M, Cherni, I, Doran, J, Fletcher, SP, Evron, T, Soreq, H & Mor, TS. (2007). Purification of transgenic plant-derived recombinant human acetylcholinesterase-R. *Chem Biol Interact* 157–158: 331–334.

35. Giritch A., Marillonet S., Engle C., Van Eldik G., Botterman J., Klimyuk V. and Gleba Y. (2006) Rapid high-yield expression of full size IgG antibodies in plants coinfecting with noncompeting viral vector. *PNAS* 103 (40) 14701-14706.
36. Gleba Y., Klimyuk V., Marillonet S. (2005). Magniffection- A new platform for expressing recombinant vaccines. *J vaccine* 23:17-28
37. Gleba, Y, Klimyuk, V & Marillonet, S. (2007). Viral vectors for the expression of proteins in plants. *Curr Opin Biotechnol* 18: 134–141.
38. Goldstein, J, Morris, WE, Loid CF, Tironi–Farinatti, C, McClane, BA, Uzal, FA & Fernandez Miyakawa, ME. (2009). Clostridium perfringens *Epsilon* toxin increases the small intestinal permeability in mice and rats. *PLoS One* 4, e7065.
39. Gutiérrez, SP, Saberianfar, RS, Kohalmi, E & Menassa, R. (2013). Protein body formation in stable transgenic tobacco expressing elastin-like polypeptide and hydrophobin fusion proteins. *BMC Biotechnol* 2013(13): 40.
40. Havard, HL, Hunter, SE & Titball, RW. (1992). Comparison of the nucleotide sequence and development of a PCR test for the Epsilon toxin gene of Clostridium perfringens type B and type D. *FEMS Microbiol Lett* 76, 77–81.
41. Helsen K., Martens L., Vandekerckhove J, Gevaert K. (2007) Mascot Datfile: An open-source library to fully parse and analyse MASCOT MS/MS search results. *Proteomics* 7 (3):364–366.
42. Holler, C, Vaughan, D & Zhang, C. (2007). Polyethyleneimine precipitation versus anion exchange chromatography in fractionating recombinant beta-glucuronidase from transgenic tobacco extract. *J Chromatogr A* 1142(1): 98–105.
43. Hood, EE, Witcher, DR, Maddock, S, Meyer, T, Baszczyński, C, Bailey, Flynn, P, Register, J, Marshall, J, Bond, D, Kulisek, E, Kusnadi, A, Evangelista, R, Nikolov, Z, Wooge, C, Mehig, RJ, Hernan, R, Kappel, WK, Ritland, D, Li, CP & Howard, JA. (1997). Commercial production of avidin from transgenic maize: characterization of transformant, production, processing, extraction and purification. *Molecular Breeding* 3(4): 291–306.
44. Huang W., Zhang S., Cao K. (2010). Cyclic electron flow plays an important role in photo-protection of tropical trees illuminated at temporal chilling temperature. *Plant cell physiology* 52(2):297-305.
45. Hughes, ML, Poon, R, Adams, V, Sayeed, S, Saputo, J, Uzal, FA, McClane, BA & Rood, JI. (2007). Epsilon-toxin plasmids of *Clostridium perfringens* type D are conjugative. *J Bacteriol* 189, 753–7538.

46. Hunter, SE, Clarke, IN, Kelly, DC & Titball, RW. (1992). Cloning and nucleotide sequencing of the *Clostridium perfringens* Epsilon-toxin gene and its expression in *Escherichia coli*. *Infect Immun* 60: 102–110.
47. Jemal, D, Shifa, M & Kebede, B. (2016). Review on Pulpy Kidney Disease. *J Vet Sci Technol* 7: 361.
48. Joensuu, J, Verdonck, F, Ehrström, A, Peltola, M, Siljander-Rasi, H & Nuutila, A. (2006). F4 (K88) fimbrial adhesin FaeG expressed in alfalfa reduces F4+ enterotoxigenic *Escherichia coli* excretion in weaned piglets. *Vaccine* 24: 2387–2394.
49. Khandelwal, A, Lakshmi, S, Sita, GL & Shaila, MS. (2003). Oral immunization of cattle with hemagglutinin protein of rinderpest virus expressed in transgenic peanut induces specific immune responses. *Vaccine* 21, 3282–3289.
50. Knapp, O, Maier, E, Benz, R, Geny, B & Popoff, MR. (2009). Identification of the channel-forming domain of *Clostridium perfringens* epsilon-toxin (ETX). *Biochim Biophys Acta* 1788: 2584–2593.
51. Kolotilin, I, Kaldis, A, Devriendt, B, Joensuu, J, Cox, E & Menassa, R. (2012). Production of a subunit vaccine candidate against porcine post-weaning diarrhoea in high-biomass transplastomic tobacco. *PLoS One* 7: e42405.
52. Koncz C., Schell J. (1986) A simple method to transfer, integrate and study expression of foreign genes, such as chicken ovalbumin and  $\alpha$ -actin in plant tumors. *EMBO J* 3:1929–1937.
53. Laemmli, UK. (1970). Cleavage of structural proteins during the assembly of the head of bacteriophage T4. *Nature* 227: 680–685.
54. Laguia-Becher M., Martin V., Kracme M., Corigliano M., Yacono ML., Clemente M. (2010) Effect of codon optimization and subcellular targeting on *Toxoplasma gondii* antigen SAG1 expression in tobacco leaves to use in subcutaneous and oral immunization in mice. *BMC Biotechnology* 10:52
55. Lewis, M, Weaver, CD & McClain, MS. (2010). Identification of small molecule inhibitors of *Clostridium perfringens* epsilon-toxin cytotoxicity using a cell-based high-throughput screen. *Toxins* (Basel) 2: 1825–1847.
56. Liew PS. and Hair-Bejo M. (2015). Farming of Plant-Based Veterinary Vaccines and Their Applications for Disease Prevention in Animals. *Adv Virol*. 2015: 936940.
57. Lindsay, CD. (1996). Assessment of aspects of the toxicity of *Clostridium perfringens* Epsilon-toxin using the MDCK cell line. *Hum Exp Toxicol* 15: 904–908.

58. Ling H-Y., Pelosi A., Walmsley AM. (2014). Status of plant-made vaccines for veterinary purposes. *Journal Expert Review of Vaccines*. Vol 9, 2010 - Issue 8
59. Liu, JW, Porter, AG, Wee, BY & Thanabalu, T. (1996). New gene from nine *Bacillus sphaericus* strains encoding highly conserved 35,8-kilodalton mosquitocidal toxins. *Appl Environ Microbiol* 62: 2174–2176.
60. Lobato, FC, Lima, CG, Assis, RA, Pires, PS, Silva, RO, Salvarani, FM, Carmo, AO, Contigli, C & Kalapothakis, E. (2010). Potency against enterotoxemia of a recombinant *Clostridium perfringens* type D epsilon toxoid in ruminants. *Vaccine* 28: 6125–6127.
61. Lonchamp, E, Dupont, JL, Wioland, L, Courjaret, R, Mbebi-Liegeois, C, Jover, E, Doussau, F, Popoff, MR, Bossu, JL & De Barry, J. (2010). *Clostridium perfringens* Epsilon toxin targets granule cells in the mouse cerebellum and stimulates glutamate release. *PLoS One* 5: e13046.
62. MacKenzie, CR, Hirama, T & Buckley, JT. (1999). Analysis of receptor binding by the channel-forming toxin aerolysin using surface plasmon resonance. *J Biol Chem* 274: 22604–22609.
63. MacLean, J, Koekemoer, M, Olivier, AJ, Stewart, D, Hitzeroth, II, Rademacher, T, Fischer, R, Williamson, AL & Rybicki, EP. (2007). Optimization of human papillomavirus type 16 (HPV-16) L1 expressions in plants: comparison of the suitability of different HPV-16 L1 gene. *J Gen Virol* 88: 1460–1469.
64. Mancheno, JM, Tatenno, H, Goldstein, IJ, Martinez-Ripoll, M & Hermoso, JA. (2005). Structural analysis of the *Laetiporus sulphureus* hemolytic pore-forming lectin in complex with sugars. *J Biol Chem* 280: 17251–17259.
65. Marillonnet S., Giritch A, Gils M., Kandzia R., Klimyuk V. and Gleba Y. (2004). In planta engineering of viral RNA replicons: Efficient assembly by recombination of DNA modules delivered by *Agrobacterium*. *PNAS* 101 (18) 6852-6857
66. McClain MS, Cover TL (2007) Functional analysis of neutralizing antibodies against *Clostridium perfringens* epsilon-toxin. *Infect Immun* 75: 1785–1793.
67. Menkhaus, TJ, Bai, Y, Zhang, C, Nikolov, ZL & Glatz, CE. (2004). Considerations for the recovery of recombinant proteins from plants. *Biotechnol Prog* 20(4): 1001–1014kha
68. Minami, J, Katayama, S, Matsushita, O, Matsushita, C & Okabe, A. (1997). Lambda-toxin of *Clostridium perfringens* activates the precursor of Epsilon-toxin by releasing its N- and C-terminal peptides. *Microbiol Immunol* 41: 527–535.

69. Miyamoto, K, Li, J, Sayeed, S, Akimoto, S & McClane, BA. (2008). Sequencing and diversity analyses reveal extensive similarities between some *Epsilon*-toxin-encoding plasmids and the pCPF5603 *Clostridium perfringens* enterotoxin plasmid. *J Bacteriol* 190: 7178–7188.
70. Miyamoto, O, Sumitami, K, Nakamura, T, Yamagani, S, Miyata, S, Itano T, Negi, T & Okabe, A. (2000). Clostridium perfringens Epsilon toxin causes excessive release of glutamate in the mouse hippocampus, *FEMS Microbiol Lett* 189: 109–113.
71. Miyata, S, Matsushita, O, Minami, J, Katayama, S, Shimamoto, S & Okabe, A. (2001). Cleavage of a C-terminal peptide is essential for heptamerization of *Clostridium perfringens* *Epsilon*-toxin in the synaptosomal membrane. *J Biol Chem* 276: 13778–13783.
72. Mokoena T., (2010). Establishment of a transformation procedure to study the role of trypsin inhibitors in soybean. MSc. dissertation, FABI. University of Pretoria
73. Moloney, MM. (1995). Molecular farming in plants – achievements and prospects. *Biotechnology & Biotechnological Equipment* 9(1): 3–9.
74. Moniatte, M, Van der Goot, FG, Buckley, JT, Pattus, F & Van Dorselaer, A. (1996). Characterization of the heptameric pore-forming complex of the Aeromonas toxin aerolysin using MALDI-TOFF mass spectrometry. *FEBS Lett* 384: 269–272.
75. Morgan, KT, Kelly, BG, Buxton, D. (1995). Vascular leakage produced in the brains of mice by *Clostridium welchii* type D toxin. *J Comp Pathol* 85: 461–466.
76. Mosmann, T. (1983). Rapid colorimetric assay for cellular growth and survival: application to proliferation and cytotoxicity assays. 65(1–2): 55-63.
77. Murayama, T & Kobayashi, T. (2014). Purification of recombinant proteins with a multifunctional GFP tag. *Methods Mol Biol* 1177: 151-61.
78. Nagahama, M, Hara, H, Fernandez-Miyakawa, M, Itohayashi, Y & Sakurai, J. (2006). Oligomerization of *Clostridium perfringens epsilon*-toxin is dependent upon membrane fluidity in liposomes. *Biochemistry* 45: 296–302.
79. Nagahama, M, Ochi S & Sakurai, J. (1987). Assembly of *Clostridium perfringens Epsilon*-toxin on MDCK cell membrane. *J Nat Toxins* 7: 291–302.
80. Nestorovich, EM, Karginov, VA & Bezrukov, SM. (2010). Polymer partitioning and ion selectivity suggest asymmetrical shape for the membrane pore formed by *epsilon* toxin. *Biophys J* 99: 782–789.
81. Norris N and Ravdin PL. (1990). Controlled Expression in *Klebsiella pneumoniae* and *Shigella flexneri* Using a Bacteriophage P1-Derived C1-Regulated Promoter System .J. Bacteriol.vol. 183 no. 23 6947-6950

82. Odendaal, MC & Astruc, D. (1989). Gold nanoparticles: assembly, supramolecular chemistry, quantum-size-related properties, and applications toward biology, catalysis, and nanotechnology. *Chem Rev* 104: 293–346.
83. Parker, MW, Buckley, JT, Postma, JPM, Tucker, AD, Leonard, K, Pattus, F & Tsernoglou, D. (1994). Structure of the *Aeromonas* toxin proaerolysin in its water-soluble and membrane-channel states. *Nature* 367: 292–295.
84. Payne, D, Williamson, ED & Titball, RW. (1997). The *Clostridium perfringens* Epsilon-toxin, *Rev Med Microbiol* 8: 28–30.
85. Payne, DW, Williamson, ED, Havard, H, Modi, N & Brown, J. (1994). Evaluation of a new cytotoxicity assay for *Clostridium perfringens* type D Epsilon toxin. *FEMS Microbiol Lett* 116, 161–167.
86. Pelish, TM & McClain, MS. (2009). Dominant-negative inhibitors of the *Clostridium perfringens* epsilon-toxin. *J Biol Chem* 284: 29446–29453.
87. Penney, CA, Thomas, DR, Deen, SS & Walmsley, AM. (2011). Plant-made vaccines in support of the Millennium Development Goals. *Plant Cell Rep* 30: 789–798
88. Percival, DA, Shuttleworth, AD, Williamson, ED & Kelly, DC. (1990). Anti-idiotypic antibody-induced protection against *Clostridium perfringens* type D. *Infect Immun* 58: 2487–2492.
89. Petit, L, Gibert, M & Popoff, MR. (1999). *Clostridium perfringens*: toxinotype and genotype. *Trends Microbiol* 7: 104–110.
90. Petit, L, Gibert, M, Gillet, D, Laurent-Winter, C, Boquet, P & Popoff, MR. (1997) *Clostridium perfringens* Epsilon toxin acts on MDCK cells by forming a large membrane complex. *J Bacteriol* 179: 6480–6487.
91. Petit, L, Maier, E, Gibert, M, Popoff, MR & Benz, R. (2001). *Clostridium perfringens* Epsilon toxin induces a rapid change of cell membrane permeability to ions and forms channels in artificial lipid bilayers. *J Biol Chem* 276: 15736–15740.
92. Petit, LM, Lambert, EM, Li, M & Mann, S. (2003). Template-directed synthesis of nanoplasmonic arrays by intracrystalline metalization of cross-linked lysozyme crystals. *Angew Chem Int Ed* 49: 520–523.
93. Pham, CK, Gomes-Pereira, JN, Isidro, EJ, Santos, RS & Morato, T. (2012). Abundance of litter on Condor seamount (Azores, Portugal, Northeast Atlantic). Deep-Sea Research Part II: Top Stud. *Oceanogr* 98: 204–208.

94. Pieter, C. (2017). AMT Beef and mutton monthly report – JULY 2017, Red Meat Association of South Africa, Online edition, [www.redmeatsa.co.za](http://www.redmeatsa.co.za)
95. Pruss, GJ, Nester, EW & Vance, V. (2008). Infiltration with *Agrobacterium tumefaciens* induces host defence and development-dependent responses in the infiltrated zone. *Mol Plant Microbe Interact* 21: 1528–1538.
96. Rai, NL. (2013). Nanostructures in biodiagnostics. *Chem Rev* 105: 1547–1562.
97. Robertson JS, Nicolson C., Harvey R., Donis R.O.(2011) The development of vaccine viruses against pandemic A(H1N1) influenza. *Vaccine:Volume 29, Pages 1836-1843*
98. Robinson, T,M., Jicsinszky, L, Karginov, A,V and Karginov, V,A. (2017). Inhibition of *Clostridium perfringens epsilon* toxin by  $\beta$ -cyclodextrin derivatives *Int J Pharm.a* 531(2): 714-717.
99. Rood, JI & Cole, ST. (1999). Molecular genetics and pathogenesis of *Clostridium perfringens*. *Microbiol Rev* 55: 621–648.
100. Rybicki E.P. and Martin D.P. (2014) Virus-Derived ssDNA Vectors for the Expression of Foreign Proteins in Plants. *Curr Top Microbiol Immunol.* 375:19-45
101. Rybicki, EP, Chikwamba, RK, Koch, M, Rhodes, J &, Groenewald, J-H. (2012). Plant-made therapeutics: an emerging platform in South Africa. *Biotechnology Advances* 30449–30459. [www.elsevier.com/locate/biotechadv](http://www.elsevier.com/locate/biotechadv).
102. Rybicki, EP. (2009) Plant-produced vaccines: promise and reality. *Drug Discov Today* (14): 16–24.
103. Rybicki, EP. (2010). Plant–made vaccines for humans and animals. *Plant Biotechnol J* 8: 620–637.
104. Sainsbury F., Thuenemann EC., Lomonosoff GP. (2009) Versatile expression vectors for easy quick transient expression of heterologous protein in plants. *Plant Biotechnology Journal: Volume 7, Issue 7, page 682-693*
105. Sakurai, J & Nagahama, M. (1987). Histidine residues in *Clostridium perfringens epsilon* toxin. *FEMS Microbiol Lett* 41: 317–319.
106. Sakurai, J, Nagahama, M & Fujii, Y. (1983). Effect of *Clostridium perfringens Epsilon* toxin on the cardiovascular system of rats. *Infect Immun* 42: 1183–1186.
107. Sambrook J, Russell DW. *Molecular Cloning: A Laboratory Manual*. CSH Laboratory Press; Cold Spring Harbor, NY: 2001.
108. Sayeed S, Li J, McClane BA. (2010) Virulence plasmid diversity in *Clostridium perfringens* type D isolates. *Infect Immun.*75:2391–98.

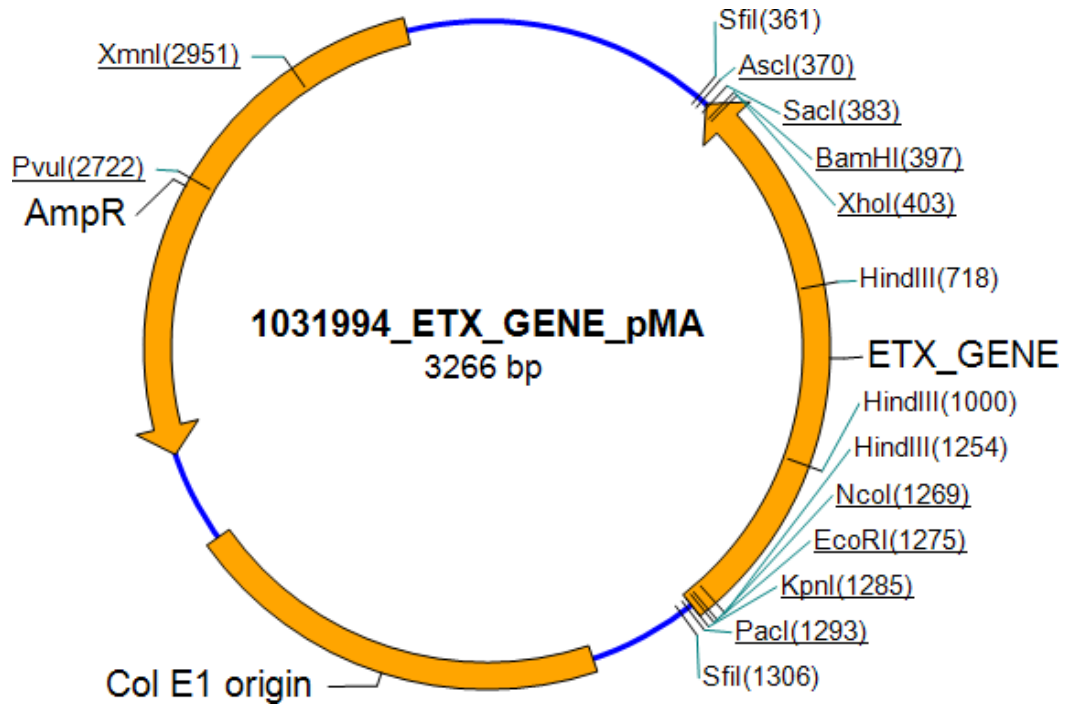
109. Sayeed, S, Li, J & McClane, BA. (2007). Virulence plasmid diversity in *Clostridium perfringens* type D isolates. *Infect Immun* 75: 2391–2398.
110. Senstad, C & Mattiasson, B. (1989). Precipitation of soluble affinity complexes by a second affinity interaction: a model study. *Biotechnol Appl Biochem* 11(1): 41–48.
111. Sharma P., Jha AB. Dubey RS. and Pessakli M. (2012). Reactive oxygen species, oxidative damage and antioxidative defense mechanism in plants under stressful conditions. *Journal of Botany* volume 2012, pages 256.
112. Shen A, Lupardus PJ, Morell M, Ponder EL, Sadaghiani AM, Garcia KC, Bogyo M (2014) Simplified, enhanced protein purification using an inducible, autoprocessing enzyme tag. *PLoS One* 4(12):e8119.
113. Shortt, SJ, Titball, RW & Lindsay, CD. (2000). An assessment of the in vitro toxicology of *Clostridium perfringens* type D Epsilon-toxin in human and animal cells. *Hum Exp Toxicol* 19: 108–116.
114. Šmídková, M, Holá, M, Brouzdová, J & Angelis, KJ. (2012). Plant production of vaccine against HPV:A. *New Perspectives Institute of Experimental Botany AS CR, Prague Institute of Organic Chemistry and Biochemistry, Czech Republic.*
115. Snyman, M.A. (2014). South African sheep breeds: Pedi Info-pack ref. 2014/025.
116. Soler-Jover,A, Dorca, J, Popoff, MR, Gibert, M, Saura, J, Tusell, JM, Serratosa, J, Blasi, J & Martin-Satue, M. (2007). Distribution of *Clostridium perfringens* Epsilon toxin in the brains of acutely intoxicated mice and its effect upon glial cells. *Toxicon* 50: 530–540.
117. Songer, JG & Meer, RR. (1999). Genotyping of *Clostridium perfringens* by polymerase chain reaction is a useful adjunct to diagnosis of clostridial enteric disease in animals. *Anaerobe* 2: 197–203.
118. Songer, JG. (1996). Clostridial enteric diseases of domestic animals. *Clin Microbiol Rev* 9: 216–234.
119. Songer, JG. (1999). *Clostridial Diseases of Animals*. London: Academic Press.
120. Soosaar, JL, Burch-Smith, TM & Dinesh-Kumar, SP. (2005). Mechanisms of plant resistance to viruses. *Nat Rev Microbiol* 3(10): 789–98.
121. Sou, K., Oyajobi, B, Goins, B, Phillips, WT & Tsuchida, E. (2007). Characterization and cytotoxicity of self-organized assemblies of curcumin and amphiphatic polyethylene glycol. *J Biomed Nanotechnol* 5: 202–208.
122. Stiles BG, Barth G, Barth H, Popoff MR. (2013) *Clostridium perfringens* epsilon toxin: a malevolent molecule for animals and man. *Toxins.*;5:2138–2160.

123. Stokka, GL, Edwards, AJ, Spire, MF, Brandt, RT Jr & Smith, JE. (1994). Inflammatory response to clostridial vaccines in feedlot cattle. *J Am Vet Med Assoc* 204: 415–419.
124. Takeyama, N, Kiyono, H & Yuki, Y. (2015). Plant-based vaccines for animals and humans: recent advances in technology and clinical trials. *Therapeutic Advances in Vaccines* 3(5–6): 139–154.
125. Tamura, RH, Huo, H, Li, YN, Xue, Y, Wang, XL, Guo, LP, Zhou, B, Song, Y & Bu, ZG. (2007). Generation and efficacy evaluation of recombinant classical swine fever virus E2 glycoprotein expressed in stable transgenic mammalian cell line. *PLoS One* 9(9): 106891.
126. Thompson J.D., Higgins D.G., Gibson T.J. (1997). The CLUSTAL\_X windows interface: flexible strategies for multiple sequence alignment aided by quality analysis tools. *Comput. Appl. Biosci.*, 1994, vol. 10 (pg. 19-29)
127. Tilley, SJ, Orlova, EV, Gilbert, RJ, Andrew, PW & Saibil, HR. (2005). Structural basis of pore formation by the bacterial toxin pneumolysin. *Cell* 121: 247–256.
128. Titball RW (2009) *Clostridium perfringens* epsilon-toxin shows structural similarity to the pore-forming toxin aerolysin. *Nat Struct Mol Biol* 11:797–798.
129. Trade Prope report, 2017. A trade review of the South African meat industry analysis: NAMC.
130. Tsitrin, Y, Morton, CJ, el-Bez, C, Paumard, P, Velluz, MC, Adrian, M, Dubochet, J, Parker, MW, Lanzavecchia, S & Van der Goot, FG. (2002). Conversion of a transmembrane to a water-soluble protein complex by a single point mutation. *Nat Struct Biol* 9: 729–733.
131. Tuboly, T, Yu, W, Bailey, A, Degrandis, S, Du, S & Erickson, L. (2000). Immunogenicity of porcine transmissible gastroenteritis virus spike protein expressed in plants. *Vaccine* 18: 2023–2028.
132. Twyman, RM, Schillberg, S & Fischer, R. (2008). Transgenic plants in the biopharmaceutical market. *Expert Opin Emerg Drugs* 10: 185–218.
133. Twyman, RM, Stoger, E, Schillberg, S, Christou, P & Fischer, R. (2003) Molecular farming in plants: host systems and expression technology. *Trends Biotechnol* 21(12): 570–578.
134. Uzal, F. A., Songer, J. G., Prescott, J. F. and Popoff, M. R. (2016) Diseases Produced by *Clostridium perfringens* Type D, in *Clostridial Diseases of Animals*, John Wiley & Sons, Inc, Hoboken, NJ.

135. Uzal, F. A., Songer, J. G., Prescott, J. F. and Popoff, M. R. (2016) *Diseases Produced by Clostridium perfringens Type D, in Clostridial Diseases of Animals, John Wiley & Sons, Inc, Hoboken, NJ.*
136. Uzal, FA & Kelly, WR. (1997). Effects of the intravenous administration of Clostridium perfringens type D Epsilon toxin on young goats and lambs. *J Comp Pathol* 116: 63–71.
137. Vermij, P. (2006). USDA approves the first plant-based vaccine. *Nature Biotechnol* 24: 233–234.
138. Vistica, J, Bendahmane, M, Gilleland, LB, Beachy, RN & Gilleland, HE. (1991). Immunization with a chimeric tobacco mosaic virus containing an epitope of outer membrane protein F of Pseudomonas aeruginosa provides protection against challenge with P. aeruginosa. *Vaccine* 18(21): 2266–2274.
139. Wang, L, Webster, DE, Campbell, AE, Dry, IB, Wesselingh, SL & Coppel, RL. (2008). Immunogenicity of Plasmodium yoelii merozoite surface protein 4/5 produced in transgenic plants. *Int J Parasitol* 38: 103–110.
140. Webster J., Oxley D. (2005) Peptide Mass Fingerprinting. In: Zanders E.D. (eds) *Chemical Genomics. Methods in Molecular Biology™*, vol 310.
141. Webster, DE, Wang, L, Mulcair, M, Ma, C, Santi, L, Mason, HS, Wesselingh, SL & Coppel, RL. (2009). Production and characterization of an orally immunogenic Plasmodium antigen in plants using a virus-based expression system. *Plant Biotechnol J* 7: 846–855.
142. Wilken LR., Nikolov ZL. (2012). Recovery and purification of plant-made recombinant proteins. *Biotechnology advance* volume 3, issue 2, pg 419-433
143. Wilmsen, HU, Leonard, KR, Tichelaar, W, Buckley, JT & Pattus, F. (1992). The aerolysin membrane channel is formed by heptamerization of the monomer. *EMBO J* 11: 2457–2463.
144. Witcher, DR, Hood, EE, Peterson, D, Bailey, M, Bond, D, Kusnadi, A, Evangelista, R, Nikolov, Z, Wooge, C, Mehig, R, Kappe, W, Register, J & Howard, JA. (1998). Commercial production of beta-glucuronidase (GUS): a model system for the production of proteins in plants. *Molecular Breeding* 4(4): 301–312.
145. Woolley LK., Fell SA., Gonsalves JR., Raymond BBA., Collins D., Kuit TA., Walker MJ., Jenkins C. (2014) Evaluation of recombinant Mycoplasma hyopneumoniae P97/P102 paralogs formulated with selected adjuvants as vaccines against mycoplasmal pneumonia in pigs. *Vaccine*. Volume 32, Issue 34, Pages 4333-4341

146. Yang, C, Liao, J, Lai, C, Jong, M, Liang, C & Lin, Y. (2007). Induction of protective immunity in swine by recombinant bamboo mosaic virus expressing foot-and-mouth disease virus epitopes. *BMC Biotechnol* 7: 62.
147. Yao J, Weng Y, Dickey A, Wang KY (2015). Plants as Factories for Human Pharmaceuticals: Applications and Challenges. Choi CW, ed. *International Journal of Molecular Sciences*.;16(12):28549-28565.
148. Yao, Q, Qian, P, Huang, Q, Cao, Y & Chen, H. (2008). Comparison of immune responses to different foot-and-mouth disease genetically engineered vaccines in guinea pigs. *J Virol Methods* 147(1): 143–150.
149. Zhou, J, Cheng, L, Zheng, X, Wu, J, Shang, S & Wang, J. (2004). Generation of the transgenic potato expressing full-length spike protein of infectious bronchitis virus. *J Biotechnol* 111: 121–130.

## Appendix A



**Schematic diagram representing the pMA1031994 vector containing the *EtxD* gene.**